Summer 8-31-2002

Remediation of chromium contaminated soils with colloidal silica

Netnapid Yossapol
New Jersey Institute of Technology

ABSTRACT

REMEDIATION OF CHROMIUM CONTAMINATED SOILS WITH COLLOIDAL SILICA

By

Netnapid Yossapol

The low-viscosity stabilizer, colloidal silica, is extensively used as a grouting material in the construction of grout curtains. It has low viscosity and is non-toxic, which is suitable for injection to stabilize fine-grained soils. It is also applied as a stabilizer in the in-situ treatment of hazardous waste. Once the colloidal silica solution is injected into contaminated soil, it moves through the pores inside the soil matrix, initiating the stabilization process. The viscosity of the colloidal silica mixture increases while it moves until solidifications. This process is called gelation and results in the creation of a gel barrier around contaminated soil particles, causing a substantial reduction of fluid flow in the soil, this will minimize the movement of water and hence movement of contaminants through the gel mass.

In this research, the stabilization process of chromium contaminated soils using colloidal silica were investigated. The transport of colloidal silica during injection was simulated at the microscopic level to further understand the gelation process. Diffusion of chromium through colloidal silica gel was modeled to evaluate the effectiveness of the technology. A new optical method to estimate the diffusion coefficient of chromium in gel was purposed. The diffusion coefficient obtained using the above optical method was used to evaluate the long term effectiveness of colloidal silica grouting technology.

The movement of colloidal silica during the injection was modeled using the change in gel viscosity with time. The simulation showed that during the grouting process, solidification starts at the soil surface and expands to fill the void space within

1.2 hours. The different soil geometries resulted in the different velocity contours and different colloidal silica solidification patterns. The greater the ellipsoid axial ratio of soil resulted in faster solidification.

The measured diffusion coefficients of chromium in the colloidal silica gel, NYACOL DP5110® from Eka Chemical Inc., ranges from 1.76 to 8.48 x 10^{-10} m^2/sec depending mainly on the concentration of silica in the gel and initial concentration of chromium. Higher silica concentrations yielded greater diffusion coefficients due to the obstruction to the free movement of chromium. The adsorption isotherm of chromate to colloidal silica gel was found to be linear at pH 7; partition coefficient was calculated to be 0.549 liter/gm. Mass balance calculations were performed to evaluate the accuracy of the proposed method and the error was less than 6.5%. Therefore, the optical method using digital imaging is an effective and reliable technique for measuring the diffusion coefficient of metal contaminated colloidal silica gel.

Using the measured diffusion and partition coefficients, a simulation was performed for worse case scenario, where chromium is continuously dissolved from soil into the water interface between soil and gel, and moves to groundwater without obstruction from soil particles. The thickness of the gel barrier used in this simulation was 5 cm (Heisher, 1997). The solubility of chromium in water was 109 mg/liter (Rock et al, 2001). The results showed that it would take approximately eight days before the groundwater would exceed the USEPA standard for chromium (0.1 mg/liter).

Based on these initial test results, the use of NYACOL DP5110® to treat chromium contaminated soil appears to be ineffective due to high diffusion. The diffusion of contaminant in gel will be a major concern when applying this technology. Further research of more realistic simulation of diffusion and refined gel formulation with capacity to convert the chromium to immobile form is recommended.

REMEDIATION OF CHROMIUM CONTAMINATED SOILS WITH COLLOIDAL SILICA

by

Netnapid Yossapol

A Dissertation
Submitted to the Faculty of
New Jersey Institute of Technology
In Partial Fulfillment of the Requirements for the Degree of
Doctor of Philosophy

Department of Civil and Environmental Engineering

August 2002

APPROVAL PAGE

REMEDIATION OF CHROMIUM CONTAMINATED SOILS WITH COLLOIDAL SILICA

Netnapid Yossapol

Dr. Jay N. Meegoda, Dissertation Advisor — Date
Professor of Civil and Environmental Engineering Department, NJIT

Dr. James M. Grow, Committee Member — Date
Research Professor of Department of Chemical Engineering, Chemistry and Environmental Science, NJIT

Dr. Lisa Axe, Committee Member — Date
Associate Professor of Civil and Environmental Engineering Department, NJIT

Dr. Methi Wecharatana, Committee Member — Date
Professor of Civil and Environmental Engineering Department, NJIT

Dr. Mohamed E. Labib, Committee Member — Date
Research Professor of Civil and Environmental Engineering Department, NJIT

BIOGRAPHICAL SKETCH

Author: Netnapid Yossapol

Degree: Doctor of Philosophy

Date: August 2002

Education:

- Doctor of Philosophy in Environmental Engineering,
  New Jersey Institute of Technology, Newark, USA, 2002
- Master of Science in Environmental Engineering,
  New Jersey Institute of Technology, Newark, USA, 1997
- Bachelor of Science in Environmental Engineering,
  Khon Kaen University, Khon Kaen, Thailand, 1993

Major: Environmental Engineering

Presentations and Publications:

Netnapid Yossapol and Jay N. Meegoda

"Physical mechanisms of colloidal silica grouting in remediation of chromium contaminated soil." Proceedings of the 33rd Mid-Atlantic Industrial and Hazardous waste Conference, Manhattan College, Riverdale, New York, June 18-20, 2001, 19-28.

Netnapid Yossapol and Jay N. Meegoda

"Remediation of Heavy Metal Contaminated Soil with Colloidal Silica." Proceedings of the 32nd Mid-Atlantic Industrial and Hazardous Waste Conference, Rensselaer Polytechnic Institute, Troy, New York, June 2000, 787-796.

This dissertation is dedicated to

"my family".

ACKNOWLEDGMENTS

I would like to express my deepest appreciation to my Thesis advisor, Dr. Jay N. Meegoda, for both his guidance and encouragement. I also deeply value the input and suggestions from the rest of my Committee Dr. James M. Grow, Dr. Lisa Axe and Dr. Mohamed E. Labib. Their help and advice profoundly impacted my research. I wish to express my gratitude to my graduate advisor, Dr. Hsin-Neng Hsieh, whose counsel aided me greatly during the course of my study. I am also grateful to him for giving me an opportunity to work as a NJIT Teacher Assistant. That experience was invaluable in helping me to prepare for an academic career. My thanks also go to various other professors who delivered informative and motivating lectures here at NJIT.

The support and inspiration from Dr. Methi Wecharatana will be always recognized in my heart. He did not only serve as a member of my dissertation Committee but was also personally available to provide guidance in life. His involvement and advice has had a special influence for my life and my future.

Both the NJIT staff and my fellow graduate students in the Civil and Environmental Engineering Department are deserving of recognition for their assistants. Without the help with technical skills, the laboratory instrument instruction, and equipment from Mr. Chandrakant Patel, Mr. Robert Morris and Mr. Frank J. Johansson, this work would have never been completed. In addition, the help from the NJIT librarians will be always recognized especially the inter-library loan staff.

Helps from outsiders in information and chemical supply are recognized as well. Thanks to Dr. Gorge J. Moridis from Earth Science Division Lawrence Berkeley National Laboratory, Ms. Marry North-Abbott and Dr. Marek Zaluski from MSE Technology for providing me with copies of their work. Thanks to Eka Chemical Inc. for providing me a sample of DP51110. Thanks for Mr. David Westlake for lending me a digital camera.

I am grateful to Khon Kaen University, Thailand, for providing me with a full scholarship during my study here in NJIT.

Lastly, my special thank goes to my friends and family: to my friends, May, Peep, Or, Tep, Aoy, Kae, Cris and Pooh-Poo for their help and encouragement, my brother, Chatpet Yossapol, for his support, my mother, Naunpen Yossapol, for her endless love, and my husband, Nitass Tantemsapya, for his love, help, support and being a source of strength when I was tired and discouraged.

TABLE OF CONTENTS

TABLE OF CONTENTS
(Continued)

Chapter **Page**

TABLE OF CONTENTS
(Continued)

Chapter **Page**

LIST OF TABLES

LIST OF FIGURES

Figures **Page**

LIST OF FIGURES
(Continued)

Figures **Page**

LIST OF FIGURES
(Continued)

Figures **Page**

LIST OF SYMBOLS

A	cross section area (m^2)
A_{ba}, A_{bs}, A_{be}	boundaries of a the unit cell
a_i	fitting parameters for the gelation-time curve
C_{water}	chemical concentration in water (mg/liter)
C_{gel}	chemical concentration in gel (mg/gm)
C_0	chemical at the gel interface (mg/gm)
D	diffusion coefficient (m^2/sec)
S	chemical adsorbed in gel (mg/gm)
j_i	molar flux at distance i
K	partition coefficient. (liter/gm)
k	ratio of C_{gel} to C_{water} (-)
P	pressure (N/m^2)
t	time (sec)
V	velocity (m/sec)
z	distance in the diffused direction (m)
ρ	mass density (g/liter)
θ	porosity (-) (volume of void/volume total)
τ	tortuosity factor (-) (actual path length between two points to the shortest distance between same two point)
μ	absolute dynamic viscosity (Poise, $N.sec/m^2$)

CHAPTER 1

INTRODUCTION

Between 1905 and 1971, more than two million tons of chromite ore processing residue (COPR) were generated from three chromite ore processing plants in Hudson and Essex Counties, New Jersey, which were used as a "clean-fills" in nearby areas. The COPR was disposed in Hudson and Essex Counties causing soil contamination in Jersey City, Bayonne, Kearny, Newark and Secaucus. The New Jersey Department of Environmental Protection, NJDEP, identified over 180 sites contaminated with COPR. The chromate waste has been found in residential, commercial and industrial zones, resulting in contamination of walls and floors of buildings, interior and exterior building surfaces, driveways, parking lots and in the surface and subsurface of unpaved areas. In the late 1990s, NJDEP (2000) performed Remedial Investigations (RI) at 45 sites to delineate the extent of the contamination and identify cleanup options. Treatment has started, currently most of the residential contamination sites has been remediated. The remediation actions for the rest of the residential site are now in progress (NJDEP, 2002). Since the problem aforementioned is a major one in New Jersey, it needs a comprehensive study to look into the applicability of other emerging technologies.

The effectiveness of emerging technology in treating metal contaminated soils was investigated by the USEPA (1991). The Solidification/Stabilization (S/S) technology is the most commonly used one to treat metal contaminated soils. Solidification/Stabilization technology is appropriate to stabilize soil and prevent hazardous substances in soil from migrating to the environment. There are numbers of S/S technologies, depending on the site conditions including type of contaminants and soil conditions. In this research the applicability of injecting colloidal silica as a grouting

material, a S/S technology, was investigated to in-situ stabilize chromium contaminated soils.

Grouting is a S/S technique of injecting a stabilizer/binder into a medium to increase strength or to improve engineering performance. The injected stabilizer/binder should have the ability to penetrate into empty spaces in soil and rock, and later hardening inside the media. This causes an increase in the mechanical strength of the media. The grouting technique was first developed in the construction industry in order to facilitate underground construction. Subsequently, it was applied to control the movement of water or hazardous chemicals in groundwater and soil. Grouting techniques have several advantages over other S/S techniques including the ability to in-situ mix the stabilizer/binder with the contaminated soil. In-situ S/S techniques require less labor and energy than ex-situ techniques that require excavation, transport and disposal of the treated material.

There were several studies performed on cement based grouting for construction of hazardous waste barriers. However, the application is questionable in remediation chromium contaminated soils (USEPA, 1988) due to the fact that chromium can react with cement causing a decrease in strength (Vipulandan & Wang, 2000). Allan and Kukacka (1994) at Brookhaven National Laboratory (BNL) performed research using chemical grouting for in-situ treatment of waste landfills. The purpose of their research was to prevent the migration of chromium from a landfill and to compare the effectiveness of different stabilizers. Chemical barriers were synthesized by injecting superplasticizers, cement and silica fume into soil media. Test results showed that these materials created effective barriers in controlling chromium migration in fine soils. Superplasticizers yielded the best performance followed by silica fume then cement. They later was successfully applied this in-situ technology to a mixed waste landfill site at Sandia National Laboratory yielding excellent results.

Colloidal silica is a silicate-based material that is used for grouting. It has many advantages over other grouting materials. It has a low viscosity and hence can easily penetrate into empty spaces between fine-grained soils. In addition to its low viscosity, colloidal silica has a large surface area contributing to its potential effectiveness as an adsorbent for metals. Application of colloidal silica grouting to remedy contaminated soil was first introduced by researchers at Du Pont (Noll & Bratlett et al., 1992). The possibility of using colloidal silica to control migration of waste and the effect of soil properties on this approach were further investigated by researchers at Lawrence Berkeley National Laboratory (Moridis, 1994; Persoff et al., 1995; Moridis et al., 1997; Apps et al., 1998). These groups demonstrated that colloidal silica can be injected into soil creating an impermeable wall, preventing the migration of radio nuclides. Persoff et al. (1999) performed additional studies to physically and numerically evaluate the possibility of using colloidal silica in controlling the movement of non-aqueous phase liquid (NAPLs).

Based on the discussion above, in-situ S/S of contaminated soils using colloidal silica is a well-established technology. However, the theoretical understanding of how colloidal silica functions as an effective S/S agent is not well understood. This research attempts to perform a theoretical study to understand the stabilization mechanisms of colloidal silica grout.

This study is divided into two parts. The first part models the movement of colloidal silica during the stabilization process using a microscopic model of fluid flow through soil. The second part of this study models the transport of chromium after the contaminated soil is stabilized with colloidal silica.

A literature survey is reported in Chapter 2. Detailed descriptions of the objectives of this study are given in Chapter 3. Chapter 4 describes the movement and the subsequent solidification of colloidal silica, where a microscopic model developed by

Meegoda (1989) was adopted to simulate the stabilizer behavior. The simulation results graphically demonstrated gradual solidification of stabilizer after injection into the soil media, which explains the movement of stabilizer as a function of time and distance. The model and the associated computer program can be further developed for the design and implementation of in-situ stabilization using colloidal silica.

In Chapter 5, an optical method to determine the diffusion coefficient is introduced. In Chapter 6, the diffusion coefficient estimated from the optical method is used to calculate the release of chromium ions from the solidified/stabilized matrix as a function of time. Conclusions and suggestions for future research are presented in Chapter 7

CHAPTER 2

LITERATURE SURVEY

In this chapter, chemistry of chromium, effectiveness of stabilization and solidification processes for chromium contaminated soils, treatment of chromium contaminated soils with colloidal silica and the chemistry of colloidal silica are explained. The first section is devoted to chromium. Next, applicable technologies to treat chromium contaminated soils and a summary of the treatment of soil using colloidal silica are discussed. Finally, an extensive description of colloidal silica is presented, focusing on its chemistry, structure and aggregation.

2.1 Chemistry of Chromium

Chromium found in nature occurs in many oxidation states, often in the form of iron chromite, $FeCr_2O_4$. Chromium is mined, processed and used in many industries such as wood preservation, leather tanning, electroplating, metal finishing and pigment manufacturing. During extraction, iron chromite is processed and oxidized to hexavalent chromium, Cr(VI), and then recovered in a soluble form. Hexavalent chromium species found in contaminated areas are often chromate (CrO_4^{2-}) and dichromate ($Cr_2O_7^{2-}$). These two forms of hexavalent chromium are pH dependent.

The Eh-pH (Dragun et al., 1997) and pC-pH diagrams presented in Figure 2.1 shows the chromium species dominant under equilibrium conditions as a function of redox potential and pH. Figure 2.2 shows equilibrium of chromium as a function of pH with Ionic strength= 10^{-3} M, $P_{CO_2}=10^{-3.5}$ atm, $C_{T,Cr(VI)}$ = 1.0 M calculated by MINEQL+ V4.5. At high pH and under oxidizing conditions, chromate and dichromate are dominant.

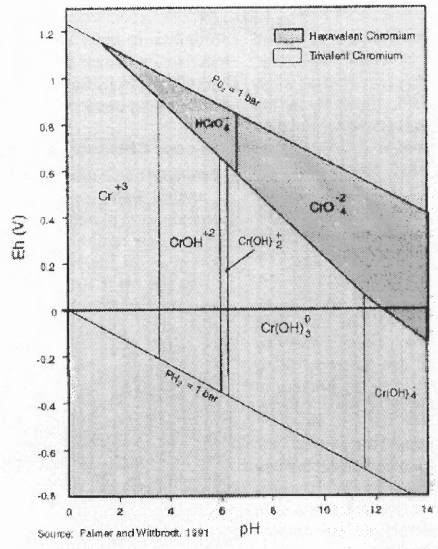

Figure 2.1 Eh-pH Diagram for Chromium (USEPA, 2000).

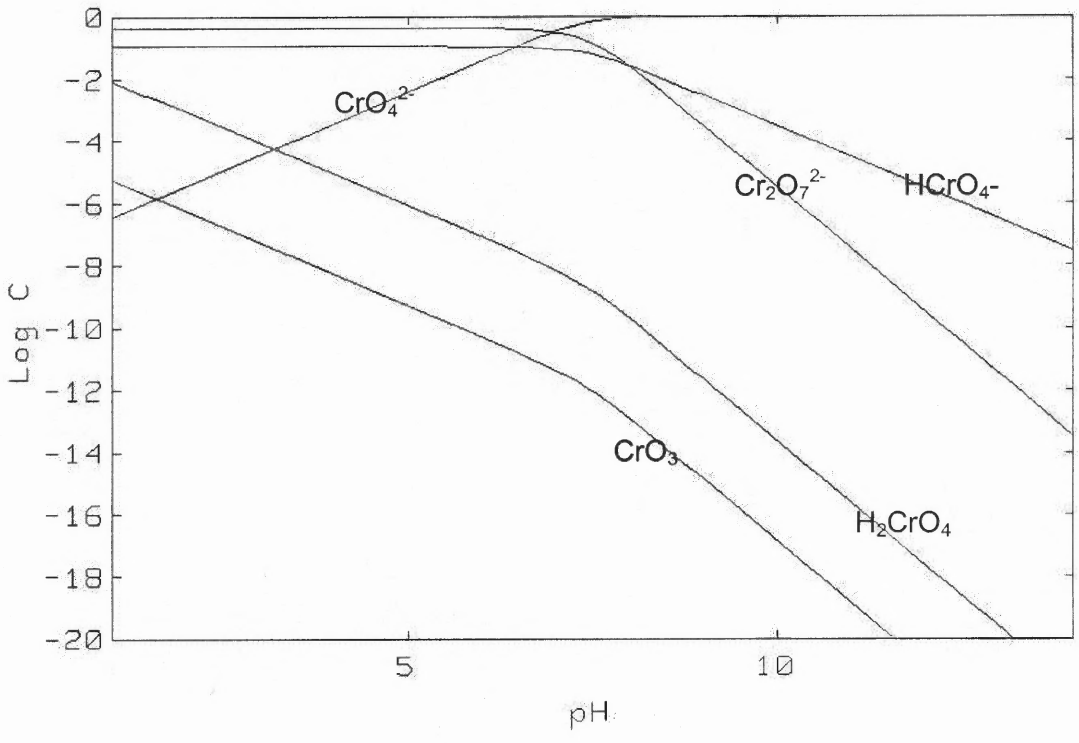

Figure 2.2 Equilibrium Diagram of Cr(VI) as a Function of pH.

For the same redox potential, hexavalent chromium can be oxidized to trivalent chromium, Cr(III), under low pH conditions (pH<4). Hexavalent chromium is more water soluble and more toxic, hence problematic than trivalent chromium. Reducing rate of hexavalent chromium to trivalent chromium depends on pH, redox conditions and chemicals in the environment. The most likely reducing natural sources are oxidizable organic matter (Eary & Rai, 1989), ferrous iron (Burgre & Hug, 1999; Fendorf & Li, 1996; Pagilla & Canter, 1999; Palmer & Wittbrodt, 1991) and manganese oxide (Kožuh et al. 2000; Patterson et al. 1997).

The mobility of hexavalent and trivalent chromium are different. The mobility of hexavalent chromium depends on sorption characteristics of the soil, including clay content, iron oxide content and the amount of organic matter. In soils with metal cations, such as Al^{+}, Ba^{2+}, Pb^{2+}, and Ag^{+}, chromium will precipitate, slowing the mobility (Plus et al, 1994). The migration of hexavalent chromium increases with soil pH. For trivalent chromium, which is less soluble, the mobility is decreased by adsorption to clays and oxides below pH 5. Under anaerobic conditions in deep soil, trivalent chromium forms soluble complexes with NH_3, OH^{-}, Cl^{-}, F^{-}, CN^{-}, SO_4^{2-}, and organic ligands (Eary & Rai, 1989; Jardine et al., 1999). These chromium compounds are more soluble and can be transported by groundwater (Lay & Levina, 1996). In addition, it can also be transported by surface runoff in its soluble or precipitated form. Most of chromium found in natural water are associated with particles and can precipitate. Thus, it is quite common to find chromium compounds in the sediments.

In conclusion, there are many forms of chromium in aqueous and soil. The forms and mobility of chromium strongly depend on environment condition, e.g. redox potential, pH and chemical species in water. Therefore, the speciation and toxicity level of chromium in natural vary at each site.

2.2 Stabilization and Solidification

There are many technologies available to remediate metal contaminated soils, e.g., electrokinetic, vitrification, phytoremediation, soil flushing and immobilization (USEPA, 1989). A summary of these technologies and their applicability are listed in Table 2.1. From the Table, electrokinetic is the most effective and the most expensive technology while the physical separation provides the lowest efficiency and the lowest cost. Solidification/stabilization has advantages in terms of implementation and cost (USEPA, 1995).

The technique used in this research, in-situ stabilization with colloidal silica gel, is classified as a S/S technology. Generally, stabilization is a process where additives are mixed with waste to minimize the rate of contaminant migration from the waste and to reduce the toxicity of the waste.

Table 2.1 Summary of EPA Evaluation Criteria of Remedial Technologies for Soil Sediments, and Sludge (USEPA, 1995)

Remedial Technology	Protection of Human Health and Environment	Effectiveness and Performance		Reduction of Toxicity, Mobility, or Volume	Implementation	Cost /ton
		Long Term	Short Term			
Electrokinetic	Permanently removed of contaminant	Permanent	Air emission	Permanently reduce toxicity	Pilot scale testing is required	Expensive
Vitrification	Good	Reused option for product	Effect from Dust	Reduce volume	Off-gas production	$100-$500
Soil Flushing	Very protective	Excellent removal efficiency	Effect from Dust	Permanently reduce toxicity, reduce volume	Subject to a number of incompatibility and interference	≥ $100
Physical Separation	Can be protective	Excellent removal efficiency	Effect from Dust	Increase Volume	Complex process pilot scale testing is required	$10-$1000
Solidification/ Stabilization	Potentially protective	Limited data	Effect from Dust	Increase Volume	Widely implemented and reliable	$50-$150

Solidification is a process that employs additives by which the nature of waste is altered during the process. Thus, the S/S process may be described as a process by which contaminants are fully or partially bound by an additive or a supporting media, a stabilizer or other modifiers. This can be achieved by mixing or injecting the contaminated waste with an appropriate amount of stabilizer. After mixing or injecting the stabilizer, the mixture forms a solidified matrix. Stabilizer materials used in S/S might be either inorganic or organic. For example, inorganic material may be cement pozzolan or silicate and organic materials may be thermoplastic wax, bitumen (asphalt), gel polymer, polyester, and polysiloxane.

The most common inorganic material used in S/S process is cement-based stabilizer. Portland cement, which is a mixture of calcium, aluminum and iron, is the most popular cement-based stabilizer. During the mixing process, cement reacts with metals to form hydroxides, which are less soluble (USEPA, 1989). However, Vipulanadan & Wang (2000) showed that stabilization of chromium with cement results in the formation of a sparingly soluble complex of calcium chromate ($CaCrO_4$). Pozzolan materials which include fly ash, ground blast furnace slag and cement kilns, are also commonly used for S/S. The primary mechanism of a pozzolanic stabilizer is the physical entrapment of metals in the pozzolan matrix.

Organic stabilizers are also used to remedy metal contaminated soils through thermoplastic and microencapsulation. This process uses organic materials such as bitumen, polyethylene, paraffin, waxes and other polyolefin as thermoplastic or thermosetting resins. The fundamental mechanism of this process is to trap metal waste inside an organic binder. The organic binder is used as a liquid in mixing with metal waste, adding subsequent coats and then hardening. Bitumen is the cheapest and the most commonly used thermoplastic binder. Thermoplastic and microencapsulation

require more energy and more complex equipment than cement-based binders (USEPA, 1995).

Selection of a stabilizer depends on soil conditions and contaminants. The effect of the contaminant and stabilizer's performance should be taken into account in such efforts. Table 2.2 shows the effect of metals on different stabilizers with respect to setting time and durability. According to the table, silica is a suitable stabilizer to treat metals, as metals have no adverse effects on the final performance of the stabilizer.

2.3 Treatment of Soil Using Colloidal Silica

The treatment technique that is considered in this research is "Grouting". Grouting is classified as S/S technique where liquid material is injected in-situ into soil media. The objective of this technique is to increase the soil strength or to create a waste control barrier. The stabilizer used has the ability to penetrate into empty spaces in soils and rock, and later hardening inside the medium resulting in increasing strength and permeability. This technique was first developed in the geotechnical and construction industry in order to build underground structures.

Table 2.2 Effect of Metals Waste to Stabilizers (USEPA, 1991)

Stabilizers	Effect from Metals
Portland Cement Type I	Increase set time and decrease durability
Portland Cement Type II and V	Increase set time and no effect on durability
Bentonite	Decrease durability
Cement-Bentonite	Increase set time and decrease durability
Silicate	No effect on durability
Arcrylaminde	Increase set time

Later, it was applied as a tool to limit the movement of hazardous chemicals in groundwater and soil. Empathetically, the process creates an impermeable barrier to prevent the migration of contaminants.

Grouting techniques have many advantages over other S/S techniques. The primary advantage is that remediation can be performed in-situ by directly injecting binder/stabilizer into contaminated soil. In-situ performance indicates that less labor and energy is required than any off-site treatment that relies on excavation, transportation and disposition of the treated material (USEPA, 1997).

In the past, several studies were conducted using cement-base grouting as a barrier. As discussed earlier, chromium affects the performance of cement-base stabilizers (USEPA, 1997). Thus, an alternative stabilizer was sought to treat chromium contaminated soils. Chemicals that have low viscosity and that can be injected easily were considered. It was found that a water-soluble polymer, a crosslinking agent or a destabilized colloidal silica solution can be used. Allan & Kukacka (1994), researchers at Brookhaven National Laboratory, performed an in-situ experiment using the chemical grouting technique. The purpose of their study was to prevent the migration of chromium from a landfill. Chemical barriers were created by injecting chemicals such as superplasticizer cement and silica fume into soil. They found that the superplasticizers created an effective barrier to control chromium migration into fine-grained soils. The superplasticizers also provided better performance compared to cement. Later, this technology was successfully applied in-situ to a mixed waste landfill site at Sandia National Laboratory, New Mexico.

Colloidal silica (CS) is an alternative stabilizer that has shown to increase soil strength and reduce permeability. It is able to enhance strength of the medium after several months following injection (Watanabe, Okumura, Ando & all of Funabashi, Japan, 1987). Immersed samples in water reported a continuous strength gain for one

year (Persoff et al., 1999). Yonekura and Miwa (1993) confirmed it to be a permanent stabilizer. The conclusions based on the long term tests of colloidal silica were that it demonstrated excellent properties of strength, low syneresis (the ability to retain the original shape) and high injection permeability up to 1,200 days. They also found that after about five years, the stabilized sand with colloidal silica was impermeable and stable. The final hydraulic conductivity of treated soils was in the range of 10^{-7} to 10^{-8} cm/sec (Durmusoglu & Corapcioglu, 2000; Noll et al., 1992; Persoff et al., 1995; Persoff et al., 1998; Persoff & Apps, 1999; Zaluski et al., 2001).

Colloidal silica has advantages over other stabilizers because of low viscosity, which allows it to easily penetrate into void spaces between fine-grained soils, and the large surface area increases the possibility of adsorbing metals onto its surface. This material was used in the oil reservoir system to enhance oil recovery by blocking the flow in porous media, later it was introduced to the environmental field. Du Pont (Noll et al., 1992) pioneered the application of colloidal silica grouting for the remediation of contaminated soils. They claimed that this stabilization technology provided three levels of protection. First, it prevents potential leaching of fluids with metals through the gel mass. Second, the amount of leachable metals is reduced in treated samples when compared to untreated samples. Finally, the colloidal silica gel itself showed a high affinity for the adsorption of metals from solution. They simulated a low permeability barrier model in a sand box, and concluded that colloidal silica is able to form a low permeable barrier due to its low viscosity.

The application of colloidal silica grouting technique in controlling the migration of waste was thoroughly studied by researchers from Lawrence Berkeley National Laboratory. They named the technology "Viscous Liquid Barrier". Over a period of eight years, DOE invested $12 million in designing, testing, and implementing this technology. The work was supported originally by CERCLA action at the Savannah River Site (SRS)

Retention Basin, 281-3H (Pearlman, 1999). A series of work including laboratory experiments and numerical studies were published. Initially, the possibility of using colloidal silica in controlling waste and the effect of soil content to the gel property was investigated. Numerical analysis was also performed. Data for the behavior of colloidal silica in soil, used in the calculation was obtained from a series of experiments conducted by Finsterle et al. (1994). They showed that the saturation within the permeability of solidified soil reduces from $8x10^{-11}$ to $1x10^{-13}$ m^2 which is sufficient enough to slow down the groundwater flow. Then, another study of using colloidal silica as an injectable barrier was reported by the same group (Persoff et al., 1995). In this study the injection experiments were performed in the laboratory. Later, the viscous liquid barrier application was scaled up and demonstrated at SRS to retain nuclear isotopes, ^{137}Cs, ^{90}Sr and ^{238}Cu (Moridis et al, 1996; Moridis et. al., 1996).

Moridis et al. (1997) physically and visually inspected the results. Figure 2.3 shows excavated colloidal silica grout plume from direct injection. From this test, it was reported that the permeability could be reduced from 10^{-5} to less than 10^{-8} cm/s after injection. Colloidal silica injection in SRS was scheduled to begin on September 23rd, 1996. It was estimated that 2,350 tons of colloidal silica would be required to fully isolate the basin (Worldwide Performance and Innovative, 1996). Unfortunately, a different technology, groundwater treatment, was chosen for the SRS at the last minute for political reasons (Westinghouse Savannah River Company, 2002). However, the potential use of viscous liquid barrier as a treatment technology still exits.

Apps et al. (1998) continued their study to produce a design guide for the viscous liquid barrier to control migration of waste. Subsequently, the LBNL staff assisted in designing and establishing another demonstration at Brookhaven National Laboratory.

Figure 2.3 Colloidal Silica Grouted Soil (Moridis et al. 1997).

A colloidal silica waste barrier was chosen to apply around the underground LINAC isotope producer facility to slow down the movement of isotopes in soil (Heisher et al., 1998). Further experiments were performed and numerical studies were made for the design of waste barriers for this site. The sand solidification process was simulated (Zulaski et al., 2000(1); Zulaski et al., 2000(2)). The injection was designed to deliver the stabilizer solution into the activation zone ensuring the complete encapsulation of the contaminated soil. Column injection tests were conducted to select the colloidal silica and additional sand tank tests were conducted to select the injection diameter. Results indicated that the test panel, and thus, the colloidal silica barrier, met the BNL performance goal of less than 4 cm/yr or 0.22 m^3/yr of flux through the barrier (North-Abbott et al., 2001).

Gellagher (2000) and Gellagher & Mitchell (2001) proposed a slightly different injection process by slowly applying stabilizing materials at the edge of site and delivering the stabilizer to the target location using the natural groundwater flow called

"Passive Site Remediation". Colloidal silica was considered as a potential stabilizer because it has long, controllable gel time and low viscosity, thus, it can flow into a liquefiable formation slowly over a long period of time. This study was performed to physically and numerically find the possibility of using this new technology with colloidal silica (Gellagher, 2000).

In addition, Apps & Persoff (1998) and Persoff & Apps (1999) used colloidal silica grout to control the contamination of non-aqueous phase liquids, NAPLs in soil. The hydraulic conductivity and unconfined compressive strength of soil after grouting was evaluated and found that it is sufficient to prevent NAPLs migration. Afterward, Durmusoglu & Corapcioglu (2000) expanded the above study to a small-scale demonstration and showed that colloidal silica stabilizer works well in preventing the migration of TCE or gasoline.

In the demonstration study at Brookhaven National Laboratory, colloidal silica grout was applied around the underground isotope producer to slow down the movement of isotopes in soil. The cost of this pilot scale test was $593,000 for treating 85 m^3 of soil, which included design and planning (Pearlman, 1999). Due to the low cost of colloidal silica used at this site, NYACOL DP5110 which costs $0.68/lb (Matthew C. Reed, Akzo Nobel/Eka Noble Chemicals Inc. personal communication), the viscous liquid barrier proved to be a cost-effective alternative when compared with excavation and disposal. Pearlman (1999) compared the cost of this technology to other technology where the excavation and disposal was estimated to cost $2,122,000. Construction of a slurry wall under the same conditions would cost approximately $91,000. Gellagher & Mitchell (2001) estimated that the operation cost for Passive Site Remediation using colloidal silica would be in the range of $120 to $180 per m^3 of soil.

2.4 Colloidal Silica

2.4.1 Chemistry of Colloidal Silica

Colloidal silica is known as a stable dispersion of discrete amorphous particles of silicon dioxide (SiO_2) in a liquid, typically water. The appearance of colloidal silica depends on particle size and concentration. It varies from opalescent to milky in color. If the particles are smaller than about 7 nm in diameter, colloidal silica is almost as clear as water. From 10 to 30 nm in diameter, it's appearance is opalescent or translucent, and above 50 nm in diameter it is white and milky (ESTL TechTra Inc., 2001). Colloidal silica forms long chains in solutions containing high concentrations of silica. This creates a reactive high surface area material with many practical applications. Varieties of colloidal silica product are widely used in many applications, including the use of coating material for electrical devices, the use of thin film for improving the strength and water resistance of substrate, refractory, investment casting, wafer polishing, anti skid, clarification, catalysts and gels (Iler, 1989). Colloidal silica application is based on its chemical and physical properties such as particle size, high specific surface area with good blinding ability, stability towards gelling and setting, and surface properties.

A variety of colloidal silica products are now available from several companies such as Bayer, Du Pont, Eka Noble Chemical, Nissan, and etc. (Gerhartz & Elvers, 1993). The selection of colloidal silica depends on the application. The properties to be considered are specific surface area, surface charge, pH, particle size, concentration, viscosity and density. Generally, specific surface area of colloidal silica ranges from 50 to 270 m^2/gm, where the surface charge can be cationic, anionic or non-ionic. Colloidal silica particle size ranges from 3 to 100 nm and pH ranges from 4 to 12. Normally commercial colloidal silica contains SiO_2 15 to 50% by weight. The larger the particle size and the lower concentration of colloidal silica, yield the lower surface area. It is

sparingly soluble in water, 100-150 mg/l at 25°C between pH ranges 2 and 8 (Gerhartz & Elvers, 1993; Dean, 1992). Figure 2.4 shows equilibrium diagram of silica as a function of pH, ionic strength = 10^{-3} M, P_{CO2}= $10^{-3.5}$M, SiO_2 = 1.0 M calculated by MINEQL+ V4.5.

Commercial colloidal silica can be destabilized chemically. The destabilization of liquid colloidal silica forming gel network is called "Gelation". Gelation is a process where silica particles link together in branched chains. During gelation, colloidal silica appears to remain homogeneous and often remains clear as it becomes viscous and sets to a firm gel. After the gel is formed, colloidal silica becomes more viscous and rigid by a coherent network of particles which retain pore liquid by capillary action.

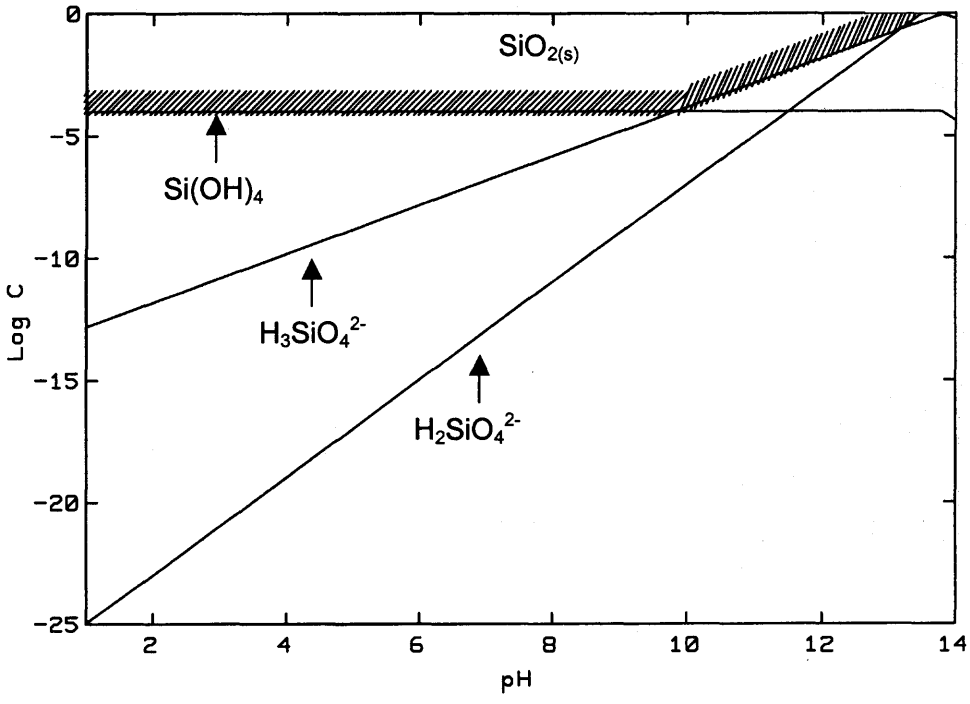

Figure 2.4 Equilibrium Diagram of Silica as a Function of pH.

2.4.2 Structure of Colloidal Silica

Colloidal silica consists of inorganic polymer, $(SiO_2)_n$, particles (Iler, 1989). Each silicon atom is covalently bonded to four oxygen atoms in a tetrahedral arrangement. Each silica atom adheres to form either a siloxane, Si-O-Si, with oxygen or silanol, Si-O-H, with hydrogen. Colloidal silica is synthesized by making a solution of $Si(OH)_4$ at a concentration greater than saturation concentration of amorphous silica (100-200 mg/l). Since the concentration is high, the reactions occur toward the minimizing energy, increasing the formation of external silanol linkage, forming more adhesion particles with internal siloxane groups. Silica particles attach to other silica particles in order to maintain stable conditions, forming species with higher molecular weights. The reactions continue leading to the formation of long chain structures as shown in Figure 2.5.

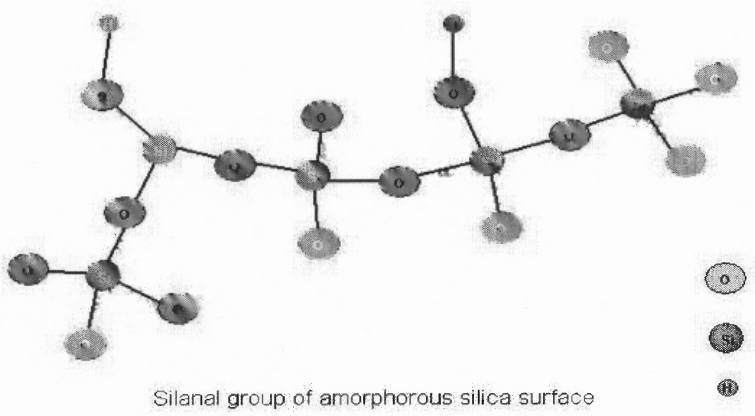

Figure 2.5 Structure of Silica Particles with Siloxane linkage and Silanol Groups. (Gerhartz & Elvers, 1993)

After the silica structure is formed, the particles condense forming a high molecular weight ring as shown in Figure 2.6. It then randomly arranges to form complex structures as shown in Figure 2.7. These complex structures serve as nuclei of three-dimensional molecules while the growth of particles occur. Because of the solubility differences, small particles will dissolve and deposit on larger particles, growing in size. When it becomes stable, the growth stops. The final structure is generally spherical with a high molecular weight and high surface area.

There are two possibilities of particle growth, growth in size as discussed above and growth in three-dimensional gel network which is discussed as follows. Impacts to colloidal silica size and the growth direction are shown in Figure 2.8. Commercial colloidal silica growth is controlled to form large stable particles.

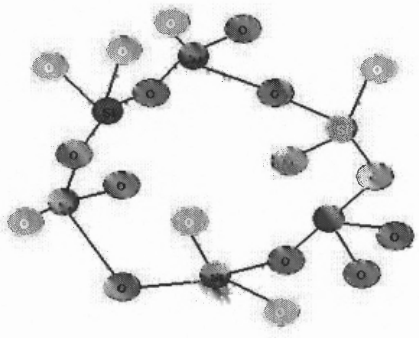

Figure 2.6 The Silica Particles Ring Structure.
(Gerhartz & Elvers, 1993)

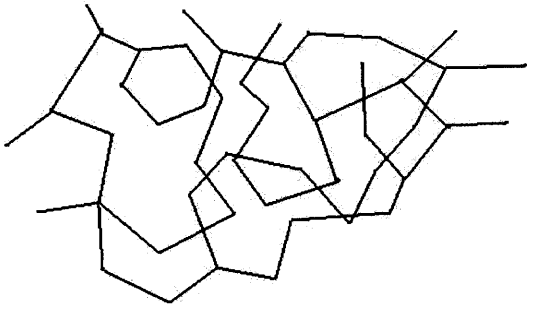

Complex ring structure in SiO2 Polymer

Figure 2.7 Complex Ring Structures of Silica Particles.
(Gerhartz & Elvers, 1993)

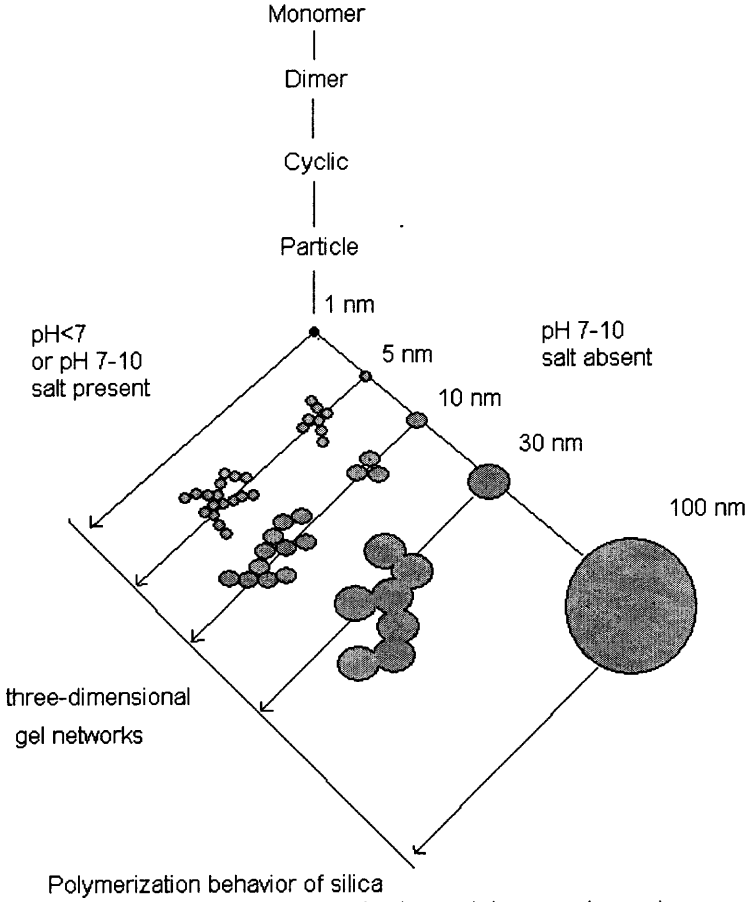

Polymerization behavior of silica
In basic solution particle grow in size and decrease in number
In acid solution or present of salt, particle growth into the network and form gel

Figure 2.8 Synthesis Route of Colloidal Silica (Iler, 1989).

Adjusting pH and adding salt can easily control the development direction and size of colloidal silica formed. For example, above pH 7, silica particles tend to grow larger in size with radius of about 100 nm. At lower pH, silica particles attach to others particles forming chains and ultimately three-dimensional gel networks.

After colloidal silica becomes stable, colloidal silica can retain its colloidal stability for many years. It was reported that colloidal silica remained stable even after aging for 25 years at room temperature (Iler, 1989). The possibility of stable colloidal silica may occur by either electrostability or steric stabilization. Eletrostatic forces due to the charge on particles keep them apart. Steric forces occur due to a layer of inert material on silanol surface that prevents the direct contact of silanol groups (Gerhartz & Elvers, 1993).

The stability of colloidal silica can also be explained in terms of minimizing the energy in the system. In nature, stable silica forms exist in variety status: polymorphic crystalline form, amorphous modification and liquid state. The main crystalline silica forms at atmospheric pressure are quartz, stable below 870°C, tridymite, stable from about 870 to 1470°C, and cristabalite, stable from about 1470°C to the melting point at about 1723°C. The most common silica form is quartz, which is found in nature as sand. The crystallization does not occur in colloidal silica solution because the solid phase grows with no particular order to form the structure. For simple compounds, the ions or molecules rapidly rearrange to satisfy minimum energy requirement. In the case of silica, the energy difference between the amorphous and crystalline state is small. Furthermore, a high energy of activation is required to break siloxane bond to permit the rearrangement. As a result, colloidal silica can preserve its stability for long time (Patterson, 1992; Lekkerkerker et al., 1995).

2.4.3 Aggregation of Colloidal Silica

Aggregation is a process that causes colloidal silica particles to link and therefore grow. Aggregation occurs with the instability of colloidal silica. There are three types of aggregation: gelation, coagulation and flocculation. Gelation is a process where silica particles link together in branched chains. After colloidal silica particles form a gel, it becomes viscous and rigid. Coagulation is a process where the particles come together in close-packed clumps. After the coagulation, the concentration of silica is much greater than original colloidal silica, causing precipitation. Flocculation process involves the use of flocculating agents. Particles link together by bridges of flocculating agent, creating sufficient long chain structures (Figure 2.9).

During the stabilization, the reaction is directed toward the gelation. Thus, only gelation will be discussed herein. The basic step in gelation is the collision of two silica particles with sufficiently low charge on the surface that come into contact such that siloxane bonds are formed (Iler, 1989):

$$\equiv Si\text{-}OH + O\text{-}Si\equiv = \equiv Si\text{-}O\text{-}Si\equiv + OH$$

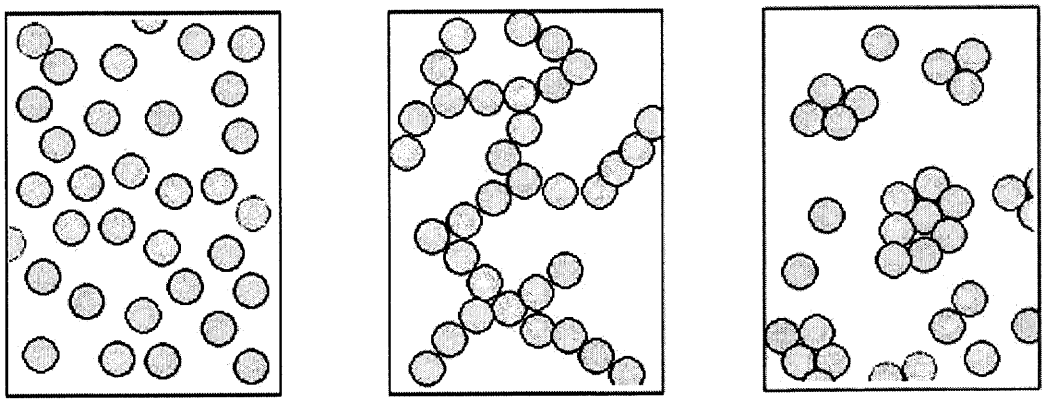

Figure 2.9 Aggregation of Colloidal Silica (Iler, 1989).

The gelation can be explained by double layer theory as follows. Essentially, the negatively charge particles are surrounded by an electrical double layer of cations. When the ionic strength of the colloid is increased, the double layer is depressed allowing the particles to approach each other to form siloxane linkage. This creates an irreversible silica gel network as shown in Figure 2.10 (Heiney et al., 2000). Formation of this linkage requires the catalytic action of hydroxyl ions and ionic strength of solution, which means that gelation occurs at high pH and in the presence of a salt. Figure 2.11 shows the effect of pH on colloidal silica-water system. Figure 2.11 illustrates that the gelation starts at a pH greater than 6. Above pH 6, gelation rate increases with pH. For pH value between 8 to10, colloidal silica is generally stable in the absence of salt. In addition to pH, gelation rate also depends on particle size, surface area, and concentration of colloidal silica.

After salt ions are added to solution, the surface charges are neutralized by soluble salts that ionize and reduce the size of the double layer (Patterson, 1992). Salt ions may also act as a bridge between two or more silica particles creating a group of silica compound (Iler, 1989). Conservation of gel volume may be a consequence of some mechanistic constraint on network growth, or the volume itself may constitute a thermodynamic boundary conditions (Heiney et al, 2000).

Since controlling of colloidal silica aggregation by adjusting pH and adding salt is practical, this method is applied in the use of colloidal silica in grouting techniques. In the grouting application, before injecting it into soil, pH will be adjusted and salt (e.g., sodium chloride or calcium chloride) will be added to modify colloidal silica solution. The aggregation occurs while the solution is in the soil matrix creating the gel network resulting in new soil properties such as porosity, permeability and hydraulic conductivity (Finsterle et al. 1996).

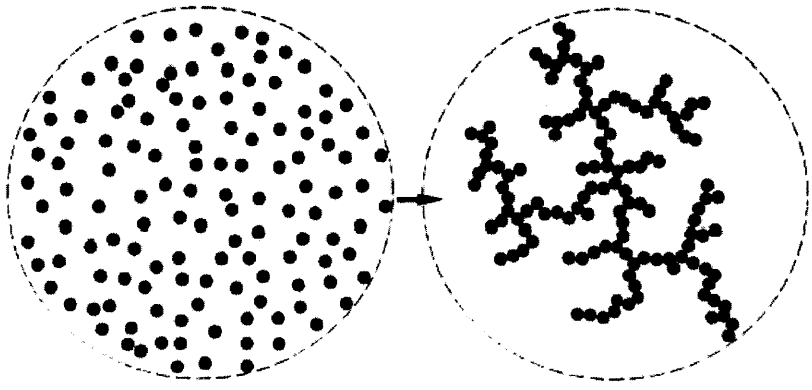

Figure 2.10 Gelation of Colloidal Silica (Poon & Haw, 1997).

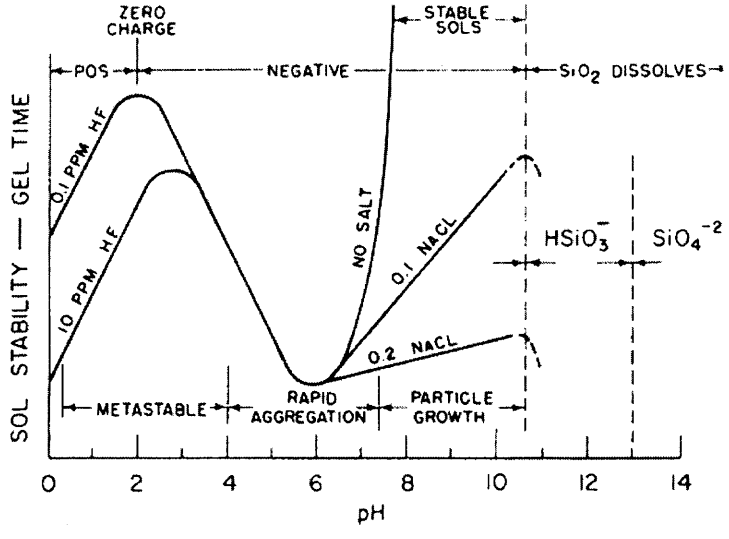

Figure 2.11 Effect of pH on Colloidal Silica-Water System (Patterson, 1992).

2.5 Adsorption of Chromium to Silica

Generally, there is no chemical reaction between chromium and silica. However, silica is able to attract metals onto its surface by physical adsorption (Fendorf, 1992; Mikolaichuk et al., 1993; Sattar & Francis, 1995; Weckhuysen et al., 1996). During the adsorption, chromium is bonded directly onto the silica surface by creating a metal oxide layer comprised of supported clusters (Mikolaichuk et al., 1993).

The adsorption capacity of chromium on silica oxide depends on environmental conditions (hydrated, dehydrated, oxidized, and reduced) and on the type and composition of the support (Csobán et al., 1998; Nakano et al., 2001). Chromium ions on surfaces of silica oxides process a wide variability in oxidation states, coordination and molecular structure (Weckhuysen et al., 1996). The adsorption capacity of ions in gel depends on silica gels pore size. Tran et al. (1999) showed that the adsorption process of heavy metals on silica gel comprise two steps: a rapid initial step on the external site followed by a slower one. The fast step is a reversible reaction between the bulk aqueous phase and external surface site. The slow step is an adsorbed at the surface slowly diffuses in the micropore of the oxide particle (Axe & Anderson, 1995; Ruthven, 1991).

Tran et al. (1999) reported that the adsorption of by silica the ion-exchange reaction on the silica gel surface is accomplished through the substitution of proton of the surface silanol group by the metal ions from solution as follows:

$$x(\equiv \text{Si-OH}) + M^{n+} \leftrightarrow M(\equiv \text{Si-O})_x^{(n-x)+} + xH^+$$

For trivalent chromium, the complexation is described by (Csobán & Poó.,1999):

$$\text{Si-OH} + Cr^{3+} + H_2O \leftrightarrow \text{Si-OCrOH}^+ + 2H^+$$

Under hydrate conditions, the adsorption of chromium strongly depends on pH. At low chromium loading, the species on silica surface are chromate and dichromate. Increasing of chromium loading results in the formation of polychromates. Berka & Banyái (2000) and Csobán & Poó (1999) showed that the adsorption of trivalent chromium as a function of pH increase in the pH higher than 3 as shown in Figure 2.12. Figure 2.12 shows the distribution of Cr^{3+} ions among dissolved, sorbed, and precipitated forms in the presence of silica gel adsorbent (silica gel 10 g/L, $[Cr^{3+}]_T$ = $5x10^{-4}$ M, KNO_3 = 0:1 M.). The dashed line shows the precipitate ($Cr(OH)_{3s}$) in the blank solution.

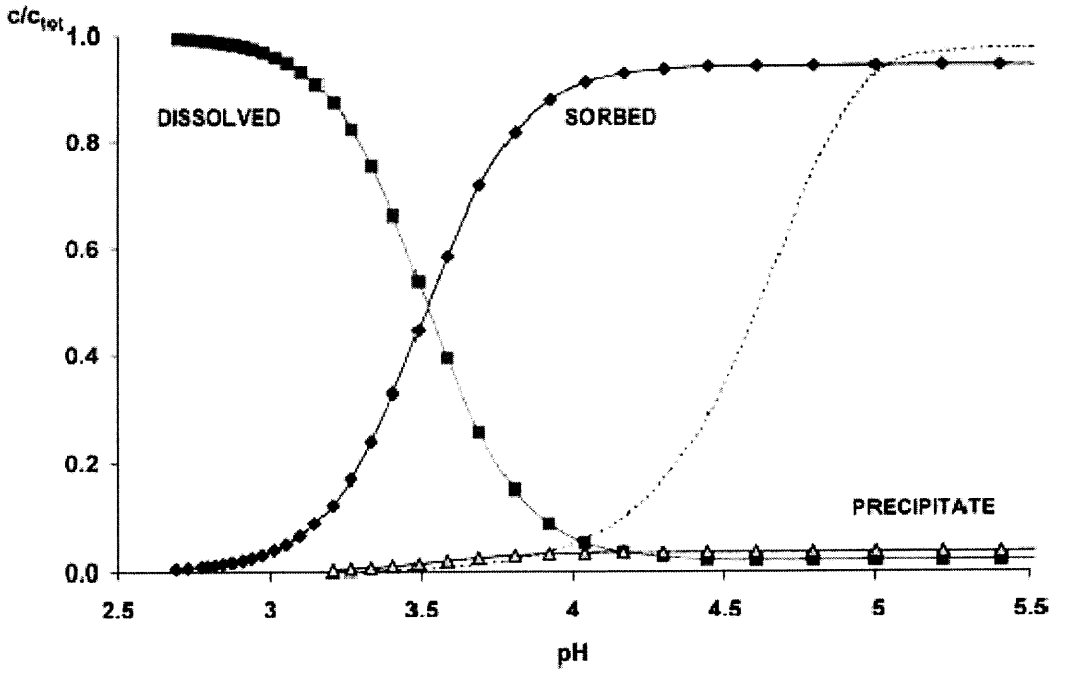

Figure 2.12 The Distribution of Cr^{3+} Ions in the Presence of Silica Gel Adsorbent. (Berka and Banyái 2000).

When trivalent chromium is in contact with silica surface, a three-dimensional growth mechanism occurs forming an inner-sphere monodentate surface complex on silica. Silanol groups on silica surface are replaced by monovalent hydrolysis species of metal cations where a γ-COOH-type structure formed (Tran et al., 1999). The structure formed is shown in Figure 2.13.

Fendorf (1994) observed a Si-Cr bond of 3.39 Å; a linear Cr-O-Si arrangement would result in a distance of 3.59 Å, and a bond angle of 150°. Monodentate coordination with a bond angle of 150° implies that reactive surface O atoms are singly coordinated by Si atom. As surface coverage increases, nucleation grows with a γ-COOH-type structure and expands over the surface before expands outward (away from the surface). This is similar to the precipitate forms crystalline clustered structures, which extrude away from the surface (Fendorf, 1992; Fendorf et al., 1994).

In conclusion, chromium ions can adsorb onto silica surface with variety of oxidation state and molecular structure. The adsorption rate and chromium species depends on type of adsorbent surface, pH and concentration of chromium in solution.

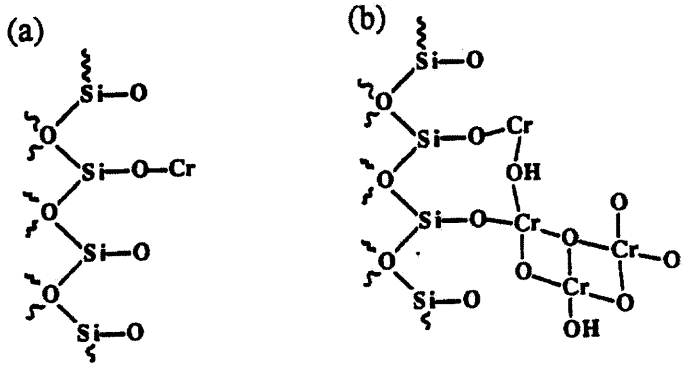

Figure 2.13 The Structure of Cr(III) on Silica Surface:
(a) The Monodentate Complexation of Cr(III) on Silica
(b) The Nucleation and Distorted γ-COOH-type Structure.
(Fendorf 1992)

2.5 Summary of Literature Survey

The literature survey presented above invoked several queries that are the basis for this study. The literature study resulted in several methods for treating contaminated soils using colloidal silica. The direct in-situ treatment was successfully applied. Colloidal silica binding ability is proven to be sufficient to prevent migration of chromium molecules. In addition, silica could be used as a waste barrier preventing the transport of waste via ground water. Colloidal silica possesses attractive properties that make it excellent for remediation of chromium contaminated soils by direct injection. For example, it is nontoxic, stable for long period of time and able to increase soil strength. Moreover, the unit cost of colloidal silica is lower when compared to other stabilizers.

In short, colloidal silica has strong potential to be a stabilizer. However, there are not many conclusive studies performed to evaluate the effectiveness of colloidal silica in treatment of chromium contaminated soils. Therefore, this research is a comprehensive theoretical study of silica as a stabilizer to treat chromium contaminated soils.

CHAPTER 3

OBJECTIVES

Colloidal silica as a stabilizer/binder works due to two distinct mechanisms. First, the solidification gel mass decreases soil permeability and prevents potential leaching from contaminated soils (Noll et al., 1992). Second, the adsorption of chromium onto silica surfaces decreases the possibility of chromium migration into groundwater system (Noll et al., 1992; Fendrof, 1992). In order to understand these two mechanisms and potential uses of colloidal silica as a grouting technique to treat chromium contaminated soils, the immobilization mechanisms were extensively studied. The study can be divided into two major parts, the microscopic behavior of colloidal silica during the injection process and the transportation of chromium through silica gel.

In the first part, microscopic behavior of colloidal silica in anisotropic granular media was studied by numerically solving Navier-Strokes Equation. This part explains the short term effectiveness of the technology. In the second part of the study, the long term effectiveness of the technology was studied using the diffusion of chromium through colloidal silica gel. In order to model the diffusion process, the diffusion coefficient of chromium in colloidal silica gel is needed. However, the numerical value of the parameter is not available in the literature. Hence, an experiment was designed and conducted to evaluate the diffusion coefficient of chromium in colloidal silica gel. The experimental design was based on a new optical technique. Hence, the overall objective of this study can be divided into three parts as described below.

3.1 Microscopic Behavior of Colloidal Silica Stabilizer in Anisotropic Granular Media

The main objective of this section of the study is to understand the stabilization mechanisms during gelation period. The stabilization technology of interest is the grouting technique where the stabilizer is directly injected into a soil medium. The gelation process was studied immediately after injecting the stabilizer mixture into the soil matrix.

The behavior of colloidal silica mixture during the process was studied using a microscopic model for fluid flow through soil. Using the model and the change of viscosity of colloidal silica mixture with time, the movement of the colloidal silica in the soil medium with time and the effect of soil geometry to gelation were simulated.

3.2 Measurement of Diffusion Coefficient

Since the current measuring techniques for determining the diffusion coefficient are complicated and time-consuming, a digital photography method that utilizes advantage of computer graphic technology was proposed to determine the diffusion and partition coefficients of chromium in colloidal silica gel.

The diffusion and partition coefficients of chromium in colloidal silica gel depend on many factors. A number of study have reported that the major factors that influent the diffusion of chromium in colloidal silica gel are silica content in gel, gelation time and initial chemical concentration (Kim, 1999; Lakatos & Lakatos-Szabó, 1998; Moridis et al., 1998). Hence, an experimental program was conducted to investigate diffusion and partition coefficients of chromium in the gel at varying: 1) silica concentrations, 2) initial chromium concentration and 3) gelation times.

3.3 Transport of Chromium in Colloidal Silica Gel

The movement of chromium through silica gel was mathematically modeled to evaluate the long term effective of the technology. The model was based on molecular transportation governed by Fick's law. The diffusion and partition coefficients for the model were obtained from experiments as described in previous section. The worse case scenario for diffusion in an infinite gel media was considered in this simulation.

CHAPTER 4

MICROSCOPIC BEHAVIOR OF COLLOIDAL SILICA STABILIZER IN ANISOTROPIC GRANULAR MEDIA

This chapter provides an explanation to the stabilization mechanisms of colloidal silica solution during stabilization using a numerical solution of the Navier-Stokes equation. The stabilization technology of interest is the "grouting technique" which injects stabilizer directly into the soil media. The colloidal silica mixture performance during the period of injection was simulated using a microscopic model of fluid flow through soil. The numerical equations were solved for the velocity and pressure distributions in pore space. The change of the solution viscosity with time was incorporated as a variable parameter resulting in the variation of velocity fields of colloidal silica in soil medium with time. Lastly, these data were interpreted and physically explained.

In this chapter, the review of previous models, numerical modeling of colloidal silica stabilization and results are also explained.

4.1 Review of Pervious Grout Modeling Studies

There are several numerical model studies describing the simulation of in-situ gelation, mostly applied for oil recovery (Kim, 1999). These models were based on application of mass balance and gelation. The mass balance was used to determine the movement of the grout solution where the gelation was used to determine the solidification rate. When grout mixture in the pore space is solidified, pore size is reduced modifying soil properties, such as, porosity, permeability, relative permeability, capillary pressure, and initial liquid saturation. The grout mass fraction in liquid phase was considered a major

factor to determine the change in porosity, rate of solidification and rate of transport. Mass balance considered factor that contribute to the in-situ gelation, such as injection pressure, hydraulic conductivity and physical properties of soil. The reduction of permeability was due to the blocking of pores with the increase of gel mass in the soil pores. Gelation considered that gel formation is caused by the aggregation and cross-linking of a polymer (Iler, 1989). The adsorption/retention of chemicals in a gel mass is described by either chemical equilibrium or kinetics (Kim, 1999).

Persoff et al. (1995), Finsterle (1998), Kim (1999) and Zulaski et al. (2000) simulated in-situ barrier formation due to injection colloidal silica solution. Associated with these studies a number of experiments were also performed to investigate the performance of gel barrier. A brief description of these modeling studies is given in the following section.

4.1.1 DuPont Study

Noll et al. (1991) developed a model to describe the soil solidification through direct injection of colloidal silica, LUDOX®. The model combined groundwater flow and colloidal silica transport. They demonstrated validity of the technology by bench scale injection of LUDOX® in sandbox/mesocosm containing 10 mg/kg chromium. Results showed that LUDOX® created a waste barrier in the subsurface and was applicable in preventing chromium migration.

4.1.2 Lawrence Berkeley National Laboratory (LBNL) Study

Apps et al. (1998) proposed the "Injectable Barrier" for the in-situ treatment of contaminated soils. They developed a numerical model to simulate the flow and the gelation process with the aim of predicting both the location of the grout plume and the properties of the new porous medium.

When colloidal silica solution is injected into unsaturated soils, the grout plume spreads under gravity and capillary forces (Finsterle et al., 1998). The viscosity of colloidal silica increases with time and finally solidifies. This caused the soil to be partially saturated. Persoff et al. (1995) used "Gel Time Curve", the relationship between viscosity and time, "Mixing Rule", the change of colloidal silica concentration due to the dilution of groundwater, and "Solidification Model", the indicator of the point where the colloidal silica has become solidified, to explain the gelation mixing and the solidification process.

The movement of colloidal silica was numerically predicted by using a computer code, TOUGH2, which was designed for use in geothermal reservoir engineering. This software can simulate non-isothermal flows of multi-component, multiphase fluids in porous and fractured media. Results showed that reduction of porosity and permeability is a function of final silica content in solution, and multiple injections were required to achieve a complete filling of pore spaces (Finsterle et al., 1996, 1998).

Moridis (1994) and Persoff et al. (1995) found that soil properties affect the gelation rate. They proposed several methods to prevent the uncontrollable gelation during the process. Finally the problem was solved by introducing a new type of colloidal silica, NYACOL DP5110, surface-modified colloidal silica by isomorphic substitution of aluminum, which caused a permanent (not pH-dependent) surface charge (Persoff et al., 1999). Thus, with this colloidal silica, there was no contribution from soil properties to solidification of gel.

After colloidal silica is injected, it moves freely through void space and starts to solidify. During the time it travels, the solution is mixing with water reducing the silica content. After a while, the solidified gel fills the soil pore, decreases the soil pore size and reduces the soil pore water. The silica content then needs to be recalculated,

results in a concentration profile around the injection port as shown in Figure 4.1, the simulation result at 102 Kpa, four hours after the injection (Finsterle, 1994).

4.1.3 Brookhaven National Laboratory (BNL) Study

BNL researchers performed a simulation of colloidal silica injection based on real site conditions (Zulaski et al., 2000). This simulation of the flow was performed using PORFLOW™, software developed by Analytic & Computational Research, Inc. PORFLOW™ is a comprehensive computer program for simulation of transient or steady state flow, heat, salinity and mass transport in multi-phase, variably saturated, porous or fractured media with dynamic phase change. The results simulated using PORFLOW™ showed that treated soil significantly altered water retention, making the new medium less porous. The flow pattern indicated that the water moved around the solidified medium (Zulaski et al., 2001).

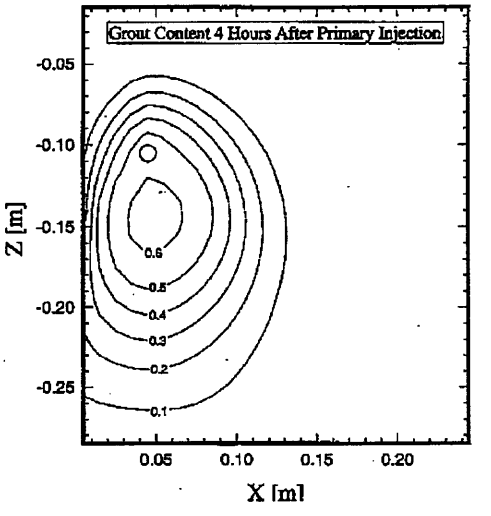

Figure 4.1 The Colloidal Silica Concentration Gradient around the Injection Port. (Finstler, 1994)

BNL researchers performed a series of laboratory tests to select the best colloidal silica and the best injection method. Column injection tests were conducted to assess the effect of colloidal silica variant and injection diameters (Manchester et al., 2001). They found that NP6010 colloidal silica from Eka Chemical Inc. provided the best results under various soil conditions, and both types of injection created grout bulbs with a core having a saturated hydraulic conductivity less than 10^{-6} cm/sec.

The simulation resulting from a grout plume is illustrated in Figure 4.2 and shows that the series injection around the waste created grout bulbs that completely covered the waste area. The colloidal silica barrier met the BNL performance goal of less than 4 cm/yr or 0.22 m^3/yr of flux through the barrier (North-Abbott et al., 2001).

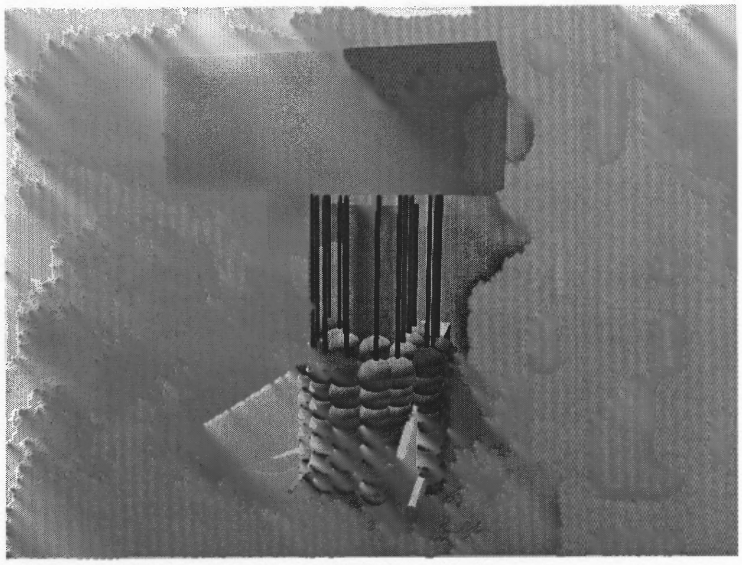

Figure 4.2 The Simulation Results for Colloidal Silica Barrier (North-Abbott et al., 2001).

4.1.4 Virginia Polytechnic Institute and State University (VPI) Study

At VPI, "Passive site Remediation" was studied employing the concept of slow injection of stabilizing materials up gradient of the contaminant plume (Gallagher, 2000; Gallagher & Mitchell, 2001). The simulation was performed using computer codes MODFLOW, MODPATH and MT3DMS. A combination of advection and dispersion was used to determine the movement of colloidal silica solution during the slow injection process. The results showed the non-uniformed colloidal silica concentrations. A contour plot of typical stabilizer concentration for one simulation with a uniform hydraulic conductivity of 0.05 cm/s and a hydraulic gradient of 0.005 are shown in Figures 4.3 and 4.4.

4.1.5 Texas A&M University Study

A simulation was performed to demonstrate the gel barrier formation by injecting colloidal silica solution into the subsurface. Several in-situ design factors were evaluated. The model tests were compared to experimental results. The colloidal silica used in this research was NYACOL 1440 from Eka Chemical Inc.

The simulation was based on the existing mass transport, flow and gelation models. In this model, the region consisting of the crosslinked colloidal silica particles and the water is classified as a gel phase, and the rest of the gelling solution is classified as a liquid phase. The reaction occurred in the direction of reducing the liquid phase and increasing the gel phase. The effect of pore water to gelation time was calibrated using the experimental results. The gel mixture viscosity was estimated from the relationship between the gel mixture and the phase volume fraction, which was determined by solving the mass transport of gel phase. The simulation result showed that the subsurface barrier construction by injecting colloidal silica solution was effective (Kim, 1999).

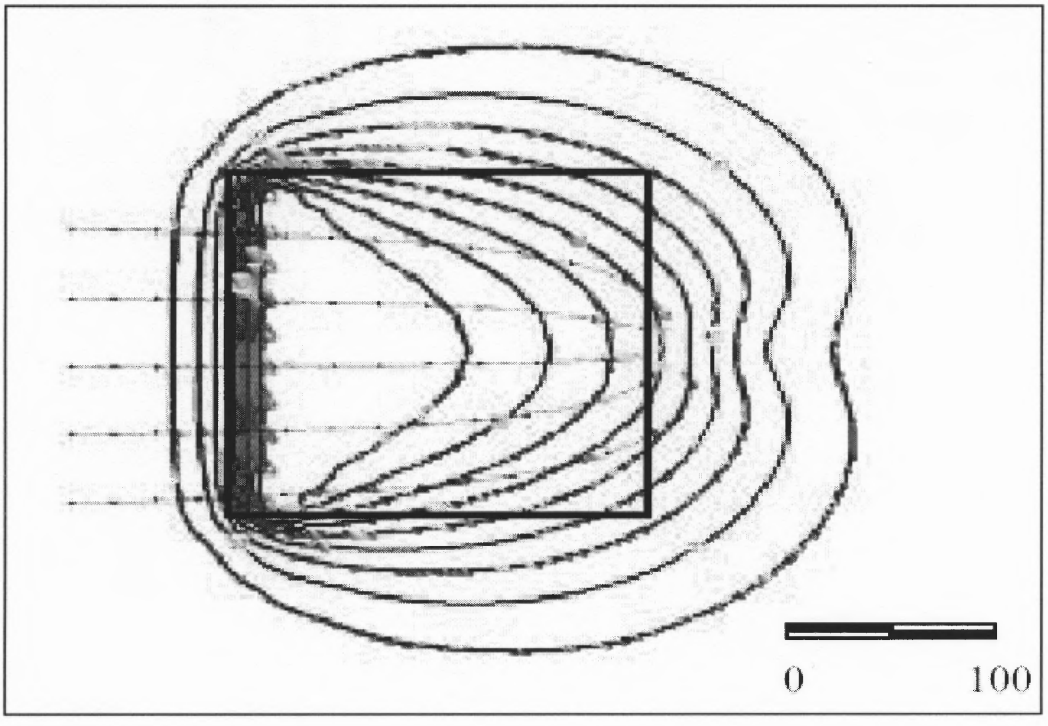

Figure 4.3 The Stabilizer Contours in Horizontal View (Gallagher, 2000).

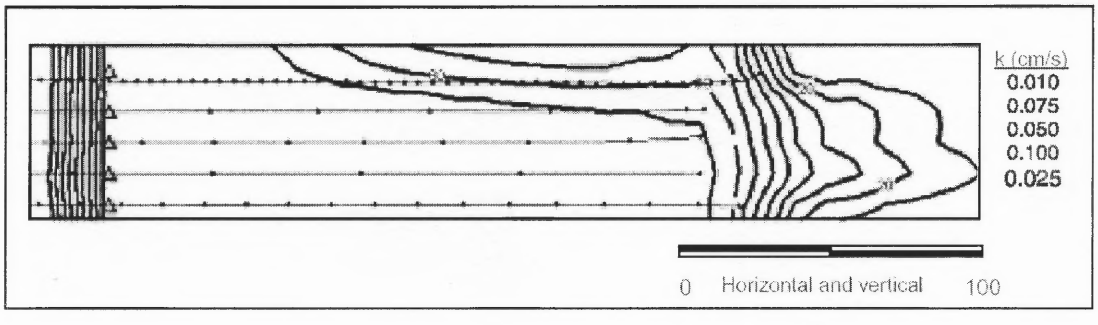

Figure 4.4 The Stabilizer Contours in Vertical View (Gallagher, 2000).

4.1.6 Summary of Review of Pervious Grout Modeling Studies

All the studies described above focused on the simulation of colloidal silica gel during injection process. All found that the reduction of soil permeability is due to the pore blocking after the stabilization process. On the other hand, the above models considered the macroscopic of engineering performance. However, the basic science or the microscopic behavior is not fully known. This research attempts to explain basic science behind the stabilization process by using a mathematical model at microscopic level. The details of the microscopic mathematical model are given in the following sections.

4.2 The Permeability in Anisotropic Granular Media

Soil permeability is a macroscopic parameter governed by the movement of pore fluid through soil at the microscopic level. Since the system concerned is a microscopic, at any specific time, the flow in the system can be assumed steady state. The steady state flow of an incompressible fluid in an incompressible porous media is governed by the equation of continuity and the steady state Navier-Stokes equation. In this research, the evolution of microstructure of contaminated soil during the treatment with colloidal silica is obtained by solving the Navier-Stokes equation with appropriate boundary conditions.

The assumption is that the porous soil mass consists of spatially periodic spherical particles of a given diameter. Thus, it is possible to analyze a unit representative cell consisting of one particle with its surrounding ambient space. Subsequently, the influence of shape, non-periodic nature, and size can be calculated by gradual alternation of the unit cell.

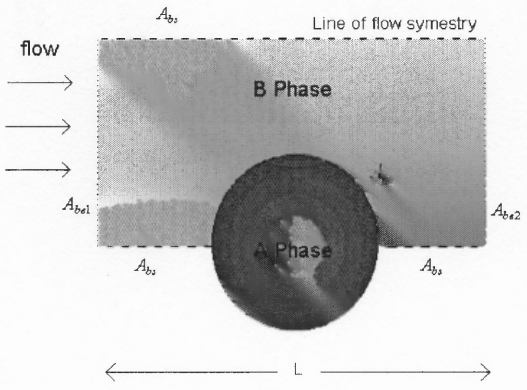

Figure 4.5 A Porous Medium Unit Cell.

The flow field through the spatially periodic porous medium for a unit cell shown in Figure 4.5 can be written using the steady-state Navier-Strokes equation:

$$\rho \underline{V} \cdot \nabla \underline{V} = -\nabla p + \mu \nabla^2 \underline{V} \tag{4.1}$$

and for continuity of the fluid motion for an incompressible fluid:

$$\nabla \cdot \underline{V} = 0 \tag{4.2}$$

Boundary conditions on velocity:

no-slip: $\underline{V} = 0$ on A_{ab}

symmetry: $\underline{n} \cdot \nabla \underline{V} = 0$ on A_{bs}

periodicity: $\underline{V}(\underline{r} + n_i \underline{I}_i) = \underline{V}(\underline{r})$ on A_{be}

Boundary condition on pressure:

periodicity: $P(\underline{r} + n_i \underline{I}_i) = P(\underline{r}) + n_i \underline{I}_i \Delta P$

The periodic boundary conditions were defined using the translation vector given by the following. If the porous medium is represented as a repetitive array of rigid particles extending indefinitely in all directions, the location of any lattice point is given by:

$$\underline{R} = \underline{R}_o + n_i \underline{I}_i \quad i=1,2,3,... \tag{4.3}$$

Where: $\underline{R}_0$ = some reference position

n_i = integers

$\underline{I}_i$ = non-unique set of basis vectors called the lattice vectors

The volume of an array is partitioned into unit cells, defined such that the entire medium can be produced from a single cell by the repeated use of the translation given by Equation (4.3).

4.3 Numerical Implementation

A triangular element was used for the finite element implementation in the above theory. The two horizontal velocities U and V (perpendicular to each other) were allowed to vary as quadratic functions over the element whereas pressure was allowed to vary linearly (Figure 4.6).

x direction or U momentum:

$$\rho\left[U\frac{\partial U}{\partial x} + V\frac{\partial U}{\partial y}\right] = -\frac{\partial p}{\partial x} + \varepsilon_x\left[\frac{\partial^2 U}{\partial x^2} + \frac{\partial^2 U}{\partial y^2}\right] \tag{4.4}$$

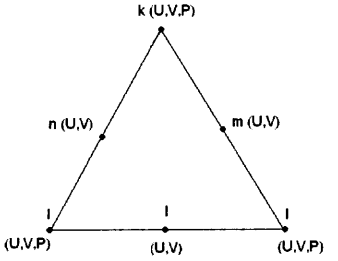

Figure 4.6 A Triangle for Finite Element.

y direction or V momentum:

$$\rho\left[U\frac{\partial V}{\partial x}+V\frac{\partial V}{\partial y}\right]=-\frac{\partial p}{\partial y}+\varepsilon_y\left[\frac{\partial^2 V}{\partial x^2}+\frac{\partial^2 V}{\partial y^2}\right] \tag{4.5}$$

and the continuity equation can be rewritten as:

$$\frac{\partial U}{\partial x}+\frac{\partial V}{\partial y}=0 \tag{4.6}$$

Where: $\varepsilon_x=\varepsilon_y=\mu$

When the Galerkin approach is utilized, the governing equations may be stated in terms of two basis function weighting factors as:

U momentum:

$$\left\{f_1^i\right\}=\int_V\langle N_i\rangle^T\left\{\rho\left[U\frac{\partial U}{\partial x}+V\frac{\partial U}{\partial y}\right]-\varepsilon_x\left[\frac{\partial^2 U}{\partial x^2}+\frac{\partial^2 U}{\partial y^2}\right]+\frac{\partial p}{\partial x}\right\}dV=0 \tag{4.7}$$

V momentum:

$$\{f_1^i\} = \int_V \langle N_i \rangle^T \left\{ \rho \left[U \frac{\partial V}{\partial x} + V \frac{\partial V}{\partial y} \right] - \varepsilon_y \left[\frac{\partial^2 V}{\partial x^2} + \frac{\partial^2 V}{\partial y^2} \right] + \frac{\partial p}{\partial y} \right\} dV = 0 \quad (4.8)$$

continuity:

$$\{f_1^i\} = \int_V \langle M_i \rangle^T \left\{ \frac{\partial U}{\partial x} + \frac{\partial V}{\partial y} \right\} dV = 0 \quad (4.9)$$

Where:

$\langle N_i \rangle$ is the quadratic basis function defined over all element adjacent to node i

or $N_i(x,y) = 1$ at node i and $N_i(x,y) = 0$ at all nodes

$\langle M_i \rangle$ is the linear basis function defined over all elements adjacent to node i

or $M_i(x,y) = 1$ at node i and $M_i(x,y) = 0$ at all other corner nodes

Equations (4.7) and (4.8) contain second order derivatives, which cannot be handled directly. Therefore, in order to lower the order of the derivative, it is necessary to use Green's transformation:

$$\{f_1^i\} = \int_V \left\{ \langle N_i \rangle^T \left[\rho \left(U \frac{\partial U}{\partial x} + V \frac{\partial U}{\partial y} \right) \right] - \left[\varepsilon_x \left(\left\langle \frac{\partial N_i}{\partial x} \right\rangle^T \frac{\partial U}{\partial x} + \left\langle \frac{\partial N_i}{\partial y} \right\rangle^T \frac{\partial U}{\partial y} \right) \right] - \left\langle \frac{\partial N_i}{\partial x} \right\rangle^T p \right\} dV \quad (4.10)$$
$$- \int_S \left\{ \varepsilon_x \langle N_i \rangle^T \left[\frac{\partial U}{\partial x} C_x + \frac{\partial U}{\partial y} C_y \right] - \langle N_i \rangle^T p C_x \right\} dS = 0$$

$$\{f_2^i\} = \int_V \left\{ \langle N_i \rangle^T \left[\rho \left(U \frac{\partial V}{\partial x} + V \frac{\partial V}{\partial y} \right) \right] - \left[\varepsilon_y \left(\left\langle \frac{\partial N_i}{\partial x} \right\rangle^T \frac{\partial V}{\partial x} + \left\langle \frac{\partial N_i}{\partial y} \right\rangle^T \frac{\partial V}{\partial y} \right) \right] - \left\langle \frac{\partial N_i}{\partial y} \right\rangle^T p \right\} dV \quad (4.11)$$
$$- \int_S \left\{ \varepsilon_y \langle N_i \rangle^T \left[\frac{\partial V}{\partial x} C_x + \frac{\partial V}{\partial y} C_y \right] - \langle N_i \rangle^T p C_y \right\} dS = 0$$

where: C_x, C_y = direction cosines normal to the surface S

and
$$\{f_1^i\} = \int_V \langle M_i \rangle^T \left\{ \frac{\partial U}{\partial x} + \frac{\partial V}{\partial y} \right\} dV = 0 \tag{4.12}$$

The surface integrals of Equations (4.10) and (4.11) may be neglected for inter-element interfaces but must account for the boundary of the system. These integrals may be computed from the known boundary conditions and incorporated into the right hand side vector of the final set of simultaneous equations.

When the Newton-Raphson method is used, the terms of the element coefficient matrix may be written in the form shown below:

$$\left.\begin{aligned} \frac{\partial f_1^i}{\partial U}\Delta U + \frac{\partial f_1^i}{\partial V}\Delta V + \frac{\partial f_1^i}{\partial p}\Delta p &= \Delta f_1 \\ \frac{\partial f_2^i}{\partial U}\Delta U + \frac{\partial f_2^i}{\partial V}\Delta V + \frac{\partial f_2^i}{\partial p}\Delta p &= \Delta f_2 \\ \frac{\partial f_3^i}{\partial U}\Delta U + \frac{\partial f_3^i}{\partial V}\Delta V + \frac{\partial f_3^i}{\partial p}\Delta p &= \Delta f_3 \end{aligned}\right\} \quad \begin{matrix} & 6cols & 6cols & 6cols \\ 6rows & \frac{\partial f_1}{\partial U} & \frac{\partial f_1}{\partial V} & \frac{\partial f_1}{\partial p} \\ 6rows & \frac{\partial f_2}{\partial U} & \frac{\partial f_2}{\partial V} & \frac{\partial f_2}{\partial V} \\ 6rows & \frac{\partial f_3}{\partial U} & \frac{\partial f_3}{\partial U} & \frac{\partial f_3}{\partial U} \end{matrix} \begin{bmatrix} \Delta U \\ \Delta V \\ \Delta p \end{bmatrix} = \begin{bmatrix} \Delta f_1 \\ \Delta f_2 \\ \Delta f_3 \end{bmatrix} \tag{4.13}$$

It should be noted that, if the pressure is specified at one node, one equation will be dropped from the system of equations. This eliminates f_3 at that nodal point and hence, the residual due to continuity of velocity is not minimized locally. To overcome this difficulty, one can assume that the specified pressure values as unknown then treat the pressure gradient across the exit and inlet boundary $[(P_{in} - P_{ex})/L]$ as a body force or make the outward force calculated from the pressure obtained from the solution be equal to the force exerted by the specified pressure values.

4.4 Application of Colloidal Silica Stabilization Process to FEM Formula Model

The viscosity of the silica grout increases with time turning colloidal silica mixture into a non-Newtonian, visco-elastic fluid that eventually becomes a solid. The gelation forms a new phase leading to changes in physical and chemical properties. In this research, the contaminated soil is idealized and modeled as a repetitive array of rigid particles extending indefinitely in all directions. The application of the above FEM formulation for a half-cell of soil results in the velocity profile. The velocity profile is a function of colloidal silica viscosity. The colloidal silica mixture does not have a constant viscosity. The colloidal silica viscosity ($\varepsilon_x = \varepsilon_y = \mu$) varies exponentially with time. In this section, the development of a mathematical relationship between colloidal silica viscosity and time are reviewed. Also, the incorporation of above relationship in microscopic model is shown. Then several simulations were performed, results were interpreted and design implications were highlighted.

4.4.1 Calculation of Viscosity

Moridis et al. (1995) proposed a relationship between the colloidal silica (NYACOL 1440 Eka Noble Inc.) viscosity and time. The "Gel Time Curve" (Figure 4.7) which shows the change of viscosity with time obtained from laboratory experiments. They also found that gelation rate of NYACOL 1440 influenced from soil composition and pH. Thus, the Al-substituted colloidal silica, NYACOL DP5110, was introduced to make it more stable at any soil condition (Kim, 1999).

Later, Moridis et al. (1996) performed a series of measurements to obtain the relationship between NYACOL DP5110 viscosity, time and salt concentration. The gel time curve from this study during the early gelation period (within the first hour) is shown in Figure 4.8. In this test, the different amounts of salt, 0.3 and 0.4 mole/liter $CaCl_2$,

were used to destabilize NYACOL DP5110 which yielded gelation times of 2 and 3 hours, respectively.

This relationship between gel viscosity and time was develop from experimental data (Finsterle et al., 1996). During the first hour of the gelation, the initial relatively low viscosity of the colloidal silica solution determines the flow behavior of the grout plume. Gravity and capillary forces affect the location and the shape of the grout plume. After the first hour, the viscosity increases rapidly and colloidal silica solution starts to loose its fluidity, see Figure 4.8. This was empirically represented as:

$$\mu_{gel} = a_1 + a_2 \cdot \exp(a_3 \cdot t) \tag{4.14}$$

Finsterle et al. (1996) showed a good correlation between the laboratory data (symbols) and the gel time curve calculated using Equation (4.14) and shown in Figure 4.9. Finsterle et al. (1996, 1998) used the above equation with TOUGH2 program to designing a colloidal silica viscous barrier. Afterward, it was applied in the design of the viscous barrier for the isolated 281-3H Retention Basin at the Savannah River Site (Apps et al., 1998).

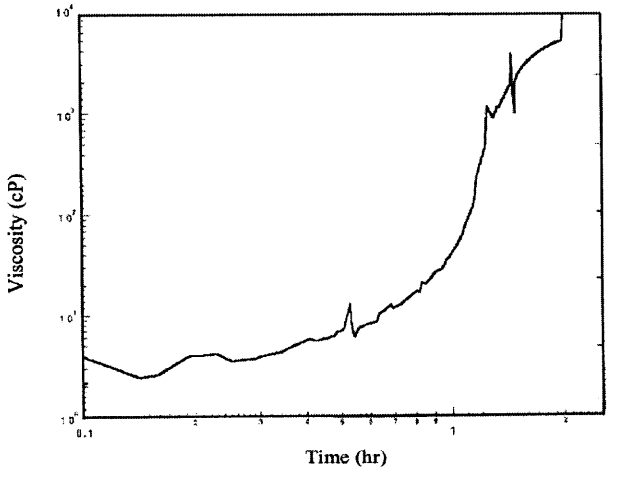

Figure 4.7 The Gel Time Curve for NYACOL 1440 (Moridis et al., 1995).

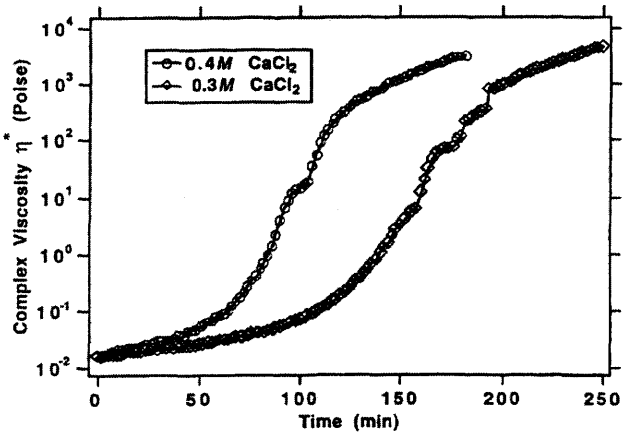

Figure 4.8 The Gel Time Curve for NYACOL DP5110 (Moridis et al., 1996).

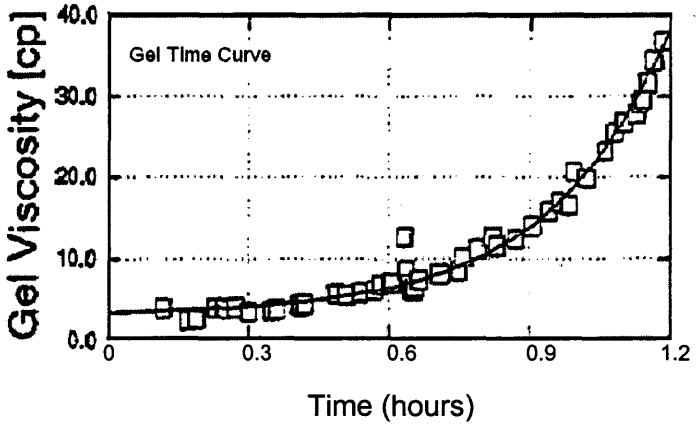

Figure 4.9 The Variation of Gel Viscosity with Time (Finsterle et al., 1996).

Equation (4.14) was later applied for the design of the injectable subsurface barrier at the Brookhaven National Laboratory demonstration site, New York (Moridis et al., 1999). The fitting parameter for viscosity equation was obtained from laboratory tests. NYACOL DP5110 colloidal silica with $CaCl_2$ at 0.26 and 0.50 mole/liter was used in this experiment. After substituting the fitting parameters, where μ_{gel} is in Pa.s and the time is in second, Equation (4.14) was rewritten as shown below. The gel time curve calculation from this equation is shown in Figure 4.10.

$$\mu_{gel} = (3.22\times10^{-2}) + (2.82\times10^{-4}) \cdot \exp\left(1.35\times10^{-3} \cdot t\right) \tag{4.15}$$

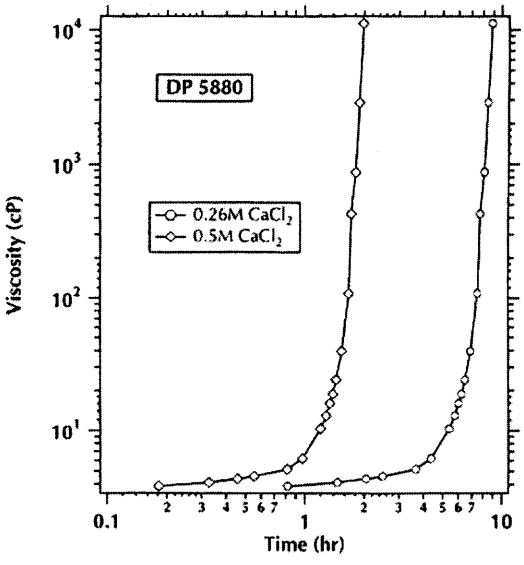

Figure 4.10 The Gel Time Curve for NYACOL DP5880 (Moridis et al., 1999).

Kim (1999) and Durmusoglu & Corapcioglu (2000) proposed another viscosity equation to fit the entire viscosity curve. An exponential function was included in the equation to provide a better fit for the curve.

$$\mu_{gel} = a_1 + a_2 \cdot \exp\left\{\left(a_3 \exp(a_4 \cdot t)\right)^{a_5}\right\} \tag{4.16}$$

As a result, the more accurate viscosity curves were obtained using different NaCl concentrations and the curve was normalized to time t^* ($t/t_{0.5}$: where $t_{0.5}$ is the time when the gel volume fraction reaches 0.5 and the viscosity becomes infinite). Thus, this viscosity equation can be expressed by ignoring the effect of NaCl. After rearranging and fitting curve where μ_{gel} is in poise and non-dimensional t^*, Equation (4.16) can be re-written as:

$$\mu_{gel} = \mu_0 - 0.3\exp(0.734^{0.01}) + 0.3 \cdot \exp\left[\left(0.734\exp(6.5 \cdot t^*)\right)^{0.01}\right] \tag{4.17}$$

This model represents the complete gel time curve and generates the same viscosity regardless of its colloidal silica and NaCl concentrations. Kim (1999) applied this model to study a colloidal silica waste barrier.

In this research, the gel time equation used was Equation (4.15). This equation provides good fitting results since the study period concerned here correspond to the beginning of gelation. In addition, the colloidal silica used in this study, NYACOL DP5110, is the same as that was used by Morisdis et al, (1996). From Figure 4.10, for 0.5 mole/liter $CaCl_2$ concentration, the viscosity increases rapidly after 1.2 hours producing complete solidification. In this research, it was assumed that colloidal silica mixture behaved as a fluid inside soil. Thus, the simulation period was limit to 1.2 hours.

4.4.2 Modeling

During the simulation of colloidal silica injection and subsequent solidification, colloidal silica was treated as a fluid that increases its viscosity with time. However, during the solidification, the new solid phase evolves, initially as a separate liquid phase then forming a new solid phase. Colloidal silica mixture maintains liquid properties and continuously changes with time, making the movement of the mixture difficult to determine. Finsterle et al. (1996) and Kim (1999) simulated the two phases by having the fluid (flow model) and solid (solidification model) model separately using colloidal silica viscosity as the indicator.

In this study, colloidal silica was treated as a liquid in the FEM model. The separation of liquid solid boundary was simplified by distinguishing the two phases with fluid velocity. Utilizing the boundary layer concept, it was assumed that when the fluid velocity drops below a predetermined minimum, the zone in the velocity profile with velocity below that minimum velocity becomes a solid. Thus, the velocity is a major indicator of the solidification in this model.

Referring to the theory of flow through a unit cell (Figure 4.5), fluid passes through the pores in soil media during the grouting process. The Navier-Strokes equation predicts velocity and pressure contours in the unit cell as shown in Figure 4.11, (the simulation of fluid flow performed using commercial software ANSYS developed by ANSYS Inc.). Bulk colloidal silica is transferred to adjoining cells from the regions with high velocity. At any locations with velocities close to zero, there is time for the gel to set and solidify. As a result, colloidal silica in the low velocity zone will solidify faster, while those in the high velocity zone transmit to the next cell.

Contaminated soil was idealized and modeled as a repetitive array of rigid spheres extending indefinitely in all directions. The variation of the pore fluid viscosity

($\varepsilon_x = \varepsilon_y = \mu$) is assumed to increase with time. This research is a microscopic simulation for colloidal silica grout by varying the microscopic viscosity with time. A minimum velocity for colloidal silica to become a solid was considered. Then it was assumed that colloidal silica with pore velocity lower than that velocity, which is the points close to the solid surface, becomes a solid later changing the pore distribution in contaminated soils. The results of the simulation are pore distribution with time.

Two Computer programs, "Three-dimensional Finite Element Model (RMA7)", developed by King et al. (1973) and input file generator, MESH, (Meegoda 1985), were used to solve the above numerical equations. These computer programs were modified to adapt to this research. These programs were initially developed in FORTRAN for a VMS system. To run on a PC, both programs were modified using software "FORTRAN Developer Studio". The post processor used by Megooda (1985) was for Tecktronic plotter. Hence, the output from RMA7 was transferred and plotted using computer software TECPLOT 5 developed by Amtec Inc.. The velocity and contour profiles obtained from TECPLOT were finalized using Acrobat PhotoShop 5.

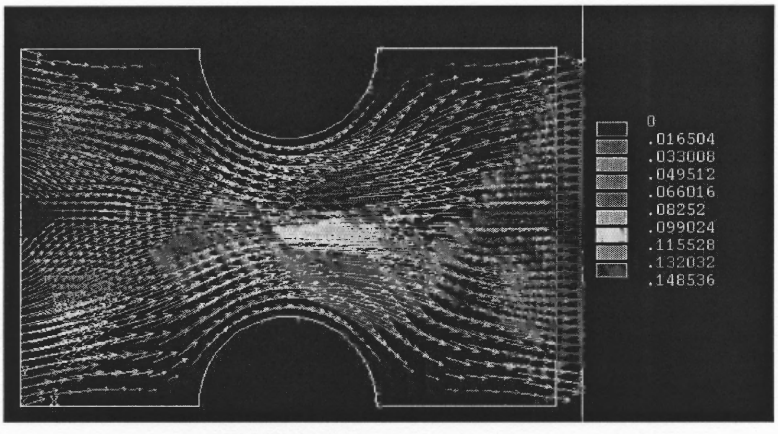

Figure 4.11 The Velocity Profile of Fluid in Unit Cell.

4.5 Simulation Results

The simulation was performed to study the effect of viscosity and unit cell geometry to solidification process. This was completed by generated six nodes triangle quadratic elements of different unit cell geometries using computer code MESH. Each unit cell contains 297 nodes and 128 elements. The unit cell with circular shaped soil particle generated from MESH and plotted by TECPLOT 5 is show as the Figures 4.12. Boundary condition A_{bs}, is defined as the repeated boundary where the fluid in unit cell boundary contact to other unit cell. A_{be} is a solid part where there is no movement. A_{be1} and A_{be2} are inlet and outlet where the normalized velocity and pressure were defined.

After the mesh was generated and all boundary conditions were defined, RMA7 was run using output from MESH. Results from RMA7 are pressure and velocity at each node. The velocity and pressure contours were plot using TECPLOT 5. The simulations were repeated using different viscosities. Base on Equation 4.14, the viscosity used ranges from 0 to $40x10^{-3}$ N.sec/m^2 (Poise) depends on the time after injection at 0.1 hour intervals up to 1.2 hours.

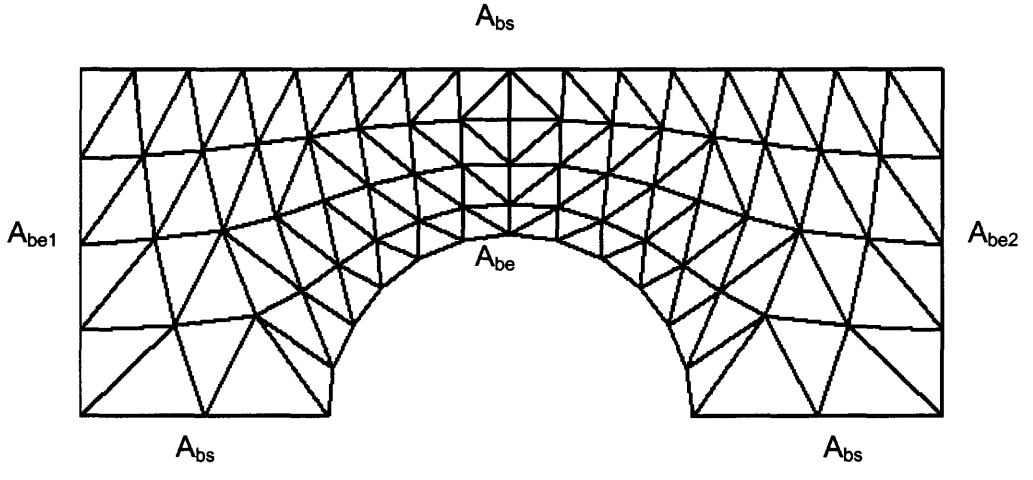

Figure 4.12 The Mesh of Circle Unit Cell of 128 Quadratic Elements.

It is assumed that colloidal silica mixture the velocity below the minimum velocity becomes a solid. In this research, the minimum velocity was set at five percent of maximum velocity. For regions in the unit cell where the velocity of colloidal silica mixture lower than five percent of the maximum velocity, the mixture was treated as a solid. The porosity of unit cell was recalculated base on new solid volume.

Beside the circle unit cells, different geometries were used in the simulation. Two scenarios with different unit cell geometries, sphere and ellipsoid, were simulated to observe the solidification pattern. The simulation results for sphere and ellipsoid are shown in Figures 4.13 and 4.14 respectively. Each Figure contains a series of plots for 1.2 hour time period.

The change in velocity profile with time is displayed with the gel time curve. The left-hand side displays the velocity contours of colloidal silica in the unit cell. The lower velocity zone is represented by the darker color while the lighter color corresponds to a higher velocity zone. The velocity ratio ranges from zero to one, normalized against the maximum velocity in the unit cell. The right hand side displays the change of viscosity ratio with time and ranges from zero to one, normalized against the maximum viscosity.

The simulations for ellipsoid of axial ratio equal to two with different angles are shown in Figure 4.15. The simulations of zero degree angle ellipsoid with different axial ratios, range from 1 to 2.5, are shown in Figure 4.16.

During the grouting process, the mixture containing colloidal silica particles in fluid travels through the soil void space (referred to a space in the unit cell). Initially, colloidal silica particles act as individual particle in the solution causing the colloidal silica mixture to have low viscosities behaving like a fluid moving through void spaces in the soil. Figure 4.13, at initial time, t = 0, represent the velocity contours of this period.

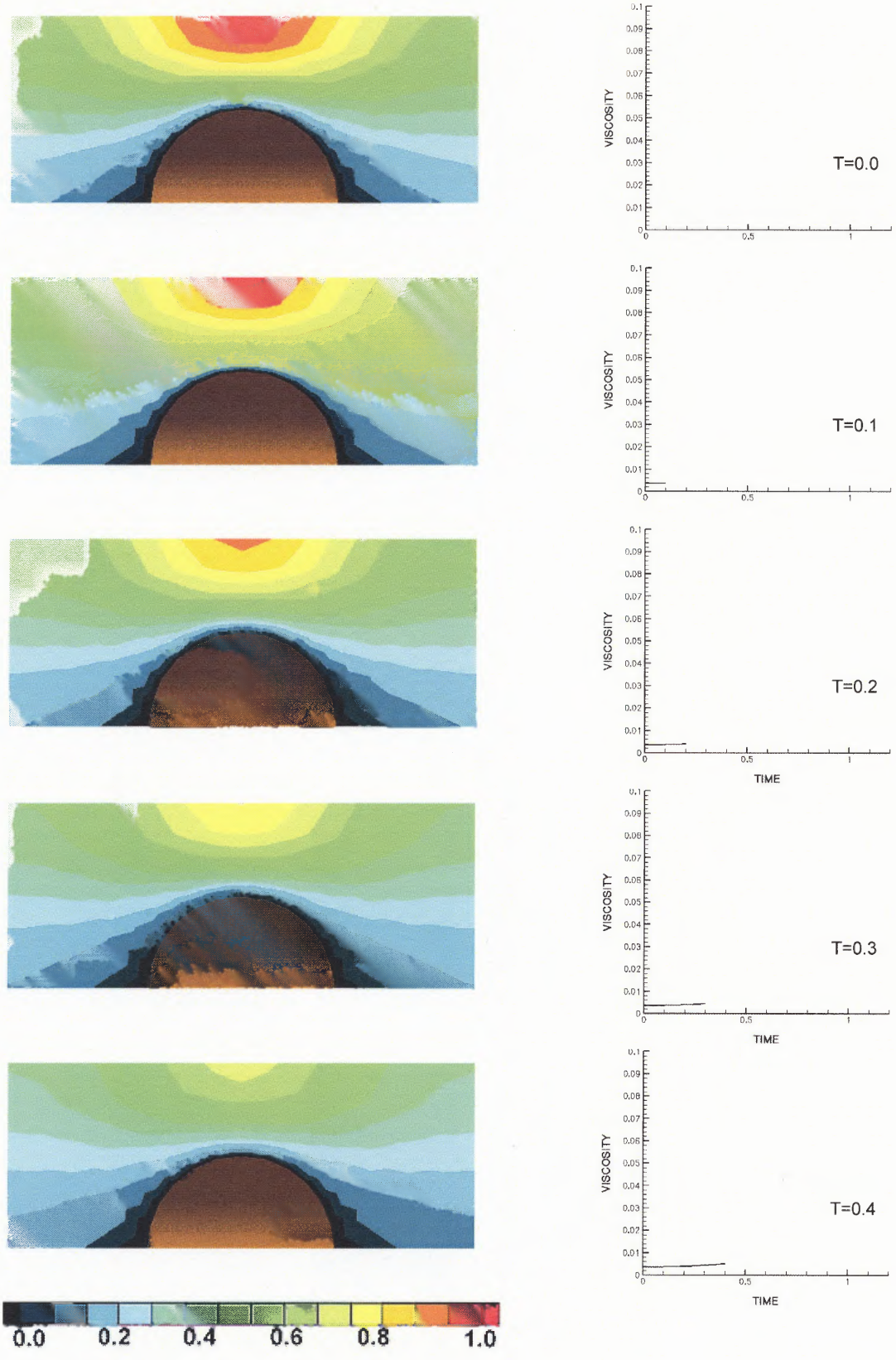

Figure 4.13 The Simulation of Solidification Process for Sphere.

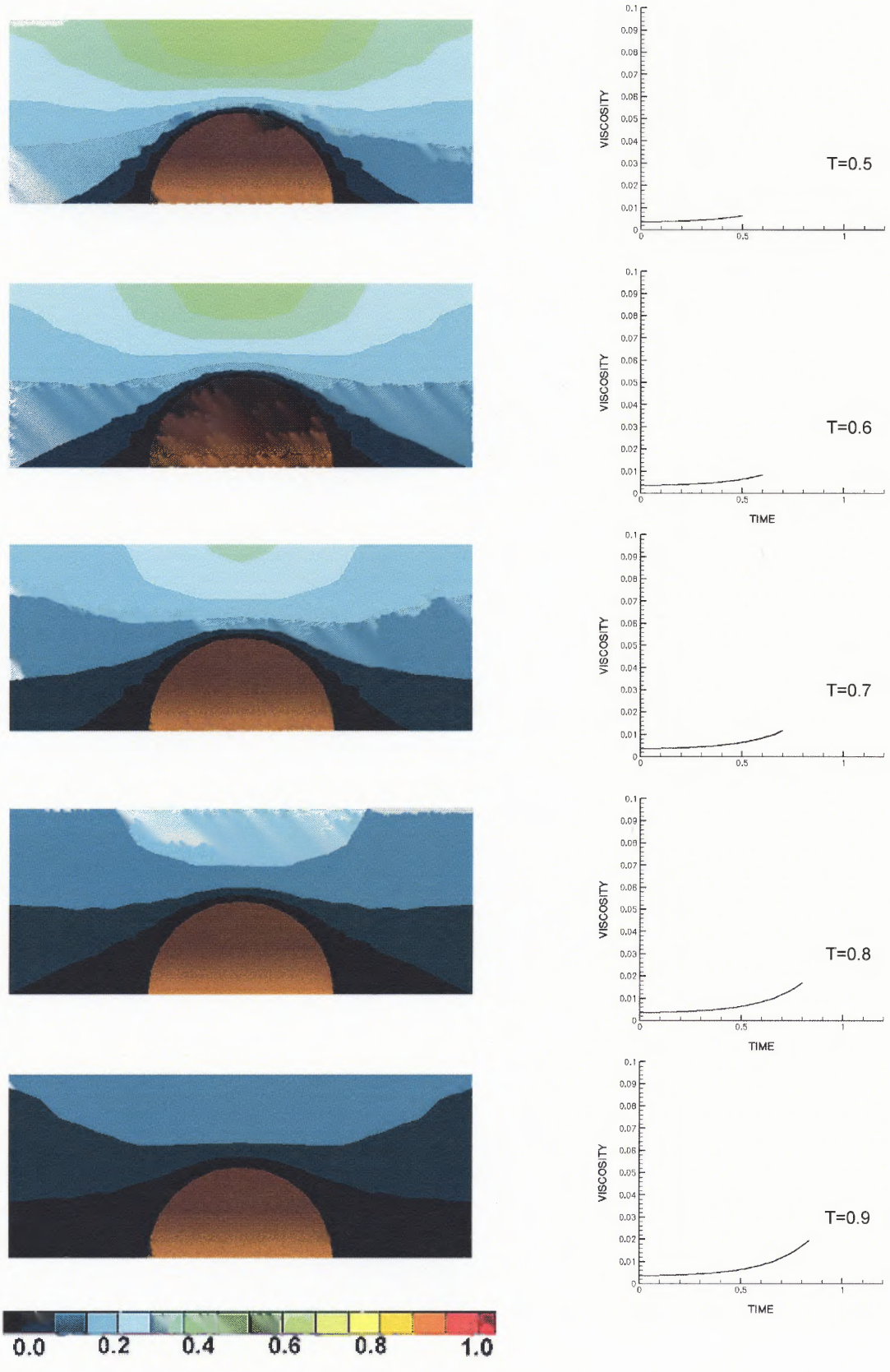

Figure 4.13 The Simulation of Solidification Process for Sphere (Contd.).

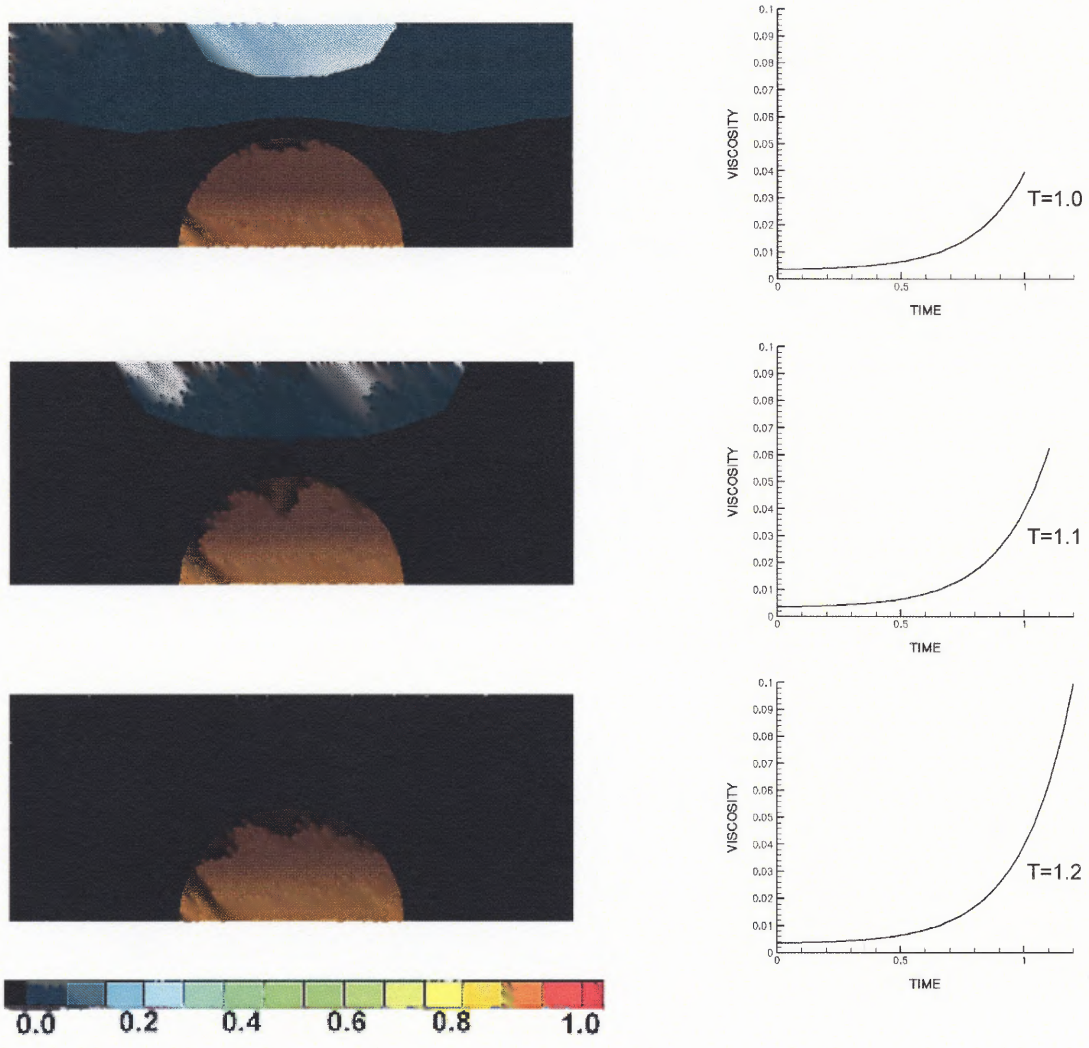

Figure 4.13 The Simulation of Solidification Process for Sphere (Contd.).

The Figure shows the low velocity closer to the soil or dead sections of the unit cell. The velocity at the center of the unit cell is the highest and that adjacent to soil surface is the lowest.

With time, colloidal silica particle attaches to other particles forming long chain to cause gelation, increasing viscosity. Corresponding velocity contours show larger areas with zero or near zero velocities close to the solid particle. At this stage, colloidal silica particles in the region that closer to the soil surface than the one in the middle between the two soil particles spend more time in the unit cell.

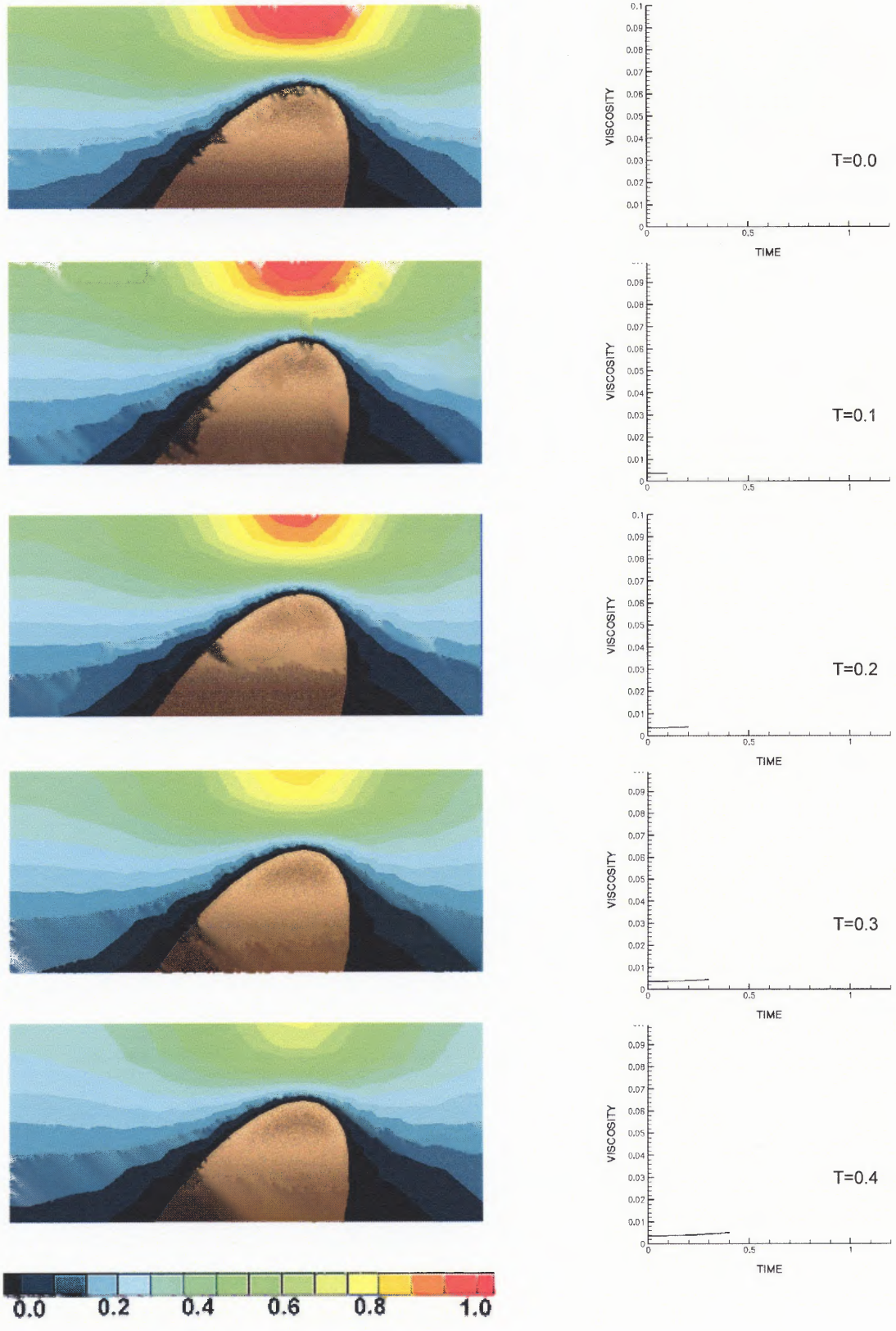

Figure 4.14 The Simulation of Solidification Process for Ellipsoid.

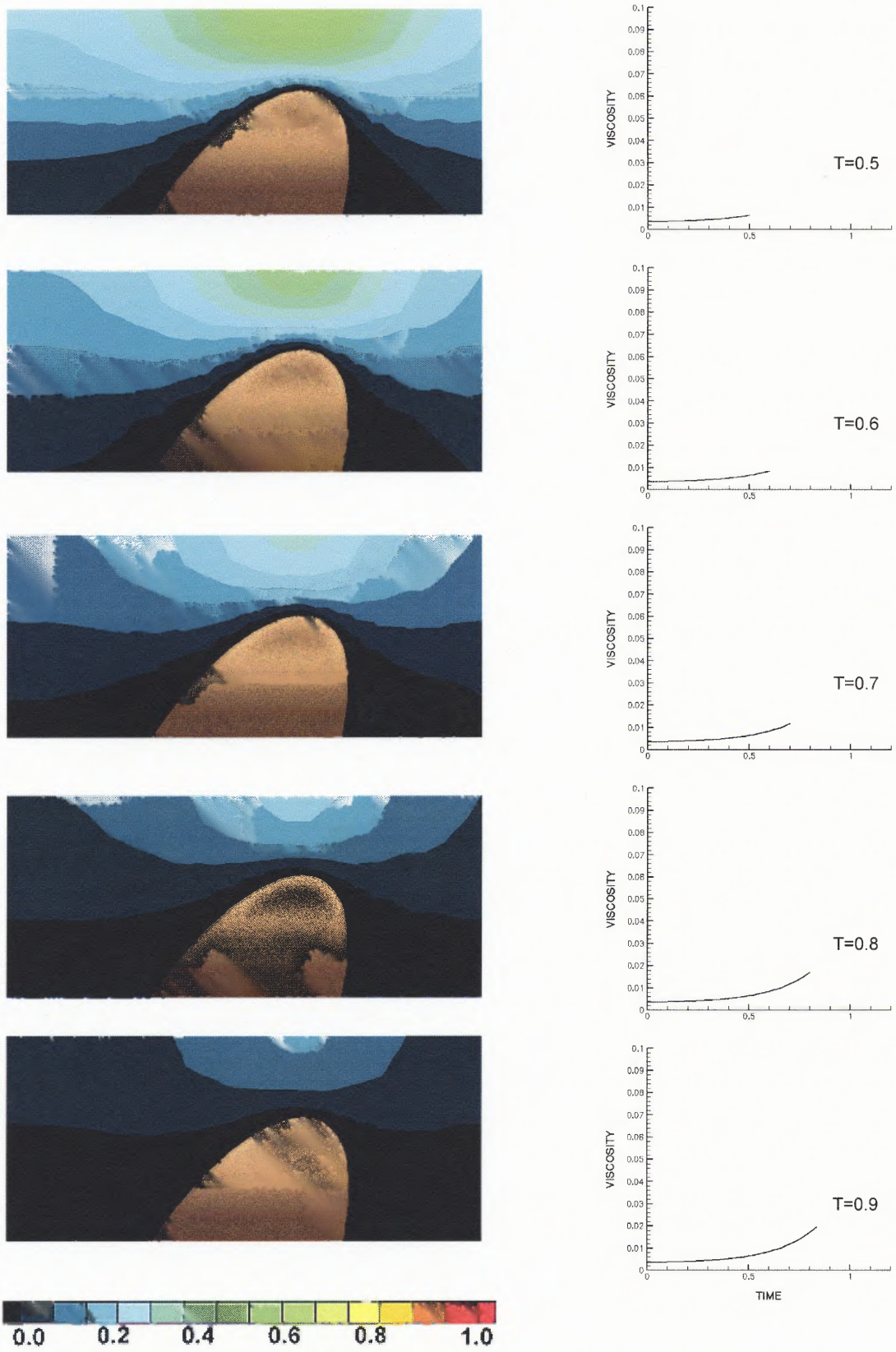

Figure 4.14 The Simulation of Solidification Process for Ellipsoid (Contd.).

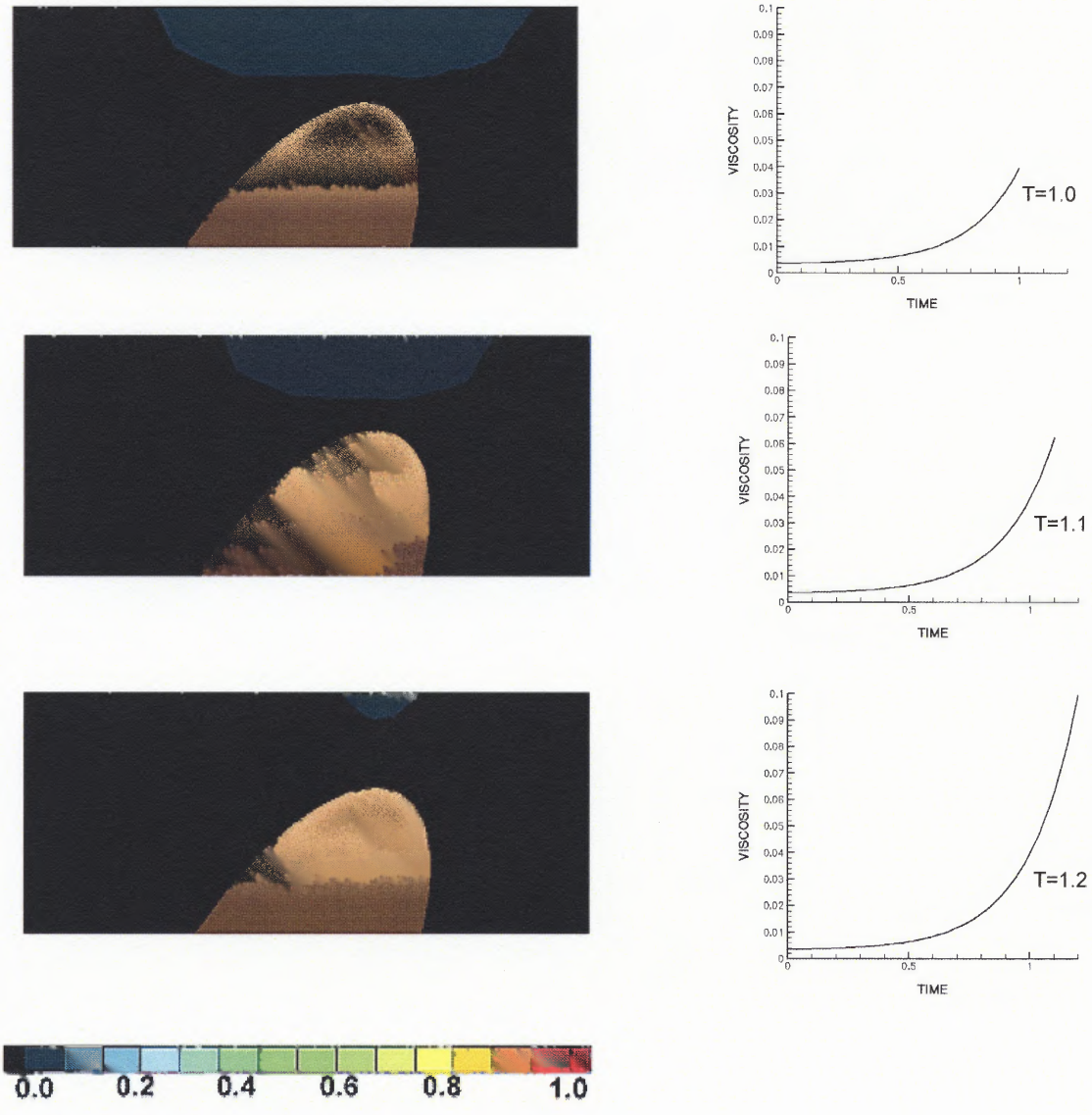

Figure 4.14 The Simulation of Solidification Process for Ellipsoid (Contd.).

As a result, the solidification starts at points closer to soil surface then expands outwards. This can be viewed as coating of soil particles resulting in the expansion of the solid volume. The gel acts like a coating, preventing chemical migration. Solidification causes increases in the solid fraction of the unit cell, with decreases in void space. The process continues until the voids are partially filled with colloidal silica gel.

The viscosity of colloidal silica is an exponential function of time. After 1.2 hours, the viscosity increases rapidly until colloidal silica becomes a solid. By the time the gelation process is completed, the gel fills most of the voids in soil resulting a partial stoppage of the fluid flow through soil. This causes a drastic reduction of the soil permeability. After complete solidification, the soil exhibits a new pore structure with different physical properties. The new pore structure that is predicted at the end of the simulation shows substantial reduction in soil properties, such as, porosity, permeability, relative permeability, capillary pressure and initial liquid saturation.

The unit cell geometry plays an important role during gelation. Comparing the two Figures, 4.13 and 4.14, different unit cell shapes yield different velocity contour. Additional simulations were performed to study the effect of different ellipsoid angles and ellipsoids with different axial ratios. The results are shown in Figure 4.15 and 4.16, respectively. It was assumed that the solidification of treated soil is completed when the soil is filled with solidified gel. The porosity is an indicator for the available space that is not occupied by solidified gel. Thus, the higher porosity reduction is the faster solidification. From Figure 4.15, different ellipsoid angles with the axial ratio equal to two, the porosity reduces from faster to slower from 90°> 45°> 30°> 0° respectively.

The effect of different axial ratio to the porosity reduction is shown in Figure 4.16. Figure 4.16 shows porosity reduction of zero degree angle ellipsoid with different axial ratios, range from 1 to 2.5. It can bee seen from the Figure that the higher axial ratio, the faster the porosity reduction rate. Thus, the shapes of soil particles affect the gelation process of colloidal silica during the grouting process. In addition, changing the unit cell geometry from smaller axial ratio to the greater one results in a faster solidification.

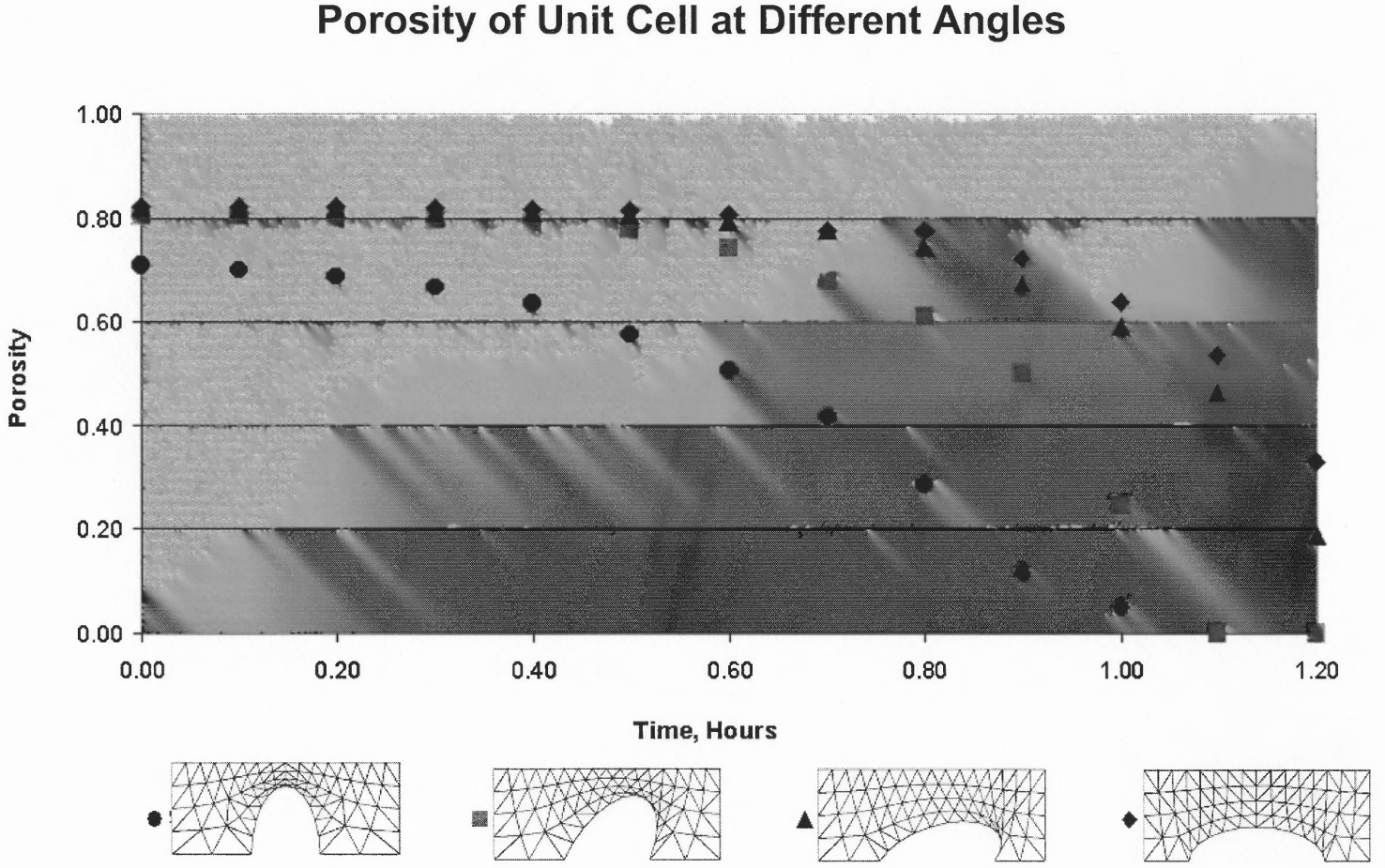

Figure 4.15 The Simulation of Solidification Process for Different Angles.

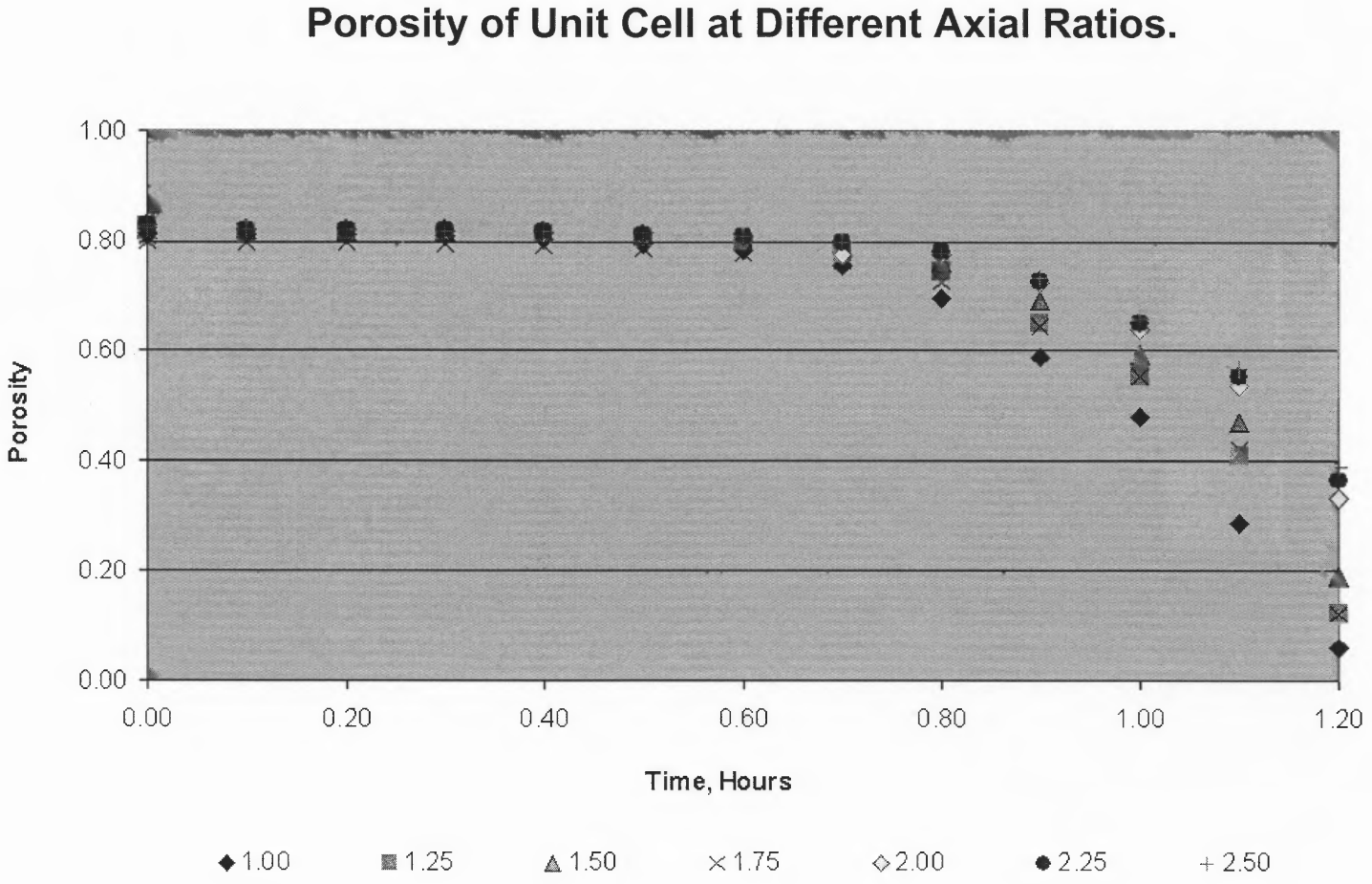

Figure 4.16 The Simulation of Solidification Process for Different Axial Ratios with Zero Degree Angle.

4.6 Discussion/Conclusions

The low-viscosity chemical stabilizer, colloidal silica, is extensively used as a stabilizer in the construction of grout curtains. Persoff et al. (1995) injected a colloidal silica mixture to stabilize fine-grained soils in some hazardous waste sites. Therefore, to understand the mechanism during the solidification, the movement of colloidal silica mixture soil was simulated.

Before injecting, colloidal silica was mixed with salt to destabilized the colloid state of silica particles. By doing so, colloidal silica viscosity increased exponentially with time until it was solidified. Right after the mixture was injected into a contaminated soil, the mixture would travel through the voids in the soil matrix. The viscosity increases while colloidal silica is moving, causing a reduction of the fluid velocity in soil. The above causes an increase in the boundary layer thickness, transforming liquid colloidal silica into a gel. The solidification starts from soil surface and expands outward. The process is continued until all void spaces are filled with colloidal silica gel. This gel in the pore would prevent or reduce flow of water into the soil, by reducing soil permeability.

A mathematical model was used in this study to explain the solidification. The simulation also showed the impact of soil geometry on velocity contours and subsequent gelation, the greater axial ratio of the unit cell, the faster solidification. This model can be further improved to aid the design of grout curtain in terms of the soil permeability and the size of stabilizer plume.

CHAPTER 5

MEASUREMENT OF DIFFUSION COEFFICIENT

5.1 Introduction

Concentration gradients occur when a chemical within a media moves from higher concentration region to lower concentration region. In other words, the concentration gradient is the difference in concentration between a high and low concentration region per unit length. During the diffusion process, chemicals will move from the area of high concentration towards the area of lower concentration until the chemical reaches equilibrium. The diffusion of chemical through gel occurs through interior pores (Masaro & Zhu, 1999).

There are three types of diffusion through pores: free molecular or Knudsen diffusion, continuum or bulk diffusion and surface diffusion. The Knudsen diffusion occurs when the pore size is of the same order of magnitude as the mean free path of the molecules, the different molecules move independent to each other and the diffusion is governed by the collisions of molecules with others and the walls. The bulk diffusion occurs when the pore size and pressure are large. The diffusion rate depends on the collision between molecules. Surface diffusion occurs when the molecules adsorb onto the surface of the pore and jump from one adsorption site to another (Doung, 1998; Bear et al., 1990; Gudmundsson, 2001).

The diffusion transport in terms of molar flux (the rate of transfer per unit area of section) can be modeled and evaluated numerically using mass balance and Fick's law. Many studies have been performed to determine diffusion coefficients. However, the diffusion coefficient of chromium in colloidal silica gel is not available. Therefore, the diffusion coefficient of chromium in colloidal silica gel needs to be determined by laboratory experiments.

There are many techniques to determine the diffusion coefficient of chemical in a gel (Maraso & Zhu, 1999; Shackelford, 1991; Westrin et al., 1994). However, these techniques are complicated and time-consuming. Recently, an optical method was proposed to measure the diffusion coefficient of metals in polymer (Axel, 1998; Morrissey & Vesely, 2000; Teasdale et al., 1999). Polymers have a similar structure to colloidal silica gel. Hence, it is proposed to adopt the optical method to measure the diffusion coefficient of chromium in colloidal silica gel.

The optical technique utilizes the advantages of computer technology with graphic applications and eliminates the need of classical methods that are tedious and time consuming. In this study, the optical technique was adopted to estimate the chromium concentration in colloidal silica gel and to obtain the diffusion coefficient. The measured diffusion coefficient is used in a simulation study to evaluate the applicability of injected colloidal silica to stabilize chromium contaminated soils, which will be explained in detail in Chapter 6.

In this chapter, the experimental procedures for estimating the diffusion coefficient of chromium in colloidal silica gel using an optical method will be explained. It also includes a literature review, theory, and numerical analysis in addition to the experimental procedure. The results obtained, specifically the diffusion coefficient of chromium in colloidal silica gel will be used to investigate the transport of chromium in soil stabilized with colloidal silica gel.

5.2 Background

5.2.1 Review of Method to Estimate the Diffusion Coefficient

Diffusion occurs in gas, liquid and solid. A gel is considered to be between a solid and a liquid state, similar to polymers. Many studies have been performed to measure the diffusion coefficients of chemicals in gels and polymers, mostly in the medical industry (Westrin et al., 1994). There are many methods that can be used to measure the diffusion coefficients of chemicals in gel. The most convenient and commonly used methods for measuring diffusion coefficient are shown in Table 5.1.

The first three methods listed in Table 5.1 are used frequently. These three methods give accurate results under practical situations. Beside these three methods, other techniques listed in Table 5.1, also provide reliable results for gels. For example, measurements of diffusion coefficients using a Diaphragm Cell (or Dual Cell) method consists of an apparatus in which two stirred chambers are separated by gel (Axelsson et al., 1991; Lakatos et al., 1998; Morisdis et al., 1998; Shackelford, 1991; Zorrilla & Rubiolo, 1994). Samples from both sides are taken and analyzed for chemical concentration at different time intervals. The diffusion coefficient can be calculated directly using the chemical concentration values at different time (Lakatos et al., 1997; Lakatos & Lakatos-Szabó, 1998). This method provides the direct measurement of diffusion with high accuracy (Westrin et al., 1994.). However, the experimental setup and sampling are difficult due to the fragile nature of wet gel. In addition, it requires the quantitative analysis of dilute solution for a long period of time, typically hundreds of hours (Takahashi et al., 2000).

In the radiotracer measurement technique, a radioactive isotope is deposited onto the gel sample. The concentration profile in the polymer matrix after allowing for

Table 5.1 The Characteristic of the Best Methods of Measuring Diffusion Coefficient (Cussler, 1997)

	Description of Transport	Apparatus expense	Apparatus Construction	Concentration Difference Required	Method of Obtaining Data	Overall Value
Diaphragm Cell	Pseudo-steady state	Small	Easy	Large	Concentration at known time; requires chemical analysis	Excellent; Simple equipment out weigh occasionally erratic results
Infinite Couple	Unsteady in an infinite slab	Small	Easy	Large	Concentration vs. position at know time; requires chemical analysis	Excellent, but restricted to solids
Taylor Dispersion	Decay of pulse	Moderate	Easy	Average	Reflective index vs. time at known position	Excellent for dilute solution
Nuclear Magnetic Resonance	Decay of pulse	Large	Difficult	None	Change in nuclear spin	Very good; works when other method don't
Dynamic Light Scattering	Decay of pulse	Large	Difficult	None	Doppler shift in scattered light	Very good for polymers
Gouy Interferometer	Unsteady state in an infinite cell	Large	Moderate	Small	Reflective- index gradient vs. position and time is photographed	Very good; excellent data at great effort
Rayleigh or Marc Zehnder Interferometer	Unsteady state out of infinite cell	Large	Difficult	Small	Reflective- index gradient vs. position and time is photographed	Very good; best for concentration dependent diffusion
Capillary Method	Unsteady state out of infinite cell	Small	Easy	Average	Concentration vs. time; requires radio active counter	Very good, commonly used only with radioactive tracers
Spinning Disc	Dissolution of solid or liquid	Small	Easy	Large	Concentration vs. time; requires chemical analysis	Good; requires diffusion controlled dissolution a stringent restraint
Wedge Interferometer	Unsteady state in an infinite cell	Moderate	Easy	Large	Reflective- index gradient vs. time is photographed	Fair; much harder to use than most authors suggest
Steady-State Method	Steady diffusion across known length	Moderate	Moderate	Large	Small Concentration changes require exception analysis	Fair; easy analysis does not compensate for very difficult experiment

diffusion is obtained by cutting a thin section from the sample perpendicular to the direction of diffusion and counting the ratio of activity of each section. The activity is directly proportional to the amount of isotope atoms in the gel sample (Willecke & Faupel,1997).

In addition, the diffusion coefficient of a chemical in a gel can be measured during the period of unsteady state. The movement of chemical in a gel can be observed in-situ by special instruments. The change in concentration profile within a gel media can be measured using instruments, such as fluorescence, absorption spectroscopy, nuclear magnetic resonance (NMR), holographic laser interferometry, ultrasonic acoustics, Rutherford backscattering (RBS) and laser scanning (McDonald et al., 2001; Burke et al., 2000). With these instruments, the chemical concentration in gel can be estimated without disturbing the solution. However, some of these instruments require more complicated steps to preserve the chemical in gel in its original state prior to the analysis.

In conclusion, there are a large number of different methods for the measurement of diffusion coefficients each having advantages and limitations. One method not widely used is the optical technique, which is considered here in this research and discussed in the next section.

5.2.2 Optical Technique

With the recent advances in digital photography and computer graphic operations, optical analysis has become an attractive measuring tool and is proposed here to estimate the variation in chemical concentration with time. When a colored chemical is transported within a gel, a concentration gradient is created. Normally the colored chemical concentration is proportion to the degree of color intensity in a digital

photograph. As a result, it is possible to digitally record the change of color with time. Then the digital data can be interpreted to obtain the concentration gradient using computer software. For examples, the method of "Infinite Couple", the concentration of chemical in gel was detected by attaching a spectrophotometer to the gel sample while diffusion took place (Dunmire et al., 1999). In the "Flow Cell" method, a gel sample was attached to a spectrophotometer making it possible to detect the in-situ color changes. The main advantage of this technique would be the elimination of a complicated sample preparation process (Takahashi et al., 2000).

5.2.3 Digital Image

Digital images are stored as raster files that "paint" colors across the computer screen in an array of square elements called pixels. The pixel is a basic building block or the smallest unit of a digital image. Each pixel is stored in an area of memory called a bit-map which contains an unique physical address, size specifications and color values.

Figure 5.1 shows how the physical addresses of pixels are stored in the computer memory. The pixel is addressed using the x and y position coordinates. One digital image can contain from thousands to millions of pixels. The amount of detail that the camera can capture is called the resolution, and it is measured in number of pixels. Higher number of pixels per unit area would yield a higher resolution (better picture quality), hence, more memory is required to store the image. The resolution is described as the number of pixels per unit length of image. For example, pixels per inch, pixels per millimeter, or pixels wide. Typical digital image resolution includes, 256x256, 640x480, 1216x912 and 1600x1200 pixels (Karim & Gerald, 2002).

One or more bits define the color value of the pixels in a digital image. The computer code that stores in the bits defines the color and its intensity. The degree of

intensity of each color reflects the color brightness in a specific pixel. The more bits used provide more variety of color in the image, which vary from 1-bit (black and white) to 24-bits (16.7 million colors). In a 24-bit image, which is a common resolution for a digital image, each pixel is described by three 8-bits representing the intensity values for red, green and blue (Figure 5.2). Each set creates 2^8 (256) intensity values and with three sets produce a total of 16.7 million colors (Kodak, 2002).

The information of its color value of any pixel in digital image is stored in terms of intensity as shown in Figure 5.3. Since each pixel contains position and color intensity information, the digital data can be easily converted to obtain physical data for diffusion.

In a diffusion study, the most critical information needed is the chemical gradient which is the concentration as a function of the position at any specific time. The concentration gradient defined as concentration (or the intensity values of the three colors in the pixel) as a function of distance (or the pixel physical addresses) can be obtained by using appropriate computer software. To achieve this, the image of the gel media that contains chemical with different color intensities at different positions is needed as a digital input. This might be done by taking a digital photograph or scanning a regular picture then converting it into a digital form. The concentration can be determined by calibration to convert color intensity to the concentration of chemical by using calibration curve (which is similar to the spectrophotometer technique). The result provides the concentration at different positions which can be used in fitting the diffusion coefficient. In addition, pictures can be taken at different time intervals providing information on the chemical movement as a function of time.

Following are advantages of the proposed digital photography method.

1. The apparatus is easy to setup.
2. The measurement can be performed within a short time.
3. The change of concentration gradient can be monitored in-situ.

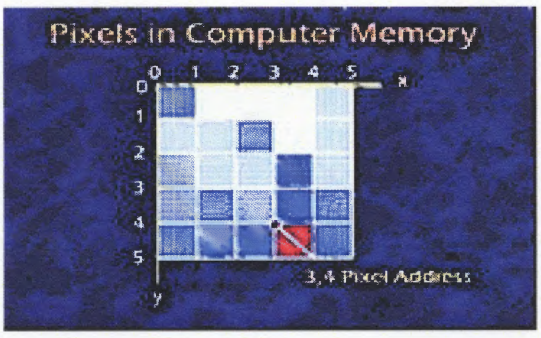

Figure 5.1 The Physical Address of a Pixel in a Computer Memory (Kodak, 2002).

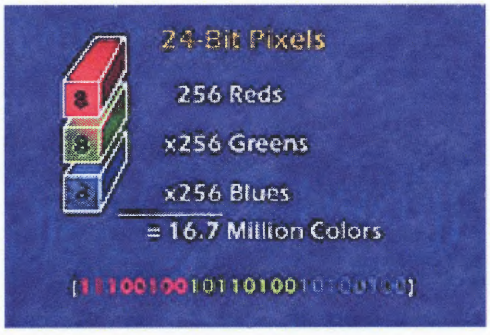

Figure 5.2 The Intensity of Color Stored in a 24-Bit Pixel (Kodak, 2002).

Figure 5.3 The Color Intensity in One Pixel of the 24-Bit Pixel Image (Kodak, 2002).

4. The diffusion coefficient can be calculated by fitting.

In a recent study, diffusion in thin films was examined in-situ by input of concentrations gradients as digital images, and the diffusion coefficient is based on Fick's law (Teasdale et al., 1999). Morrissey & Vesely (2000) studied the Non-Fickian diffusion. The diffusion front of a species in a polymer was monitored in-situ by mounting a charge coupled device (CCD) camera on the microscope, and the penetration front was measured by using a PC-Image software.

From observation, chromium in a gel is yellow in color while the gel is white. When the diffusion takes place, the white color gel becomes yellow. The degree of color is proportional to chromium concentration in the gel. Therefore, the diffusion coefficient can be determined by optical technique. Details of the experiment are described in the following section.

5.3 The Determination of the Diffusion Coefficient

5.3.1 Numerical Implementation

The experimental setup can be best described as one-dimensional diffusion of small molecule in a gel media. The gel is an isotropic medium, whose structure and diffusion properties in the neighborhood of any point are the same relative to all direction. Because of its symmetry, the diffusing substance is normal to the surface of constante concentration through point, along the z axis. Hence, the chemical gradient and flux across the gel medium can be modeled using Fick's law. For this, the mass balance on a thin layer Δz located at some arbitrary position z within the gel media must be considered as shown below:

Solute accumulation	=	Rate of diffusion into the layer at z	-	Rate of diffusion out of the layer at $z + \Delta z$	-	Mass adsorbed onto media inside the layer

Note that the gel has a capacity to retain a small fraction of chromium by adsorbing chromium inside the gel medium (Lakatos et al., 1998). Thus, adsorption phase must be included in the mass balance equation.

In mathematical terms, this is

$$\frac{\partial C}{\partial t} = j_z - j_{z+\Delta z} - \frac{\rho}{\theta}\frac{\partial S}{\partial t} \tag{5.1}$$

Where S is a concentration of chemicals adsorbed, ρ is a bulk density and θ is a porosity.

Assuming a linear relationship between the chromium to colloidal silica gel (Lakatos et al., 1998). The third term on the right hand side represent the change in concentration in the water caused by adsorption. This term can be interpreted in terms of:

$$\frac{\rho}{\theta}\frac{\partial S}{\partial t} = \frac{\rho}{\theta}\frac{\partial S}{\partial C}\frac{\partial C}{\partial t} \tag{5.2}$$

Assuming the concentration of chemicals adsorbed, S, is directly proportional to the concentration of substance free to diffusion, C.

$$K = \frac{\partial S}{\partial C} \tag{5.3}$$

The diffusion of ions in polymer and gel depends mainly on gel's geometry (Axel, 1998). Thus, it is assume that at a constant gel geometric and same amount of mass in

the system, diffusivity of chromium in colloidal silica gel, D, is constant. For, the application of Fick's law, the mass balance Equation (5.1) reduces to:

$$\frac{\partial C}{\partial t} = D\frac{\partial^2 C}{\partial z^2} - \frac{\rho}{\theta}\frac{\partial S}{\partial C}\frac{\partial C}{\partial t} \tag{5.4}$$

$$\frac{\partial C}{\partial t} = \frac{D}{1+\frac{\rho}{\theta}K}\frac{\partial^2 C}{\partial z^2}$$

A new constants diffusion coefficient D_{total} can be defined where.

$$D_{total} = \frac{D}{1+\frac{\rho}{\theta}K} \tag{5.5}$$

Thus the above equation becomes.

$$\frac{\partial C}{\partial t} = D_{total}\frac{\partial^2 C}{\partial z^2} \tag{5.6}$$

Equation (5.6) is used with the appropriate boundary condition to analyze the data obtained from digital photography and to determine the diffusion coefficient. Details of numerical analysis of Equation (5.6) are given below.

5.3.2 Numerical Solution

In this study, the problem is assumed as a one-dimensional diffusion with constant diffusivity in an infinite length medium. This is graphically shown in Figure 5.4, where the two media in the system are water and gel. The color intensity represents the chemical concentration. The concentration is originally equal to C_0 in water and equal to

zero in the gel. The chemical profile shows the movement of chemical from water to gel after some time. It can be seen that the concentration is higher in water ($z = -\infty$ to $z = 0$), and reduces upon entering into the gel media ($z > 0$), until reaching zero at a distance equal to infinity ($z = \infty$).

The following assumptions were made in the analysis.

1. Transport occurs in two different media that are water, $-\infty < z < 0$, and gel, $0 < z < \infty$.
2. Transport is controlled only by diffusion and adsorption (no advection).
3. The interface resistance, where the initial concentration of chemical entering the gel media is equal to a fraction of the chemical concentration in water and gel. This fraction is called partition coefficient. The interface resistance might transpire from: 1) the diffusion coefficients differences, 2) the mole fraction between two media (Crank, 1979) and 3) the sorption on surface (Hemond & Fechner-Levy, 2000).

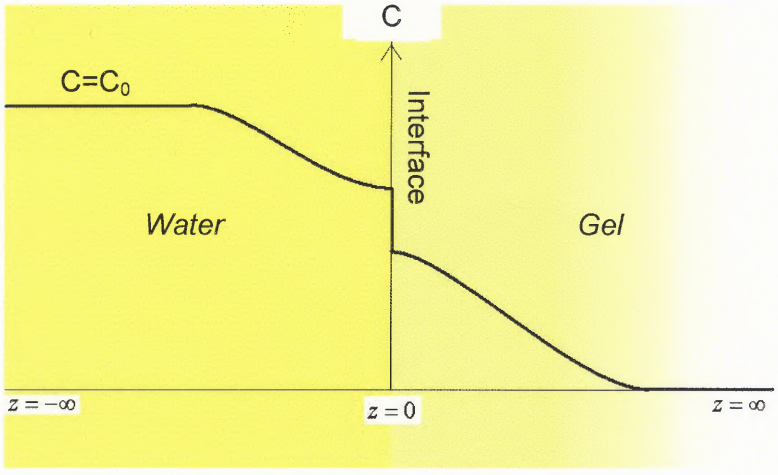

Figure 5.4 The Experimental Condition.

4. It is assumed that chemical concentration at the two ends of the cell, $z = \infty$, is zero and , $z = -\infty$, is C_0 throughout the experiment (Dunmire et al., 1999). In other words, the beds, both water and gel phases, are similar to an infinite slab (Crank, 1979). Thus, the cell can be assumed to be semi-infinite. Note that this condition is enforced by restricting the duration of the experiments.
5. The diffusion coefficient of chemical in both water and gel are constant.

Using the above assumptions, it is reasonable to state that the diffusion occurred during the experiment is based on Fick's Law as shown in Equation (5.6). The mass balance was solved using Laplace Transformation (Crank, 1979), and the solution was used to calculate the diffusion coefficient from the data obtained from the digital photography technique.

Following the experiment conditions and Equation (5.6), the numerical equation for diffusion in a gel media, $0 < z < \infty$, can be written as:

$$\frac{dC}{dt} = D \frac{d^2C}{dz^2} \tag{5.7}$$

Note that D in this equation is equal to D_{total} in Equation (5.6).

The initial boundary conditions can be written as:

$$C = 0, \qquad t = 0 \qquad 0 < z < \infty$$

$$C = C_0, \qquad t \geq 0 \qquad z = 0$$

Equation (5.7) can be solved by Laplace transformation by first multiplying both sides by e^{-pt} and integrating with respect to t from 0 to ∞. The right hand side of Equation (5.7) becomes.

$$\int_0^\infty e^{-pt}\frac{dC}{dt} = \left[Ce^{-pt}\right]_0^\infty + p\int_0^\infty e^{-pt}Cdt = p\overline{C}$$

Please note that the square bracket vanishes by applying initial condition of $t = 0$ to $t = \infty$.

And the left hand side of Equation (5.7) becomes:

$$D\int_0^\infty e^{-pt}\frac{d^2C}{dz^2} = D\frac{\partial^2}{\partial z^2}\int_0^\infty e^{-pt}Cdt = D\frac{\partial^2\overline{C}}{\partial z^2}$$

Which can be rewritten as:

$$p\overline{C} = D\frac{\partial^2\overline{C}}{\partial z^2}$$

Applying the boundary condition:

$$\overline{C} = \int_0^\infty C_0 e^{-pt}dt = \frac{C_0}{p} \qquad \text{at } z = 0$$

Also:

$$\overline{C} = \frac{C_0}{p}e^{-((\sqrt{p/D})z)}$$

The solution can be integrated, and the result is obtained as:

$$C = C_0 erfc\frac{z}{\sqrt{4Dt}} \tag{5.8}$$

Where $$erf(x) = \frac{2}{\sqrt{\pi}} \int_0^x \exp(-u^2) du$$

$$erfc(x) = 1 - erf(x)$$

From equation (5.8) the diffusion coefficient can be calculated by knowing concentration as function of distance and time. In this research, the calculation was performed by the nonlinear regression using least square optimization method. Additional details about the statistic method are given in section 5.3.4.).

From equation (5.8) the diffusion coefficient can be calculated by knowing concentration as function of distance and time. In this research, the calculation was performed by the nonlinear regression using least square optimization method. Additional details about the statistic method are given in section 5.3.4.

Considering the system with the presence of the two media, water and gel, the boundary condition at the interface, $z = 0$, can be rewritten:

$$\frac{C_{gel}}{C_{water}} = k, \qquad t \geq 0 \qquad z = 0$$

$$D_{gel} \frac{\partial C_{gel}}{\partial x} = D_{water} \frac{\partial C_{water}}{\partial x}; \qquad t \geq 0 \qquad z = 0$$

Where k is the ratio of the uniform concentration in the region $z > 0$ to that in $z < 0$ when final equilibrium is attained. C_{gel} is concentration of chemical in a gel phase (can be either concentration of pore water in gel or concentration of total chromium in gel depends on type of diffusion) and C_{water} is concentration of chemical in a water phase.

Note that the use of infinite length for the cell in Equations (5.7) reflects the assumption that the concentration did not change at the ends of the cell. The no-flux

boundary condition at the ends can therefore be replace by the approximation (Dunmire et al., 1999),

$$C_{gel} = 0, \qquad t \geq 0 \qquad z \to \infty$$

$$C_{water} = C_{water_0}, \qquad t \geq 0 \qquad z \to -\infty$$

Equations (5.7) can be solved by Laplace transformation provide the following solution.

$$C_{gel} = \frac{kC_{water_0}}{1 + k(D_{gel} / D_{water})^{\frac{1}{2}}} erfc \frac{z}{\sqrt{4D_{gel}t}} \tag{5.9}$$

$$C_{water} = \frac{C_{water_0}}{1 + k(D_{gel} / D_{water})^{\frac{1}{2}}} \left\{ 1 + k(D_{gel} / D_{water})^{\frac{1}{2}} erfc \frac{z}{\sqrt{4D_{water}t}} \right\} \tag{5.10}$$

Total diffusion coefficient where occur in gel phase, D_{gel}, can be obtained from the experiment. The diffusivity of chromium in water, D_{water}, is available in literature (Clark, 1996; Lakatos et al., 1998; Thibodeaux, 1995). The ratio of the uniform concentration at the interface, k, concentration in gel to concentration in water, can be determined from partition coefficient, K, which was obtained from the adsorption experiment (section 5.4). Thus, the diffusion profile of the two phases can be determined using Equations (5.9) and (5.10). The details of partition coefficient determination are as follows.

5.3.3 Partition Coefficient

The occurrence of interface resistance can be explained as follows. If a chemical is in contact with two different phases then it will have a different affinity for each phase. Part of the chemical will be absorbed or dissolved by one phase and the rest by the other. The relative amounts depend on the relative affinities. The ratio of concentrations at the boundary in each medium is defined as the partition or distribution coefficient of the system. The partition law states that this ratio is a constant for a given system (Xrefer Inc., 2002).

In a water-gel system, a chemical has different affinities to water and gel. The partition coefficient, K, is defined as the ratio of chemical concentration in the barrier region to that in the gel. The partition coefficient can be calculated as a function of chemical potential (Sunderrajan et al., 1996). This function is characterized by the partition coefficient as illustrated below.

$$K = \frac{S}{C} \tag{5.11}$$

The partition coefficient can be determined experimentally through isotherms (Mackay, 2001; Thibodeaux, 1996). The partition coefficient of the system was obtained from the adsorption experiment and will be discussed in section 5.4. This value was used to determine the concentration distribution between the two phases.

5.3.4 Statistical Analysis

Smoother Technique: The concentration values obtained from the experiment varied largely due to the conversion of digital images. Therefore, a statistical analysis was performed to acquire a meaningful set of data from the experimental results. The

approach used in this research is called the " Smoother Technique" (Simonoff, 1996). The smoother technique is a tool for summarizing the trend of a response measurement Y as a function of one or more predictor measurements X_1, ... , X_p. It generates an estimation of the trend that is less variable than Y itself.

An important property of a smoother is its nonparametric nature. It doesn't assume a rigid form for the dependence of Y on X_1, ... , X_p. This technique fits a curve to the data points locally, so that at any point on the curve depends only on the observations at that point and some specified neighboring points. Consequently, the level of smoothing depends on the number of data points used. The result is called a "smooth" because such a fit turns out an estimation of responses that is less variable than the original observed responses. The procedure for obtaining such fits is called "scatter plot smoothers".

There are many smoothing techniques. The common techniques used are Locally Weight Regression Smoother (Loess), Spline, Robust LTS, Robust MM, Kernel and Friedman Super (Simonoff, 1996). Since the "Friedman Super Smoother" is based on local averaging, it is best suited to nonlinear data set (Aboobaker, 2001). In addition, comparing to other techniques, in this research, this method generated the most accurate smoothing result for data obtained from digital photography. Therefore, it was used in this research. Computer software "S-Plus 2000" from MathSoft Engineering & Education Inc. provides the "Friedman Super Smoother" analysis and was used to smooth the data obtained from digital image.

Regression Analysis: A fitting procedure estimates any kind of relationship between a dependent and independent variables is called "Regression". In general, the objective of the regression analysis is to verify the relation between a dependent and independent variables. All regression models can be represented as:

$$y = F(x_1, x_2, ..., x_n)$$

The term $F(x_1, x_2, ..., x_n)$ in the above equation can be translated such that the dependent "y", is a function of the independent variables "$x_1, x_2, ..., x_n$," (Motulsky, 1996).

Two types of regressions were used in this research, multiple regression and nonlinear regression. The details of the regression analysis in determining the diffusion coefficient are explained as follow.

Multiple regression: In the case where there is more than one independent variable, the regression cannot be visualized in two-dimensional space, but can be computed. The multiple regression procedure will estimate a linear equation in the form:

$$y = F(x_1, x_2, ..., x_n) = a + b_1 x_1 + b_2 x_2 +, ..., + b_n x_n$$

The regression coefficients, b_i, represent the independent contributions of each independent variable, x_i, to predict the dependent variable, y.

Multiple regression analysis was performed to obtain chemical concentration from color intensity. A digital color image is a mixture of different brightness levels of blue, green and red. The calibration for concentration gradient from color intensity depends on the combination of these three colors. Therefore, the regression equation can be written as:

Concentration = a + $b_1 \cdot$ Blue Intensity + $b_2 \cdot$ Green Intensity + $b_3 \cdot$ Red Intensity

The above equation transformed color intensity data received from digital images to concentration data. The concentration data is then used in determining the diffusion coefficient (see section 5.4.4).

Nonlinear regression: When the relationship between the independent and dependent variables is nonlinear, the fitting procedure called "nonlinear regression" is performed. The nonlinear regression is more complicated than the linear regression. A common method used for nonlinear regression is called the "least square estimation". The least square estimation aims to minimize the sum of square deviations of the observed values from those predicted by the model. Nonlinear regression works by varying the values of the variables to minimize the sum-of-squares.

The nonlinear regression by least squares estimation can be performed by following the steps shown below (StatSoft Inc., 2002):

1. Assume a model and an initial estimated value for each variable in the equation.
2. Generate the curve defined by the initial values.
3. Calculate the sum-of-squares of the difference between the observed and the predicted values.
4. Adjust the variables in the model to make the calculated curve overlap the data points by increasing the number of the original value. Keep adjusting the variables until there is virtually no difference in the value of sum-of-squares.
5. Report the best-fit results. The accuracy depends on the predicted model, the initial values used in step 1 and the stopping criteria of step 4.

In this research, the model was defined as Equation (5.8) which unknown variable D. Equation (5.8) has the *erfc* term or an "Error Function". Normally, the commercial statistic software provides the function that can be used to calculate both linear and nonlinear regression. However, the error function is a nonlinear scientific function that cannot be directly calculated by computer-generated functions. Thus, manual calculations were needed following the steps mentioned above. The variable, D, was adjusted by increasing the number 1/100 of the original value until sum of square was minimum using "solver" in Microsoft® Excel 2000. Solver is an add-ins macro that used for optimization. In this case, it found the best D value that gives the minimum sum of square. Beside the sum of square, the best fit for the regression was able to evaluate by using statistic tool described below (Allen, 1997; Bates & Watts, 1988).

Evaluating the Fit of the Model: After estimating the regression parameters, an essential aspect of the analysis is to test the appropriateness of the overall model. A statistic test is required to verify the model fit for the reliable dependent parameter of the data. Many different tools and methods may be used to perform the test. The following steps are commonly performed to evaluate the fit of the models in the least squares method.

1. Residual: Residual is a difference between the observed values and the corresponding values that are predicted from the model. The smaller residual values will yield more precise (or accurate) predictions.
2. R^2: R^2 or *coefficient of determination* is an indicator of how well the model fits the data. An *R-square* close to 1.0 indicates that the independent variables are closely related to the dependent variables. It can be calculated by the following equations.

R^2 = 1-SSE/SST

Where SST = error sum of squares = $(\sum y^2_{observation}) - \frac{(\sum y_{observation})^2}{n}$

SSE = some of square = $\sum (y_{observation} - y_{predictiction})^2$

3. Goodness-of-fit, Chi-square: The Chi-square test is the test of significance based on the "chi-square statistics". The statistics are related to the weighted sum of squares of differences between the observed and the predicted. If the *p*- level associated with this Chi-square is significant, then the regression parameters are statistically significant.
4. Plot of Observed vs. Predicted Values: A visual comparison between a scattered plot of predictions vs. observed values would be able to assess the fit of the model. If the model appropriate for the data, the prediction plot would align to the observation plot.

In this research, the residual and the plot of observed vs. predicted values were used as a tool to evaluate the fit of the model. The difference between experimental data and model were determined to find the best fit, both data were plotted and compared visually.

5.4 Experiment

Laboratory tests were conducted to obtain the diffusion and partition coefficients of chromium in colloidal silica gel. Five sets of experiments were performed. Experimental details including objectives, materials, methods, and results are described in the following sections.

5.4.1 Objectives

The diffusivity of chromium in colloidal silica gel depends on many factors. Kim (1999), Lakatos et al. (1998) and Moridis et al. (1998) showed that the important factors that influence to the diffusion coefficient are silica content in gel, gelation time and initial chemical concentration. Therefore effects of these factors on chromium transport in colloidal silica gel were investigated using the optical method described before.

Five sets of experiments were performed; 1) the measurement of partition coefficient, 2) the diffusion coefficient of chromium in gel with different silica contents, 3) the diffusion coefficient of chromium in gel with different initial concentrations 4) the diffusion coefficient of chromium in gel with different gelling times and 5) a confirmation test for the reliability of the digital photography technique.

5.4.2 Material

Materials used in this experiment are colloidal silica, calcium chloride and chromium solution.

Colloidal Silica: Colloidal silica used in the experiments is NYACOL DP5110. It was specially made for the demonstration site (Viscous Barrier) at Brook Heaven National Laboratory. NYACOL DP5110 is a mixture of colloidal silica, water, anti-freeze and alkaline material. The alkaline material was added to establish a buffer property that makes the colloidal silica works in stabilizing the soil with little contribution from soil pH. Four liters of NYACOL DP5110 were provided by Eka Chemical Inc.. NYACOL DP5110 cost $0.68/lb. or $374.00 for a 550 lbs drum (Matthew C. Reed, Akzo Nobel / Eka Chemicals, personal communication). The physical properties of this colloidal silica are as follows:

Density	1.205 gm/ml
Silica content	30 % by weight (300 gm/liter)
pH	9
Viscosity	9.5 cps.

Calcium Chloride ($CaCl_2$): Reagent grade calcium chloride dihydrate from Fisher Scientific was used as a destabilizer. The ratio of one part of 1.0 mole/liter calcium chloride to four parts of 300 gm/liter by weight colloidal silica is required to destabilized colloidal silica to form a gel within three hours (Heisher at al., 1998). One mole/liter calcium chloride solution was prepared and used throughout the experiment.

Chromium Solution (Cr(VI)): Reagent grade potassium dichromate crystal, $K_2Cr_2O_7$, from Malinckrodt Inc. was mixed to form the chromium solution. The crystals were dried at 103^0C then transferred to a desiccator prior to use. A 1000 mg/liter, pH 7, of chromium stock solution was prepared and used throughout the experiments. Note that the solubility of potassium dichromate is 1.5×10^4 mg/liter at pH 7, 25°C (MINEQL+ V4.5, Environmental Research Software).

5.4.3 Method

The experimental methods are as the following.

The Measurement of Partition Coefficient: The sorption of chromium in colloidal silica gel was assumed linear. This assumption needs to be verified. Thus, the adsorption experiment was conducted. The partition coefficient of chromium in water and gel is required in order to solve Equations (5.9) and (5.10). The results are the concentration profile of chromium in water and gel phase.

Colloidal silica, NYACOL DP5110, 300 gm/liter was mixed with 1.0 mole/liter $CaCl_2$ 4:1 by volume (0.2 mole $CaCl_2$: 0.8 liter NYACOL DP5110in 1 liter solution). After mixing, 0.5 grams of solution was transferred to 50 ml clear plastic tube. The gelation time was expected to be three hours (Manchester et al., 2001). The gel samples were left for another 24 hours after the initial gelation to ensure that the solution is completely set before the measurements were taken.

Once the colloidal silica gel was set, 20 ml of chromium solution at different concentrations were added to the gel. Chromium addition ranged from 10^{-8} to 10^{-2} mole/liter. $NaNO_3$ was added to maintain ionic strength at 10^{-3} mole/liter. pH of the solution was kept at 7. The samples were shaken at 150 rpm at 20 ^{0}C for up to 72 hours. The samples were taken and chromium concentrations were measured using atomic absorption spectrophotometer (AAS), Perkin Elmer 370, for samples with chromium concentration higher than 10^{-3} mg/liter, and atomic absorption graphite furnace (AAGF), Perkin Elmer 4110ZL, for the rest of samples. The measurements were performed for a range of contact times (1, 3, 6, 12, 24, 48 and 72 hours).

The experiment to study the optimum adsorption pH of chromium to colloidal silica gel was conduct at pH range 3 to10. pH of the solution was adjusted before adding to the gel. Chromium concentration used in this experiment was 1000 mg/l. After shaken at 150 rpm at 20 ^{0}C for 72 hours, the samples were taken and chromium concentrations were measured using AAS Perkin Elmer 370.

The Measurement with Different Silica Contents: The amount of colloidal silica used is one factor that controls the project cost. By knowing the relationship between silica content and diffusion coefficient one could optimize the project cost. Besides the optimization, Kim (1999) and Zulaski et al., (2001) showed that direct injection would produce a concentration profile of gel in soil. Hence, the diffusion and partition

coefficients values obtained from this experiment will provide a better prediction of chromium transport where there is a gel concentration profile.

The impact of silica content relative to the diffusion coefficient was investigated for five silica concentrations, 240, 210, 180, 150 and 120 gm/liter. The concentration gradients were observed by taking digital photographs at the set time intervals for each concentration. The gel mixture was prepared with the same ratio as the previous experiment. During the experiment, the temperature was maintained at 20°C. Different silica concentrations were prepared by mixing colloidal silica solution with different amounts of de-ionized water. After preparing, 2 ml of the colloidal silica solutions with different silica concentration were transferred to 5 ml clear plastic vial. The gel samples were left for another 24 hours after initial gelation before the measurements.

The calibration curves were prepared for each gel concentration by mixing the gel with various amounts of chromium to obtain the desired concentration, then transferring them to vials. The partial concentrations of chromium used were 200, 180, 160, 140, 120, 100, 80, 60, 40, 20 and 0 mg chromium/gm of gel, respectively. This range was based on the result from the adsorption experiment (see section 5.4.4) and the concentration of chromium leached from the ore processing residue (Chapter 6.) which reveal that chromium sorbed to colloidal silica gel in the environment was about 80 mg/gm.

Once the colloidal silica gel was set, 0.20 mg chromium (in 1 cm^3 water) was added to the set gel in a plastic vial and the diffusion from aqueous phase to gel phase was observed and captured. Pictures of the vials were taken using a digital camera (Olympus Digital Camera D-460 zoom) at every ten minutes for 360 minutes to record the color change with time. The resolution of the pictures taken was 1600X1200 pixels. For the set up used in the experiment, 1 cm contains approximately 300 pixels (1 pixel $\cong$ $3.3x10^{-5}$ m). Pictures were then downloaded and analyzed for the color intensity

changes corresponding to the travel distance of chromium. Color intensity from digital image was converted to numerical value using a computer software "SigmaScan Pro" from Sigma Inc.. Later, the color intensity data were converted to concentration values using calibration curves. The chemical concentration entering gel was determined using Equation (5.11) and the partition coefficient obtained from the previous experiment. Thus, the diffusion coefficient, D, can be determined by least square optimization for the best fit of the mass balance solution (Equation(5.8)).

The Measurement with Different Initial Chromium Concentrations: In this experiment, the impact of initial chemical concentration to the diffusion coefficient is explored. From equation (5.7), the initial chemical concentration, C_0, is the function of the diffusion gradient. It is necessary to clarify this correlation for a better understanding of transport mechanism. In addition, in the application of the stabilization process, the site property in terms of chromium concentration is varies. Knowing the effect of initial chromium concentration to the diffusion coefficient provides the greater predict to the transport of chromium in the environment. The effect of initial concentration on the diffusion coefficient is investigated in this experiment.

The preparation of colloidal silica gel and the diffusion measurement is similar to the first experiment except silica concentration 240 gm/liter in the gel was used throughout the experiment. Chromium solutions at different concentrations were added to set colloidal silica gel in plastic vials as described in previous experiment. The chromium concentrations used were 200, 180, 160 140 and 120 mg/liter. These values were chosen as they were on the linear portion of the calibration curve. The color changes were observed and captured in the same manner as described in the previous set of experiment.

The Measurement with Different Gelation Times: The gelation time takes approximately three hours (Manchester et al., 2001). However, with longer settling time the gel becomes harder (Iler, 1989). The proposed experiment started after the colloidal silica gel was set. Therefore, tests were performed at different gelation times ranging from 3 to 48 hours.

The preparation of colloidal silica gel and diffusion measurements were the same as described before. A silica concentration in the gel at 240 gm/litter was used for this test. The gelation time was different for each sample and varied from 3, 6, 12, 18, 24 and 48 hours. After the required gelation time was reached, 0.20 mg chromium solution was added to colloidal silica gel in plastic vials. Then, the observation and data collection were preceded as described before.

Confirmation Test to Evaluate the Reliability of Measurements: It is uncertain whether the concentration profiles obtained from the optical method by converting color intensity using the calibration curve may result in precise values without direct measurement. Hence, this experiment was intended to confirm the reliability of the optical method. The experiment was performed by analyzing chemicals in the solution with direct measurement (atomic adsorption method). The results were compared to those obtained from the digital photography method.

The preparation of colloidal silica gel and the instruments used are similar to previous experiments. Silica concentration at 240 gm/litter in the gel was used for every sample. However, the allowed diffusion time was different for each sample. It varied from 30, 60, 90, 120, 150 to 180 minutes. After the required gelation time was reached, 0.20 mg chromium (in 1 cm^3 water) was added to colloidal silica gel in plastic vial. Data collection proceeded as described before. At the end of desired diffusion time, a sample of chromium solution was taken from the vial for the analysis after a picture was taken.

Chromium in samples were analyzed by AAGF, Perkin Elmer 4110ZL, (EPA method 7191).

5.4.4 Results

Details of five experimental results are as follows.

The Measurement of Partition Coefficient: The amount of Cr(VI) in solution after sorbed to colloidal silica gel was measured to assess the adsorption isotherm and partition coefficient. The speciation of chromium in the experiment is shown in Figure 5.5. The majors species of chromium in the system, $C_T=10^{-2}$ mole/liter, Ionic strength=10^{-3} mole/liter, $P_{CO_2}=10^{-3.5}$ atm, $CaCl_2$=0.25 mole/liter, SiO_2=4.8 mole/liter, are CrO_4^{2-}, $Cr_2O_7^{2-}$ and $CaCrO_4^{-}$.

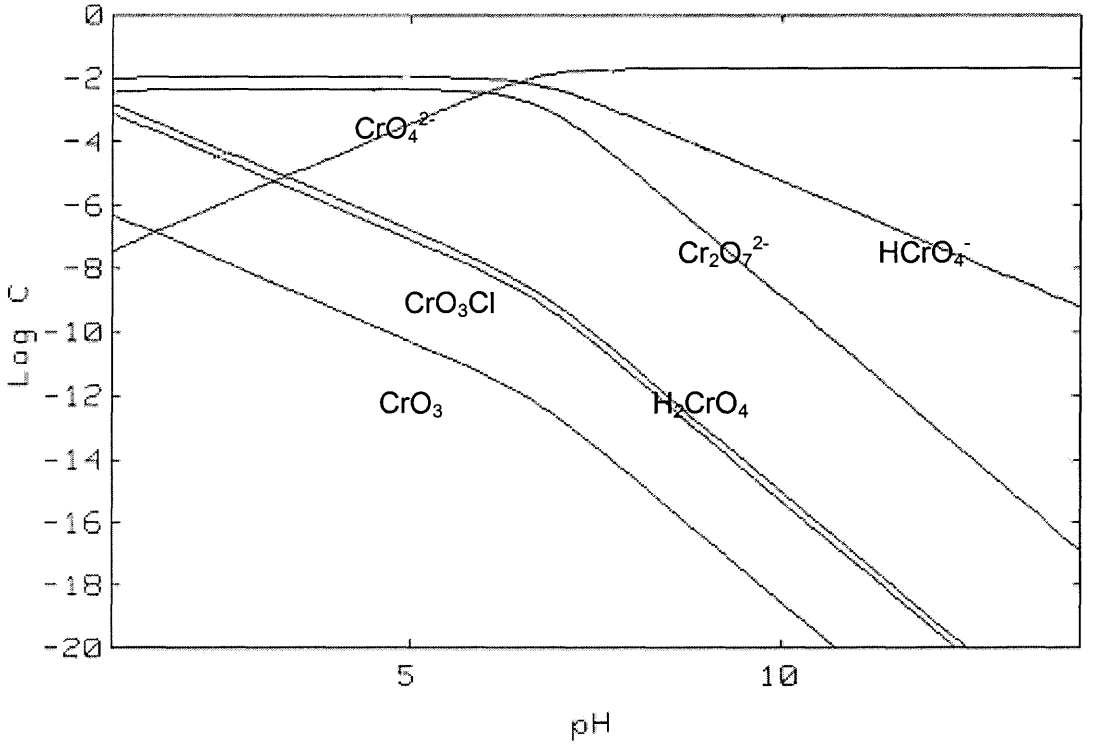

Figure 5.5 Equilibrium Diagram of Cr(VI) as a Function of pH, $C_T=10^{-2}$ M., Ionic strength=10^{-3} M., $P_{CO_2}=10^{-3.5}$ atm, $CaCl_2$=0.25 M., SiO_2=4.8 M..

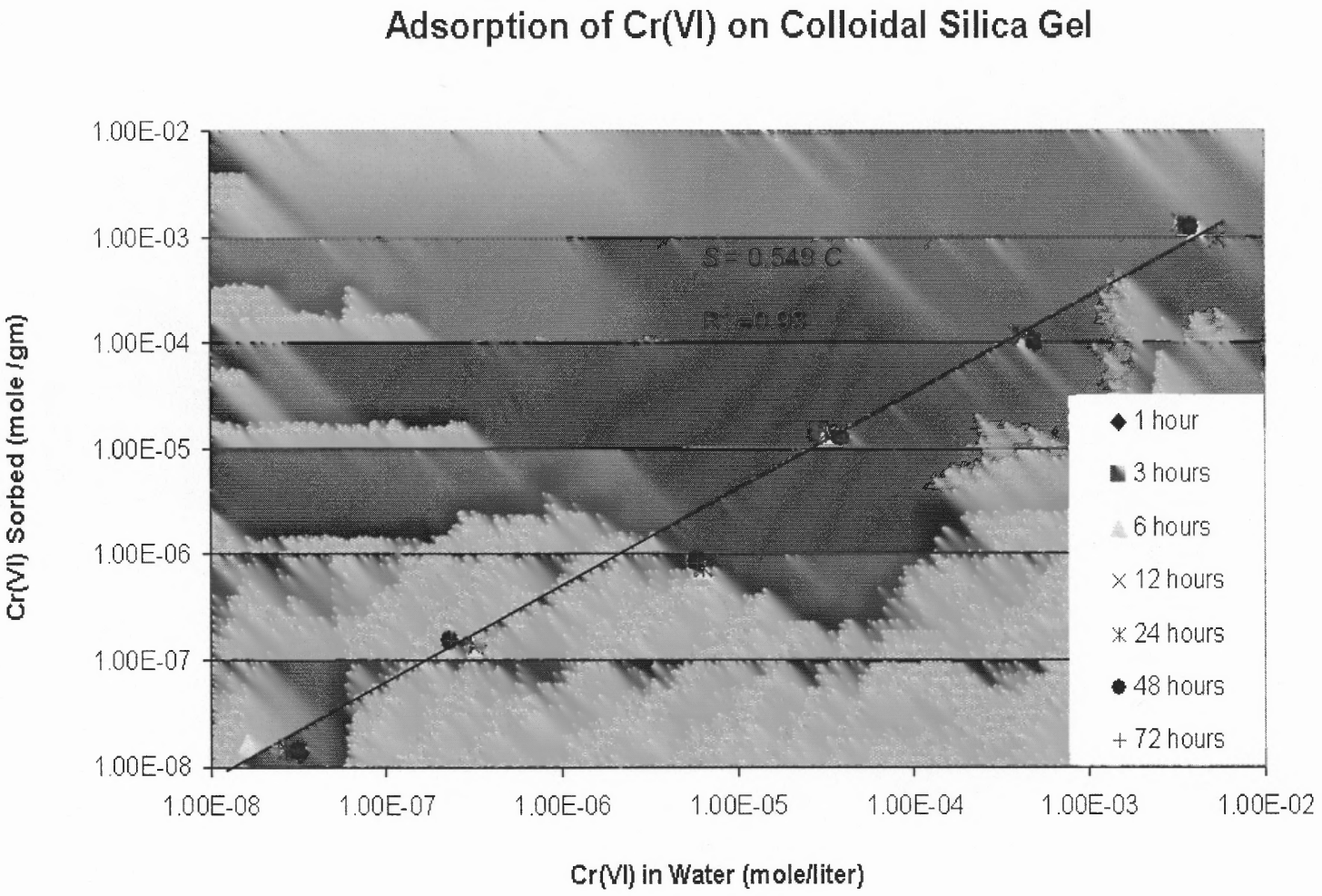

Figure 5.6 Isotherm of Chromium Sorption to Colloidal Silica Gel,

Ionic strength=10^{-3} M., $P_{CO_2}=10^{-3.5}$ atm, $CaCl_2$=0.25 M., SiO_2=4.8 gm/l, pH 7, Temp = 20 °C.

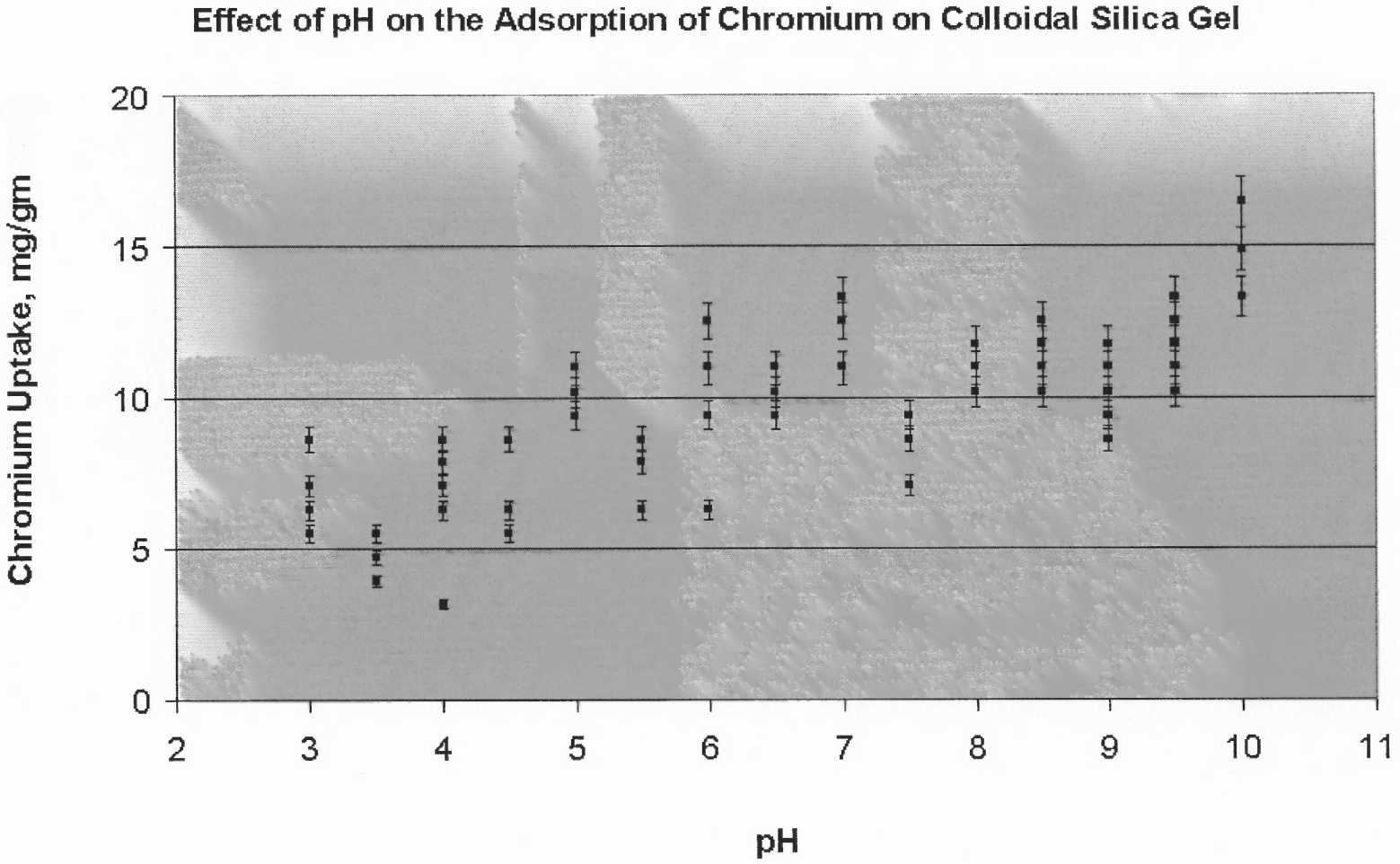

Figure 5.7 Effect of pH to the Sorption of Chromium to Colloidal Silica Gel.

C_T= 3.4x10^{-2} M, Ionic strength=10^{-3} M., P_{CO_2}=$10^{-3.5}$ atm, $CaCl_2$=0.25 M., SiO_2=4.8 gm/l, Temp = 20 °C.

From Figure 5.5, chromium species sorbed to colloidal silica gel in the experimental pH, 7, is dichromate. Cr(VI) in solution was measured and plotted on log-log scale. The experimental results (Figure 5.6) show that there is no differences in the amount Cr(VI) sorbed between 1 and 72 hours. This suggests that the sorption reached equilibrium within one hour. The isotherm was found to be linear over six orders of magnitude chromium concentration. The partition coefficient of chromium to gel in water calculated from linear regression was found to be K = 0.549 liter/gm with R^2 =0.93.

The effect of pH to adsorption is shown in Figure 5.7. The adsorption is increasing with pH. However, Cr(VI) speciation also a function of pH. Thus, the partition coefficient of chromium to colloidal silica gel is therefore pH dependent.

The assumption of the mass balance is based on the linear adsorption isotherm (section 5.3.1). Thus, Equation (5.8) is valid for the experiment condition.

The Calibration Curve: Different concentrations of chromium produced various degrees of colors intensity as shown in Figure 5.8. In these samples, silica content was 240 gm/liter and the chromium concentration varied from 0 to 200 mg Cr/gm gel. The higher the concentration the greater the yellow color.

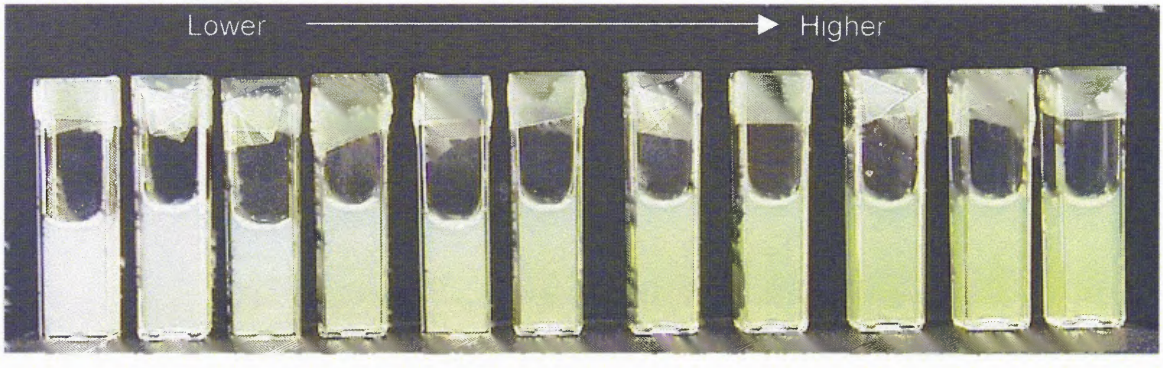

Figure 5.8 Calibration Samples.

From Figure 5.9, color intensity is linearly proportional to chromium concentration up to 300 mg/gm gel. After the color is saturated at concentration of chromium in gel greater than 300 mg/gm gel, the reading of blue color intensity from digital image yields the constant value. Thus, the concentration used in the experiment, 200 mg/gm gel, was chosen since it is in the linear range.

Calibration curves for different gel concentrations were developed for each silica concentration. Silica content used in the calibration curves were 240, 210, 180, 150 and 120 gm/liter by weight. The measured color intensity in a mixture of the three main colors: green, red and blue, was evaluated with multiple regression to determine the calibration curves. Multiple regression was conducted in Microsoft® Excel.

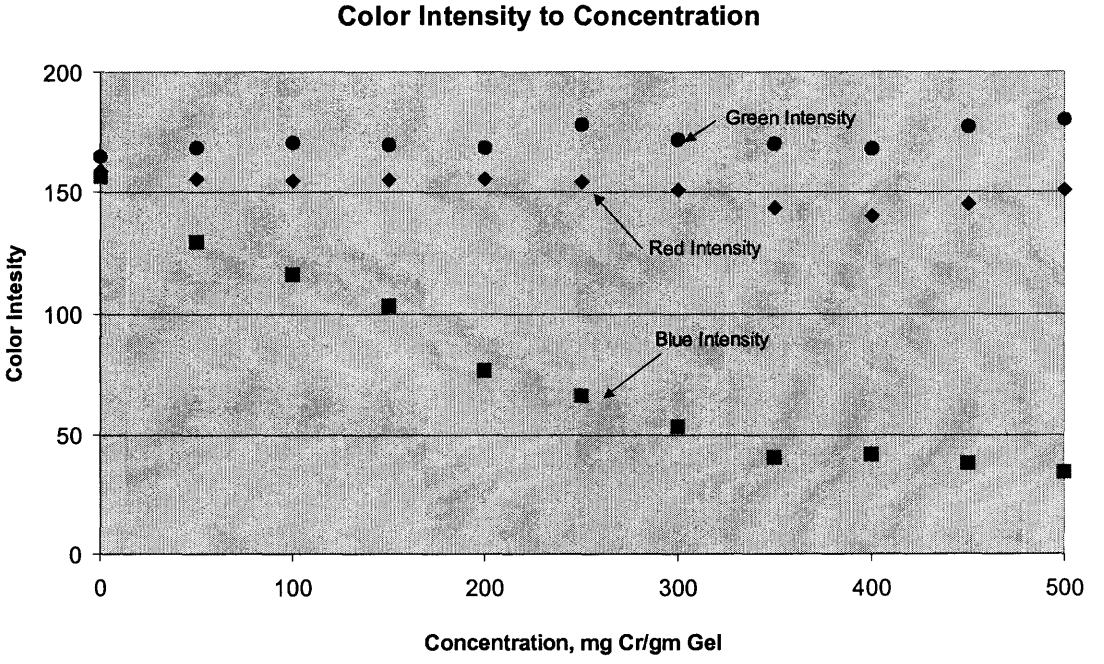

Figure 5.9 Color Saturation at High Chromium Concentration.

The concentration value obtained from each calibration curve was compared to their actual value as shown in Figure 5.10. The calibration shows high correlation between chromium concentration and color intensity, from the regression for 240 to 120 gm/liter of silica in the gel, the R^2 are 0.997, 0.968, 0.988 and 0.973 and the error are 3.51%, 6.27%, 7.08% and 6.88% respectively.

As can been seen from Figure 5.11, for different gel concentrations, similar color intensity values were obtained for each chromium concentration. This indicated that there is no variation between various gel concentrations and the color intensity calibration. In other words, average calibration curves appear to be accurate for all gel concentration. However, for greater accuracy, specific calibration curves were used for each silica concentration to determine the chemical concentration in gel.

The Measurement of Diffusion Coefficient: The diffusion was initiated by adding 0.20 mg chromium (in 1 cm^3 water) to colloidal silica gel in plastic vial. Digital photos were taken at ten minutes intervals for 360 minutes. The pictures were analyzed to obtain the change in color with depth (cm) (see Figure 5.12). Lastly, color intensities at different vertical location in "z" direction were also determined by assuming that the beginning point of diffusion, $z = 0$, at the top of the gel.

This experiment is not error free. Some of the errors that might be encountered during the analysis of the digital images are from capillary action and wall effects. Due to its high viscosity that yielded high surface tension, colloidal silica mixture created a curve as shown in Figure 5.12. In addition, wall effects may produce higher concentrations at the vial walls.

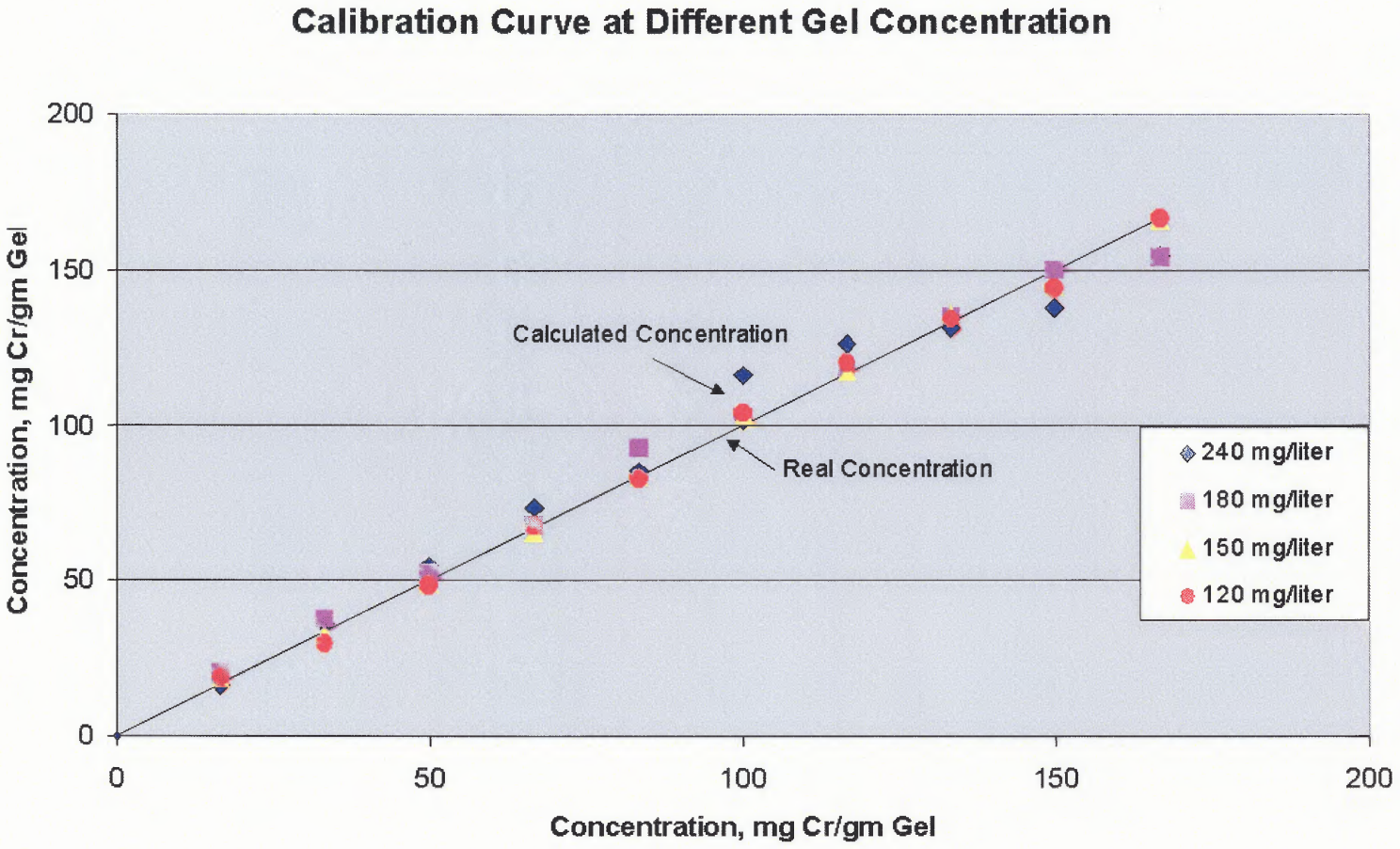

Figure 5.10 Comparison of the Predicted and Measured Concentration from the Calibration Curve.

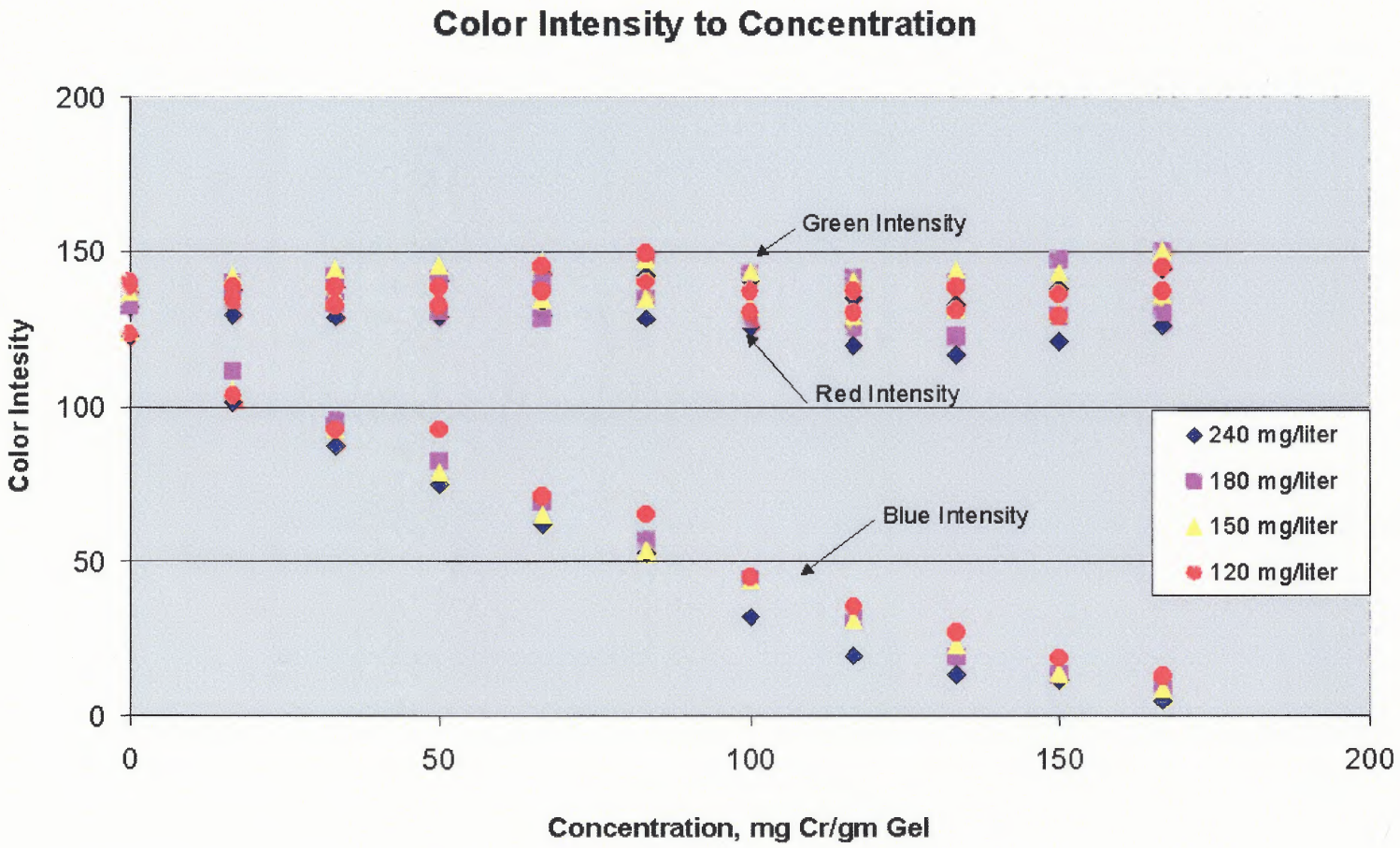

Figure 5.11 Comparison of Different Color Intensities Used in Calibration Curve.

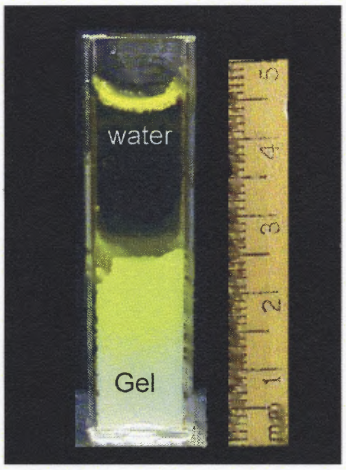

Figure 5.12 The Digital Image of the Diffusion.

However, proper measurements may circumvent these errors. For example, measuring the color intensity at the middle of the gel medium could eliminate these problems. Also, the plane perpendicular to "z" direction is required to be large relative to the "z" distance. The size of the raster image collected comes into play here. The higher the resolution the larger the perpendicular plane becomes. The digital images collected in this experiment have the resolution of 1600 and 1200 pixels horizontal and vertical respectively. The measurement of color intensity along the z direction is along vertical direction, which has 1200 pixels for the size of 4 cm. This yielded the resolution of 300 pixel/cm (1 pixel $\cong$ 3.3×10^{-5} m).

To ensure that the length of the vertical plane was great enough to eliminate wall effects, the color intensity measurement was taken around the center of the vial. For each image, the measurement was taken seven adjacent vertical lines with each line containing 150 measuring points over the 1.50 cm distance to compute the average value. The data were calibrated and plotted to check for trends of the curves. If the dataset contains outliner, the smoother technique would be applied.

After the color intensity values were acquired, they were converted to concentration using calibration curves. These data sets provided the concentrations at different locations ("z" distance) at different time intervals.

The Measurement with Different Silica Concentrations: The test results for five samples containing different amounts of silica are shown in Figures 5.13, 5.14 and 5.15 and Table 5.2.

Figure 5.13 shows raw data and those predicted using the model for 240 gm/liter silica content. The raw data are averaged over the seven points collected from the digital photograph and converted to concentration using the calibration curve. The diffusion coefficient was determined by least squares method. Diffusion coefficients at six different time intervals, 50, 100, 150, 200, 250, and 300 minutes, were determined to calculate the average value.

There are two ways to verify chromium entering gel, C_0, using partition coefficient obtained from the first experiment and Equations (5.9) and (5.10). First, the concentration in gel, C_{gel}, is considered as a total concentration which is a combination of chromium sorbed on silica surface and chromium in pore water ($C_{gel} = S$). Thus, C_{gel_0} can be calculated from C_{water_0} in Equation (5.9) and partition coefficient in Equation (5.11). The results are shown in Figure 5.13 (a). Second, the concentration in gel, C_{gel}, is considered as concentration of chromium in pore water. Assuming that the system is at equilibrium where adsorption is much faster than diffusion, the concentration of chromium in pore water can be calculated using partition coefficient, in this case, $C_{gel_0} = C_{water_0}$. The results are shown in Figure 5.13 (b). It is clear that the two methods of calculation yield the same diffusion coefficient value.

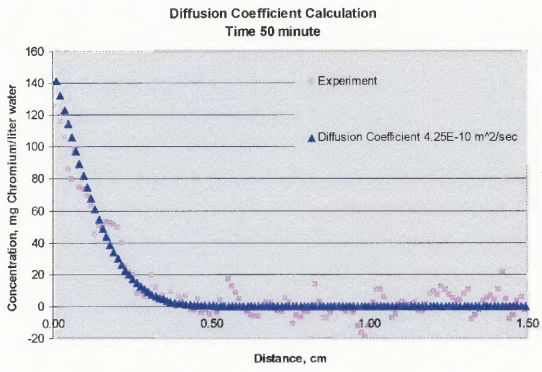

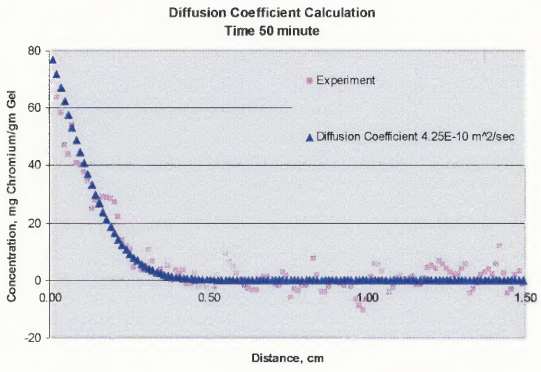

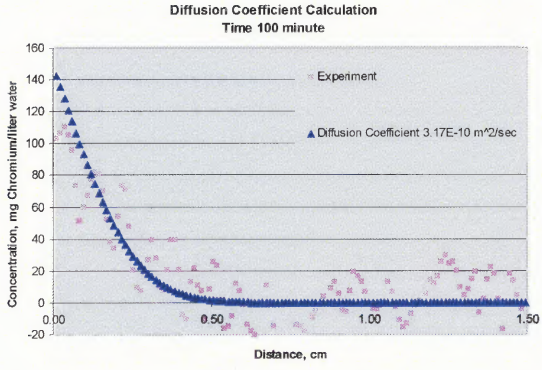

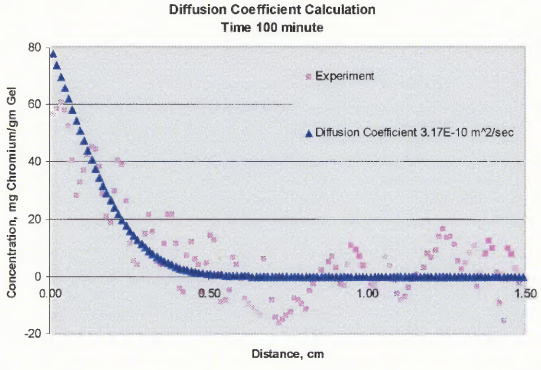

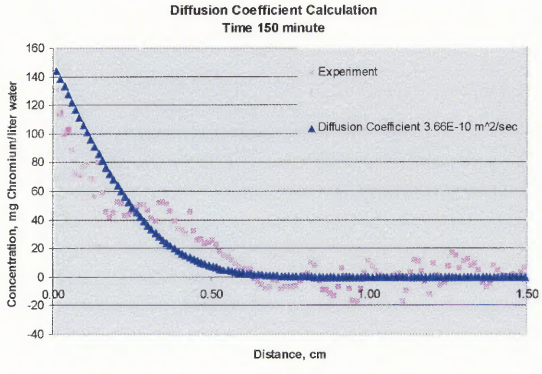

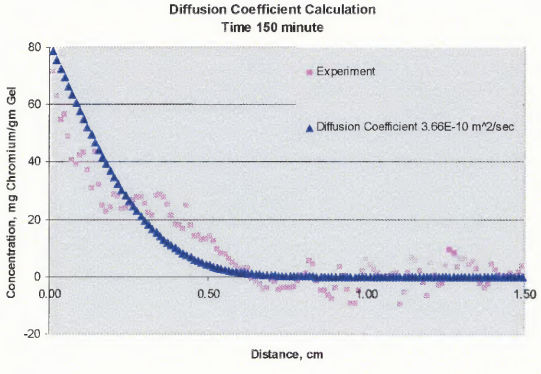

a. Distribution in Pore Water

b. Distribution in Gel

Figure 5.9 The Comparison between Predicted and Real Chemical Concentration.

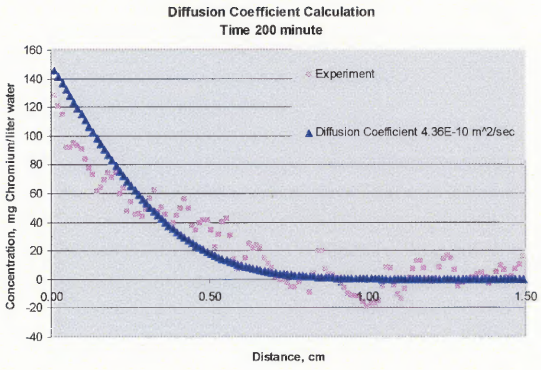

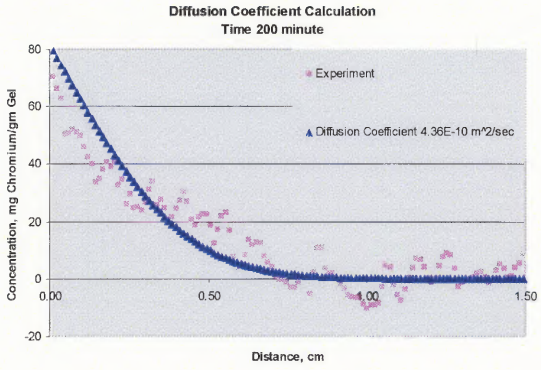

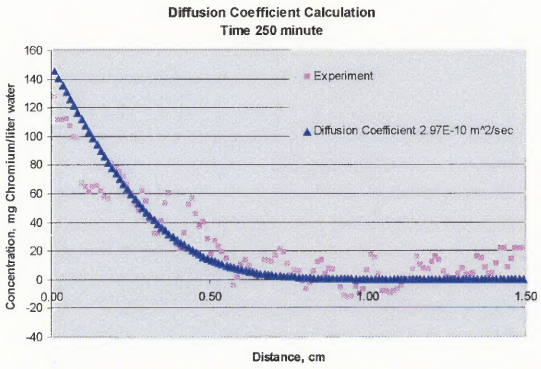

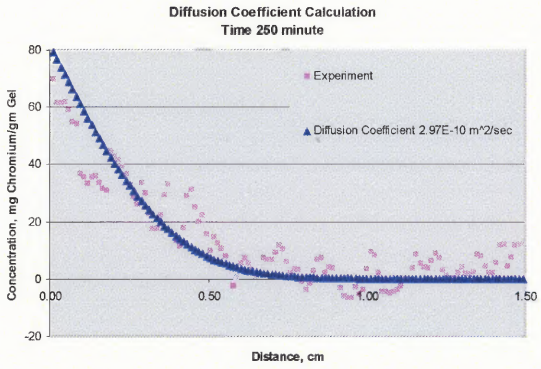

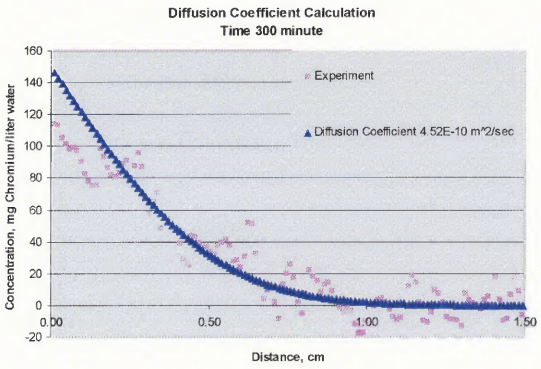

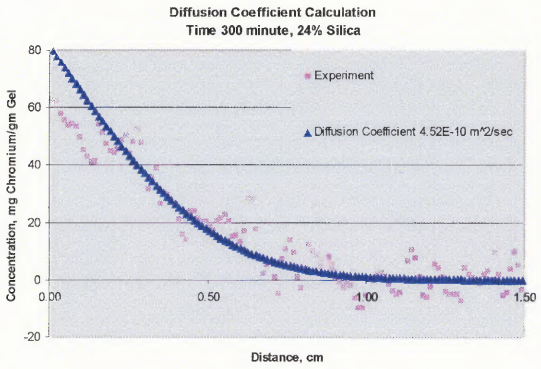

a. Distribution in Pore Water

b. Distribution in Gel

Figure 5.9 The Comparison between Predicted and Real Chemical Concentration (contd.).

Table 5.2 Diffusion Coefficient at Different Silica Concentrations in Gel

Type	Diffusion Coefficient x 10^{-10}, m^2/sec
From Experiment	
Silica Concentration 240 gm/liter	4.91 ± 0.60
Silica Concentration 210 gm/liter	5.39 ± 0.65
Silica Concentration 180 gm/liter	6.44 ± 0.50
Silica Concentration 150 gm/liter	7.16 ± 0.64
Silica Concentration 120 gm/liter	8.48 ± 0.96
From literature (Lakatos et al., 1998)	
CrO_4^{2-} in water	11.90
CrO_4^{2-} in gel (10 gm polymer and 25 gm Si/ liter)	11.00
From literature (Thibodeaux, 1995)	
CrO_4^{2-} in water	11.2
Calculation based on Stoke-Einstein Equation (Clark, 1996)	
CrO_4^{2-} in water	21.6

Table 5.2 compares the results obtained from this study with those reported in the literature. In literature, the diffusion coefficient ranged from 10^{-13} to 10^{-9} m^2/sec (Burke et al., 2000; Dunmire et al., 1999, Masaro & Zhu, 1999; Lakatos et al., 1998; Takahashi et al., 2000). Total diffusivities from this study ranged from 4.91 to 8.48 x 10^{-10} m^2/sec which are comparable.

The variation of the diffusion coefficient with silica content in gel is shown in Figure 5.14. From this Figure, the diffusion coefficient of chromium in gel decreases

linearly with increasing silica content. Lakatos et al. (1998) found a similar relationship. This relationship can be explained using the obstruction effect model (Netz & Dorfüller, 1997).

In this obstruction model, gel chains are regarded as motionless relative to the diffusive molecules. This approximation is based on the assumption that the self-diffusion of polymer/gel is much smaller than that of diffusive molecules. Thus, the presence of the motionless polymer is represented as a fix and impenetrable immersion in the solution. The presence of motionless polymer chains leads to an increase in the mean path of the diffusing molecules between two points in the system (Masaro & Zhu, 1999).

The obstruction effect can also be explained in terms of physical structure. The migration of chromium ions in gels can be described similar to the diffusion of charged

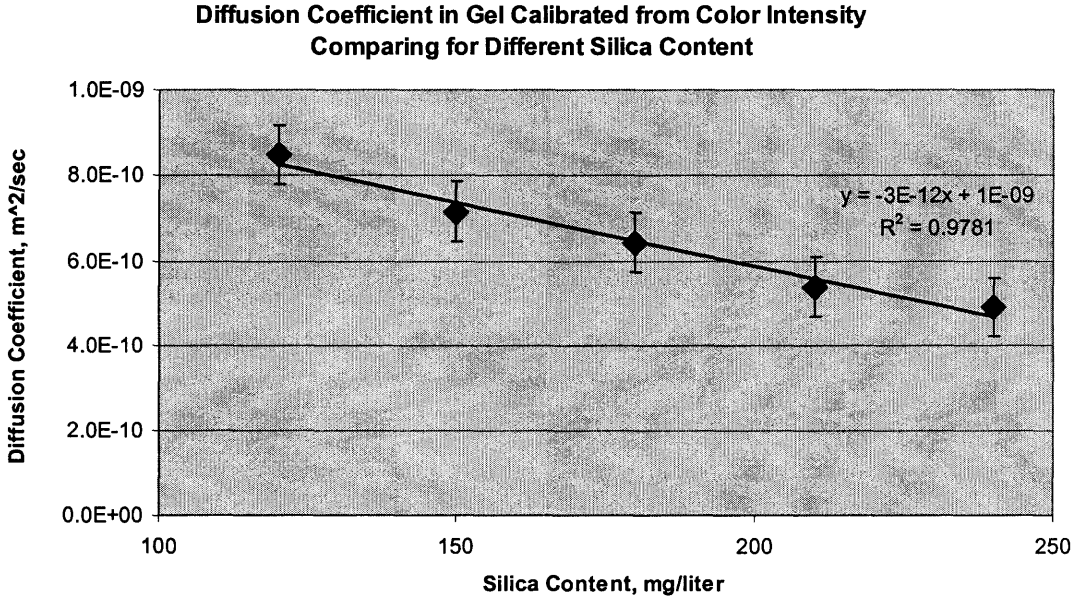

Figure 5.14 The comparison of Diffusion Coefficient at Different Silica Contents.

species in porous media saturated with water. The network of polymerized silicate forms a flexible structure of gel and its "pore space" is filled with solvent, in this case is water (Lakatos et al., 1997).

Colloidal silica gel has a non-uniform structure composed of silica chains and water. Silica chains form a porous network with water inside the pore spaces. The pore size has a wide distribution. The size of pore space depends on the concentration of silica, pH and salt content. The average diameter of colloidal silica gel pore is approximately micropore, $\phi<2.0\text{x}10^{-9}$ m, or mesopore, $2.00\text{x}10^{-9}$ m $<\phi<5.0\ \text{x}10^{-8}$ m (Poon & Haw, 1997) while the size of hydrated chromium ion is $\phi\sim 1.38\text{x}10^{-10}$ m for trivalent chromium and $\phi\sim1.04\text{x}10^{-10}$ m for hexavalent chromium (Lide, 2001), which is ten times smaller than average pore diameter of gel. Therefore, the metal ions transport in gel medium can be seen as small particles movement in water that is in pores of gel network. It is reasonable to assume that during the transport, the obstruction to free movement of chromium can occur inside the pore of the gel.

The diffusion of chromium in gel media can also be defined as Equation (5.5):

$$D_{gel} = \frac{D_{water}}{1+\frac{\rho}{\theta}K}$$

The term $1+\frac{\rho}{\theta}K$ can be defined as the retardation factor due to the transport-sorption (Stumm, 1992). The factor can be calculated based on the experimental results.

From the discussion above, the gel behaves like a porous model with silica network forms continuous solid phase and its pore space is saturated by water. Moreover, diffusion coefficient found ranges $4.91\ \text{x}\ 10^{-10}$ to $8.48\ \text{x}\ 10^{-10}$ m^2/sec which is

one order of magnitude higher than diffusion of ions in water, ranges 1 x 10^{-9} to 2 x 10^{-9} m^2/sec (Freeze & Cherry, 1979). Therefore, the diffusion dominates by bulk diffusion. In other words, it can be characterized as bulk diffusion of chromium ions in porous material with tortuosity. The expression of gel geometry as a function of diffusion coefficient can be written as (Lakatos & Lakatos-Szabó, 1998):

$$\frac{D_{water}}{D_{gel}} = \frac{\tau^2}{\theta} \tag{5.12}$$

The bulk diffusivity of chromium in aqueous phase is known from literature (D = 1.12 x 10^{-9} m^2/sec (Thibodeaux, 1996)). The density of commercial amorphous silica in colloidal silica form is 2.2 to 2.3 gm/cm^3 (Patterson, 1992). Thus, the porosity, the retardation factor and the tortuosity as a function of silica concentration can be determined from Equations (5.5) and (5.12). The calculation result is shown in Figure 5.15. Results shown that porosity of colloidal silica gel ranges from 0.05 to 0.2 which is inversely related to colloidal silica concentration in gel. The retardation factor ranges from 4 to 14 which increases linearly with silica content in gel. Tortuosity ranges from 1.25 to 2 increasing linearly with silica content in gel

The Measurement with Different Initial Chromium Concentrations: The initial chromium concentration also plays an important role in the transport of chromium in gel. Generally, higher initial concentrations will result in larger concentration gradients causing a greater flux of the chemical. It was note that the chemical concentration in solute is an important variable affecting the diffusion coefficient (Rutherford, 200; Stumm 1992; Chen & Yang, 1998). This experiment was conducted to observe the effect of initial chemical concentration on diffusion.

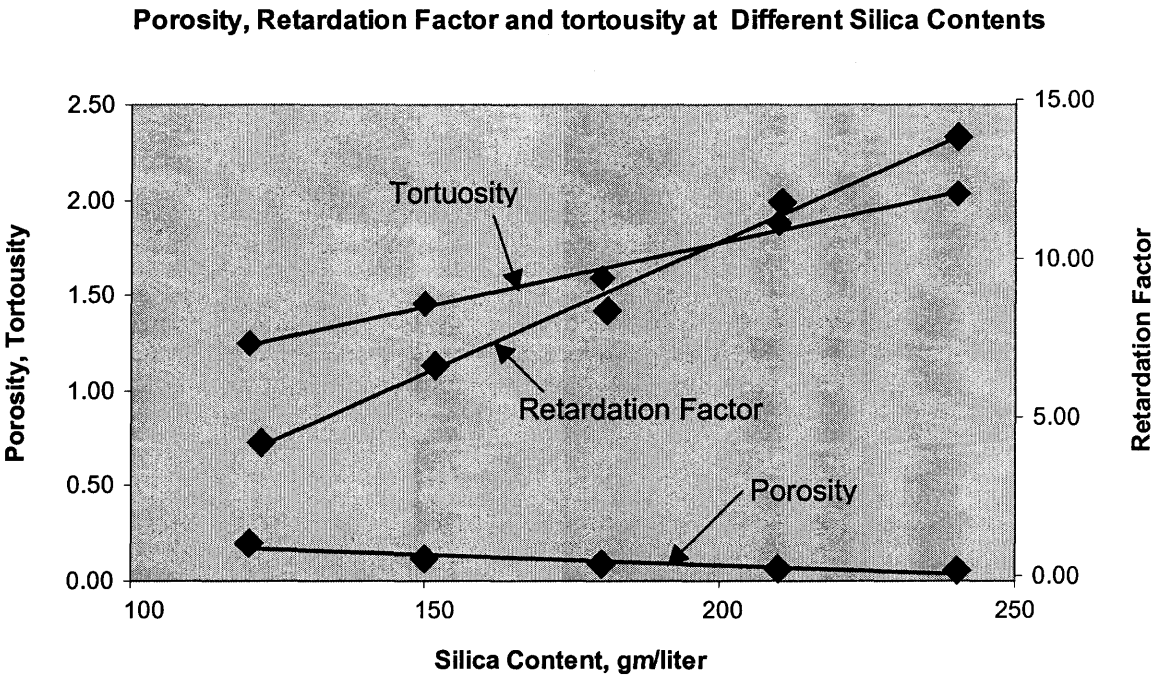

Figure 5.15 Porosity, Retardation Factor and Tortuosity at Different Silica Contents.

Initial concentrations in this test were 200, 180, 160, 140 and 120 mg/liter with silica concentration 240 gm/liter. The output, as reported in Table 5.3 and Figure 5.16, yields difference diffusion coefficient at different initial concentration. Diffusion coefficients ranged from 1.76 to 5.19 x 10^{-10} m^2/sec which is comparable to those reported in literature.

The variation of average diffusion coefficient with different initial chromium concentration was plotted in Figure 5.16. The curve shows that at low initial chromium concentration, there is no correlation between the initial chromium concentration and diffusion coefficient. However, the diffusion coefficient increase with chromium initial concentration at high concentration (greater than 180 mg/liter). This might occur because; 1) the adsorption of chromium to silica surface (Rutherford, 2001; Wang et al,

Table 5.3 Diffusion Coefficient at Different Initial Chromium Concentration

Initial Chromium Concentration, mg/liter	Diffusion Coefficient x 10^{-10} ,m^2/sec
120	1.76 ± 0.18
140	3.04 ± 0.51
160	3.46 ± 0.35
180	4.85 ± 0.23
200	5.19 ± 0.26

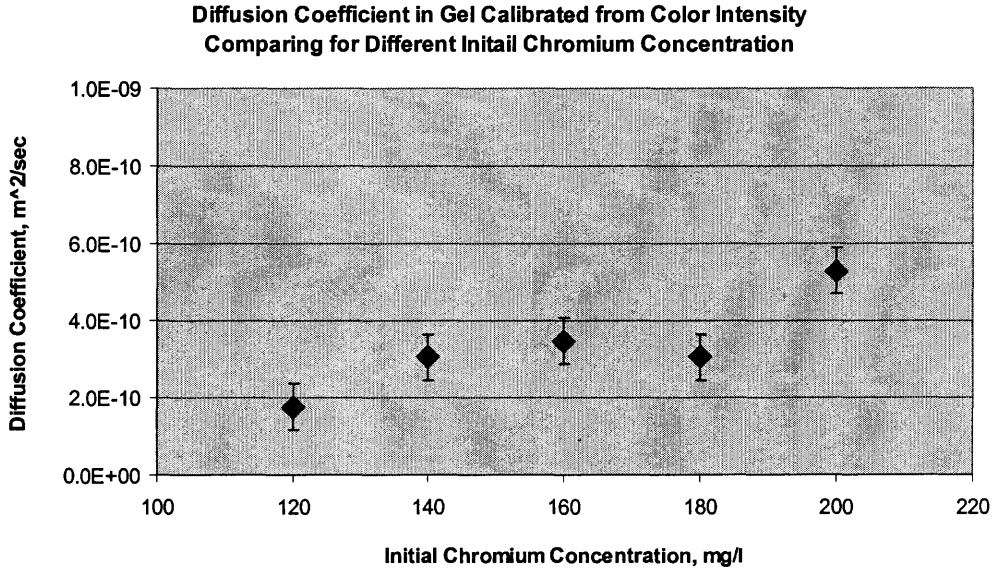

Figure 5.16 The comparison of Diffusion Coefficient at Different Initial Chromium Concentrations.

2001) or 2) the change of gel and chromium structure during the diffusion (Faupel et al, 1998). These behaviors fall under case II diffusion, non-Fickian, which have been observed in numerous works related to diffusion in gels and polymers (Camera-Roda & Sarti, 1997; Crank, 1979; Faupel et al, 1998; Friedman & Rossi, 1997).

The Measurement with Different Gelation Times: Generally, it takes time for the gel to gain its maximum strength (Yonekura & Miwa, 1993). In this study, the effect of gelation time on the diffusion coefficient was investigated. Five different gelation times were used in this experiment, 48, 24, 12, 6 and 3 hours. Diffusion coefficients calculated from least square method are shown in Table 5.4.

Diffusion coefficient values from the studies are in the range of 4.97 to 5.26 $x10^{-10}$ m^2/sec. No correlation between gelation time and diffusion coefficient was found. Thus, it is assumed that the gelation time has no contribution to diffusion. The average diffusivity, value of 5.13 $\pm$ 0.11 x 10^{-10} m^2/sec, was calculated from different gelation times, which is comparable to those reported in literature that range from 10^{-9} to 10^{-13} m^2/sec (Burke et al., 2000; Dunmire et al., 1999, MaDonald, 2001; Masaro & Zhu, 1999; Lakatos et al., 1998; Takahashi et al., 2000). Hence, it appears that there is no significant change in gel structure after three hours.

The average diffusion coefficient of chromium with silica concentration 240 gm/liter and initial chromium concentration 200 mg/l obtained from the three experiments, 4.91 x 10^{-10}, 5.19 x 10^{-10} and 5.13x10^{-10} m^2/sec, respectively, was 5.01 $\pm$ 0.15 x 10^{-10} m^2/sec with 95% confidence. The standard deviation was 1.50 x 10^{-11} m^2/sec, which yielded 2.90% error. This value was used to determine for the chromium mass balance in gel phase in the next experiment.

Table 5.4 Diffusion Coefficient at Different Gelation Times

Type	Diffusion Coefficient x 10^{-10}, m^2/sec
Gelation Time 48 hours	5.07 ± 0.83
Gelation Time 24 hours	5.26 ± 0.23
Gelation Time 12 hours	5.25 ± 0.45
Gelation Time 6 hours	5.09 ± 0.66
Gelation Time 3 hours	4.97 ± 0.35
Average	5.13 ± 0.11

Confirmation Test to Evaluate the Reliability of Measurements: The concentration profile in two media could be calculated based on the diffusion coefficient obtained from the previous experiments. The concentration profiles calculated from Equations (5.9) and (5.10) are shown in Figure 5.17. The Figure illustrates chromium concentration profiles between water and gel at different time intervals of 30, 60, 90, 120, 150 and 180 minutes respectively. The diffusion coefficient of chromate ions in water and in the gel and the partition coefficient used in the calculation are 1.12×10^{-9} m^2/sec (Thibodeaux, 1996), 5.01×10^{-10} m^2/sec and 0.549 liter/gm, respectively. In gel phase, both chromium concentrations in pore water and in gel (the combination of chromium sorbed and chromium in pore water) are shown.

From the mass balance, the total amount of chemical in the system at anytime is constant. Hence, the area under curve at anytime should be a constant. The analysis of

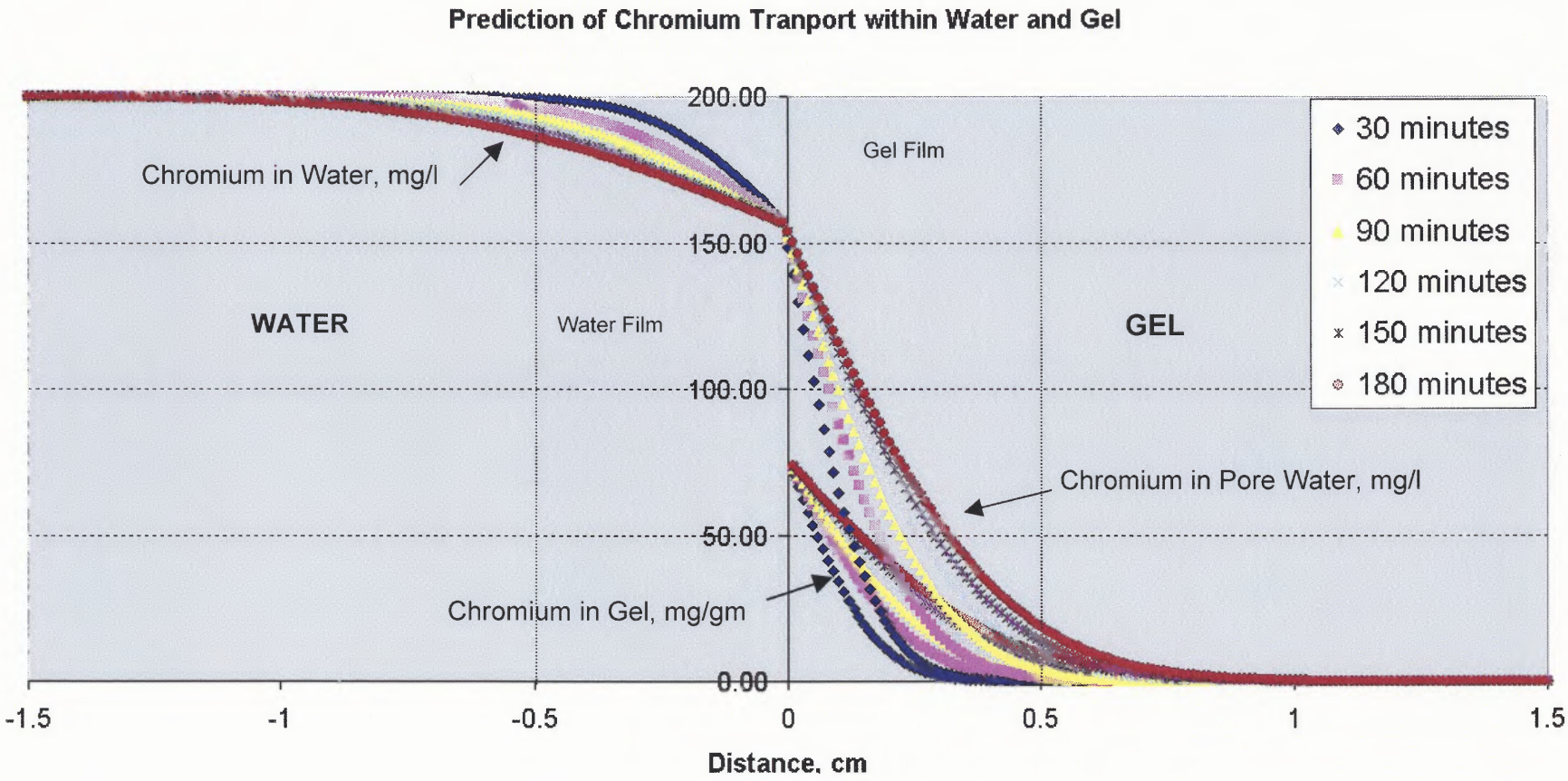

Figure 5.16 The Prediction of Chromium Transportation in Water-Gel Phase.

Table 5.5 Amount of Chromium in Water and Gel

Time, minutes	Chromium in solution, mg*	Chromium in gel, mg**	Total Chromium, mg	Error, gm/liter
30	0.190	0.011	0.201	0.57
60	0.196	0.016	0.212	5.96
90	0.196	0.017	0.212	6.22
120	0.192	0.018	0.210	4.89
150	0.186	0.021	0.206	3.11
180	0.174	0.022	0.196	2.23

* Wet analysis

** Total area under curve vs. distance obtained from digital image

chemical in water by wet analysis together with the analysis of chemicals using digital photography should yield the same amount of chemical at any time in the system. The different time intervals were used for confirmation.

The amount of 0.20 mg chromium was used which is a total mass in the system. Chromium in solution was determined directly from the wet analysis using AAGF. The amount of chromium in gel was calculated from the area under curve multiplied by cross section of the vials. The results are shown in Table 5.5.

From Table 5.5, the total amount of chromium in each sample was close to 0.200 mg. The error ranged from 0.57 to 6.22%. Hence, determination of chromium concentration from the digital photography calculation is comparable to that from wet analysis. Consequently, the proposed digital photography method is a reliable method to determine diffusion coefficients of chromium in gel.

5.5 Discussion/Conclusions

This study proposed a new method to measure the diffusion coefficient. The optical method using digital imaging proved to be an effective and reliable technique. This method was successfully performed and produced accurate chromium diffusion coefficient values in gel. This method can be easily applied to measure the diffusion coefficient of colored chemicals in clear/white media.

The adsorption isotherm of chromate ions to colloidal silica gel is linear. The partition coefficient calculated from this experiment is 0.549 liter/gm. The diffusion coefficients obtained from the experiments were in the range of 1.76 to 8.48 x 10^{-10} m^2/sec. Lakatos et al. (1998) reported the diffusion coefficient of chromium in polymer gel and in water in the rage of 10^{-9} m^2/sec. This above values fall with in the range of values expected based on reported values in the literature for polymer and gels (10^{-13} to 10^{-9} m^2/sec). The diffusion coefficient of chromium in colloidal silica gel with 240 gm/liter silica concentration at the 95 % confidential interval was (5.01 $\pm$ 0.15) x 10^{-10} m^2/sec.

Silica concentration effects tortuosity of gel, resulting in the different diffusion coefficient. The higher silica content yields a smaller diffusion coefficient due to obstruction effects. The tortuosity of colloidal silica gel ranges from 1.25 to 2.00 depends increasing linearly with silica content in gel (ranges 120 to 240 gm/liter). At low initial chromium concentration, initial chromium concentration has no attribute to diffusion coefficient. Diffusion coefficient increases with initial chromium concentration at high chromium concentration, due the adsorption and the unstable chromium and gel structure.

Accuracy of the proposed method can be evaluated by three different methods. First, the parameter D obtained from this study was compared with those reported in literature using different techniques. Second, the values obtained from this experiment

were compared to theoretically values. The diffusion coefficients of chromium in colloidal silica gel, NYACOL DP5110, are not reported in the literature. However, the reported values of diffusion coefficient in gel ranged from 10^{-13} to 10^{-9} m^2/sec.

A test was performed to further confirm the accuracy of the proposed method, where chromium concentration in both gel and water was determined. Chromium concentration in gel was analyzed by the digital photography method while the concentration in water was analyzed by using AAGF. The mass balance calculations were performed. The errors were in the range of 0.57 to 6.22%. This confirmed that the accuracy of digital photography method is comparable to the wet analysis.

Precision of the diffusion coefficient was obtained from three tests for 240 gm/liter colloidal silica, 200 mg/liter initial chromium concentration and 24 hours gelation. It was found to be $(5.01 \pm 0.15) \times 10^{-10}$ m^2/sec with 95% confidence. The standard deviation was 0.15×10^{-11} m^2/sec, which yielded 2.90% error.

The advantages of the method are: 1) the apparatus is easy to setup, 2) measurement can be performed within a short time, 3) the change of concentration can be monitored in-situ and 4) the diffusion coefficient can be calculated by simple curve fitting. The photography method has disadvantages too. It can be applied to only colored solute in wet gel. A constant of light source is needed during the experiment. The high resolution digital camera is required in order to obtain precise result.

In summary, the measurement of diffusion coefficients for chromium in colloidal silica gel using digital photograph has proven to be accurate and precise. This method is suitable for analyzing colored chemicals inside clear/white gels. This simple technique should be able to analyze the transport of ions in gel.

Suggestions

Selecting the proper camera should increase accuracy. The higher the resolution of the digital image, the better the results. Different camera types provide different resolutions ranging from thousand to millions pixels per image. Also, the consistency of light and the selection of background color are also important. The digital image is light sensitive, thus the same light source is needed throughout the experiment. The incandescent light is not a good light source, as it gives off yellowish glare and yellow happens to be one of the three colors that is analyzed by the software. Using of proper color background would provide better color gradients. The background color depends on the color of the chemical and gel. With the rapid improvement of computer technology, this method should be further improved and extensively used in the future.

CHAPTER 6

TRANSPORT OF CHROMIUM IN COLLOIDAL SILICA GEL

In this chapter, the transport of chromium in solidified colloidal silica gel was studied. The diffusion coefficients and partition coefficient obtained from the experiments were used to predict the leaching of chromium from the stabilized matrix. The simulation was performed based on the worse case scenario to obtain the long-term release of chromium from the gel.

6.1 The Determination of Chemical Transport in Colloidal Silica Gel

Colloidal silica gel is a porous silica network with a wide distribution of pore spaces filled with water. The colloidal silica gel pore size is at lease ten times larger than chromium ions. Thus, it is reasonable to assume that chromium ions move freely inside pores of the gel. From Chapter 5, the diffusion mechanism of chromium in colloidal silica gel was found a bulk diffusion of dichromate ions in pore water of colloidal silica gel. The presence of the motionless polymer chains leads to an increase in the mean path of the diffusing molecules between two points in the gel. Figure 6.1 shows the possible distribution of contaminants during the stabilization process. Chromium ions are assumed to be deposited inside soil particles, on soil surfaces and suspend in pore space of gel. Chromium exposed to water in gel media may is transported by diffusion in gel pores adjacent to soil, then diffuses into the gel pores and eventually into groundwater. The diffusion of chromium in gel matrix is explained in mathematically as.

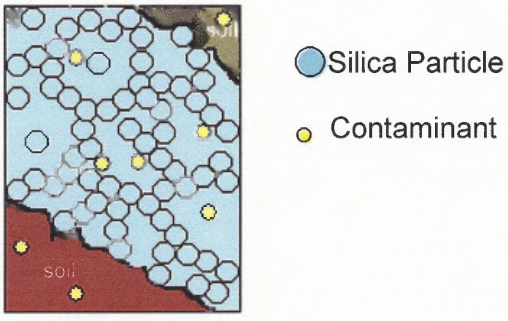

Figure 6.1 The Diffusion Process.

$$\frac{dC}{dt} = D\,\frac{d^2C}{dz^2} \tag{6.1}$$

In order to obtain the chromium concentration in groundwater, the following assumptions were made.

1. The amount of contaminant on the soil surface is sufficient to maintain a constant concentration at the soil-gel interface at all times.
2. Interface resistance occurs and the ratio of concentration at the soil-gel interface was calculated form partition coefficient.
3. The initial concentration of chromium in the gel is zero.
4. The diffusion coefficient is a function of silica concentration in gel.
5. The transport is controlled solely by diffusion and adsorption with no advection.

Consider a grout curtain as shown in Figure 6.2, contaminants travel through the barrier by diffusion. The concentration of contaminant is highest at the interface and reduces to zero at the opposite side of the grout curtain. One-dimensional diffusion was

assumed in an infinite gel media. Note that chemical path might be longer due to the soil tortuosity. However, assuming that in the worse case where the tortuosity has no effect to the diffusion, profile of chromium concentration in gel was assumed and shown in Figure 6.3.

Here, the following additional assumptions were made.

1. At the interface between soil and gel, chemical in solid states would dissolves until it reaches a saturated concentration. The chemical at the interface diffuses into the gel media.
2. The concentration of chromium in gel at the groundwater interface is zero at all time. This is based on the assumption that the groundwater mass is large compare to the gel mass.

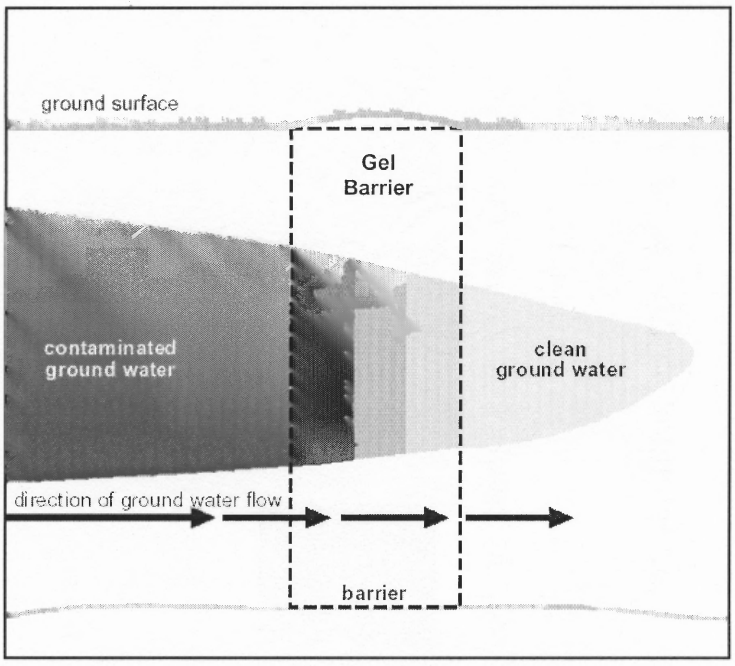

Figure 6.2 The Waste Barrier.

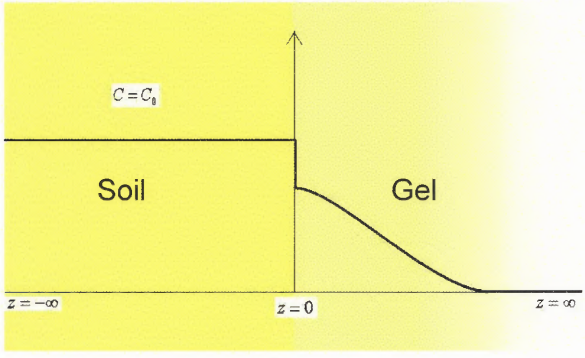

Figure 6.3 The Concentration Profile in the Gel Barrier.

Hence chemical concentration in gel at any distance can be calculated from the equation below (Crank, 1979).

$$C = C_0 erfc \frac{z}{\sqrt{4Dt}} \tag{6.2}$$

$$erfc(x) = 1 - \frac{2}{\sqrt{\pi}} \int_0^x \exp(-u^2) du$$

From the Equation (6.2), chromium concentration as a function of distance and time can be calculated. Hence, the leachate, concentration which is an amount of chemical diffusing, can be obtained.

6.2 Input Parameter for the Simulation

Input parameters required for the Equation (6.2) are concentration of chemical entering gel, C_0, and diffusion coefficient, D. Concentration of chemical entering gel can be determined from the solubility of chromium compounds and the partition coefficient, K. The coefficients used were obtained from the experiment. The details of each parameter are as follows.

6.2.1 Solubility of Chromium

The solubility of chromium depends on chromium compounds, pH, redox conditions and chemicals in the environment. Some of the particulate chromium would remain suspended and ultimately deposit in sediments. Hexavalent chromium is stable and water-soluble; however, it may be reduced to trivalent chromium by organic matter in water, and subsequently precipitate as chromium oxide. Although most of the soluble chromium in surface waters may present as hexavalent chromium, a small fraction may present as trivalent chromium complexes with organic substances. The solubility of a few important hexavalent chromium compounds is given in Table 6.1.

Chromium compounds of interest in this research are chromite ore processing residue. During the ore processing, chromite ore is crushed to less than 100 mesh size, mixed with soda ash, and roasted to produce soluble sodium chromate, Na_2CrO_4. The residue, before treatment, typically consists of 15-20% trivalent chromium as Cr_2O_3 and 0.3-1.0% hexavalent chromium as sodium chromate. The chromite ore processing residue contains sparingly soluble salts such as $CaCrO_4$, $Ca_4Al_2CrO_{10}$, and $FeOHCrO_4$ as well as insoluble trivalent chromium. The residue has pH of about 7-8 and consists of 30% moisture. The residue does not contain any hazardous volatile constituents (USEPA, 2000).

Rock et al. (2001) analyzed chemical properties of chromite ore processing residue from Kearney, NJ, and found that the waste has high levels of soluble hexavalent chromium, 940 $\pm$ 40 μM (109.04 mg/l), and low levels of trivalent chromium, <1.0 μM (<0.16 mg/l).

Table 6.1 Aqueous Solubility of Hexavalent Chromium Compounds

Compounds	Water Solubility, mg/liter
Ammonium Chromate $(NH_4)_2\ CrO_4$ [a]	4.05×10^5 at 30°C
Calcium Chromite $CaCrO_4$ [a]	2.23×10^4 at 20°C
Chromic Acid CrO_3 [a,b]	6.17×10^4 at 30°C
Potassium Chromate K_2CrO_4 [a]	6.29×10^5 at 30°C
Potassium Dichromate $K_2Cr_2O_7$ [a]	4.90×10^4 at 0°C
Sodium Chromate Na_2CrO_4 [a]	8.73×10^5 at 30°C
Sodium Dichromate Dihydrate [a]	2.30×10^6 at 0°C
Electroplating Soil (61 g/kg Cr) [c]	11.00
Ore Processing Residue (8.6 g/kg Cr) [c]	109.04
Tannery (1.3 g/kg Cr) [c]	$<1.16 \times 10^{-2}$
Chromite Mine (4.7 g/kg Cr) [c]	$<1.16 \times 10^{-2}$

Source : [a] USEPA, 1998
[b] Dean, 1992
[c] Rock et al., 2001

The chemical entering gel or the chemical in aqueous phase is equal to the solubility of chromium in the specific site. In this research, the leachate of chromium from ore processing residue is used. From Table 6.1, solubility of 109.0 mg/liter for chromite ore processing waste from Kearny, NJ, was used to estimate the leachate of chromium from colloidal silica gel.

6.2.2 Diffusion Coefficient of Chromium in Colloidal Silica Gel, D

The diffusion coefficient shows the rate of transport of chemical in medium. This parameter was used to determine the movement of chromium in the colloidal silica gel medium. The diffusion coefficient was obtained from the experiment described in detail in Chapter 5 which ranges between 1.76 to 6.64 x 10^{-10} m^2/sec depending on silica content in gel (see Figures 5.14).

In this simulation, silica concentration in the gel was assumed 240 gm/liter. From the experiment, the diffusion coefficient of the simulation condition could be estimated. Hence, the diffusion coefficient used was 5.0 x 10^{-10} m^2/sec.

6.2.3 Partition coefficient, K

The interface resistance occurs if a chemical is in contact with two different phases with different affinities to each phase. The ratio of the concentrations within the two phases is defined as the partition coefficient of the system (Xrefer Inc., 2002).

In a water-gel system, the partition coefficient, K, is defined as the ratio of the chemical concentration in the barrier region to that in the gel. From Chapter 5, it was found that partition coefficient of chromium in solution and colloidal silica gel is 0.549 liter/gm.

Chromium concentration in solution phase of 109.0 mg/liter was used in the model. In this system, chromium from soil dissolves to water in gel pore. In this case,

the water film is very small comparing to gel film. Thus, it is reasonable to assume that chromium concentration at the water interface is 109.4 mg/liter. Chromium concentration entering gel phase, C_0, calculated from the above value and partition coefficient was 60.0 mg/gm gel.

The input parameters used for the simulation are summarized below.

Solubility of chromite ore processing waste	109.0	mg/liter
Partition Coefficient, K	0.549	liter/gm
Chromium entering gel, C_0	60.0	mg/gm
Diffusion coefficient of chromium in gel, D	5.01×10^{-10}	m^2/sec

6.3 Results

The input parameters described above were used to solve Equation (6.2). In the simulation, the diffusion coefficient, the initial concentration (chromium entering gel) and distance (gel thickness) were constants while time was a variable. Four different gel thicknesses were simulated. Heisher et al. (1997) reported that average thickness of gel in the waste barrier is 5 cm. Hence, for the simulation the following thickness was used: 1, 2, 3, and 5 cm.

The prediction, a plot of concentration profile in gel at different times with 5 cm gel thickness is shown in Figure 6.4. The variation of chromium concentration as a function of time in soil, gel and groundwater with four different times is shown in Figure 6.5. Figures 6.4 shows different concentration profiles at different time from 50 to 400 hours. After 200 hours (about eight days), the concentration of chromium migrate out from the gel mass to groundwater would exceed the USEPA MCL standard (0.1 mg/liter).

Table 6.2 Cleanup Goals for Chromium (USEPA, 2000)

Leachable Metals	Chromium (mg/liter)
TCLP (Toxicity Characteristic Leaching Procedure) threshold for RCRA Waste (SW846, Method 1311)	5.00
Extraction Procedure Toxicity Test (EPTox) (Method 1310)	5.00
MCL (the maximum permissible level of contaminant in water delivered to any user in a public system)	0.10
Superfund Site Goals	0.050

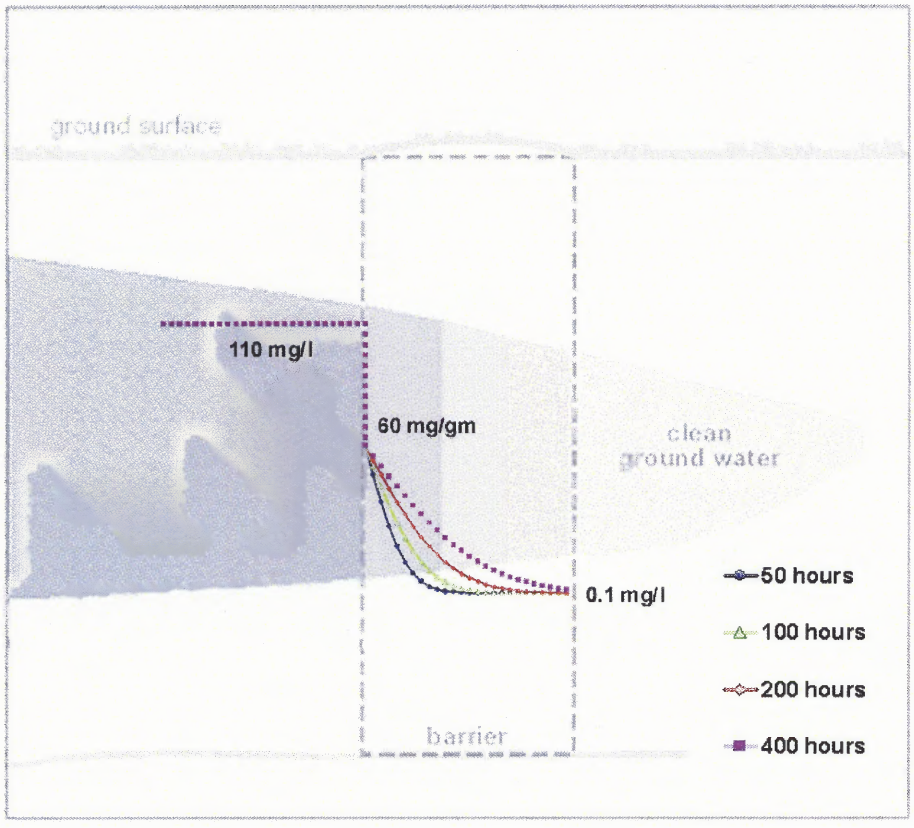

Figure 6.5 The Prediction of Chromium Transport in Gel Barrier.

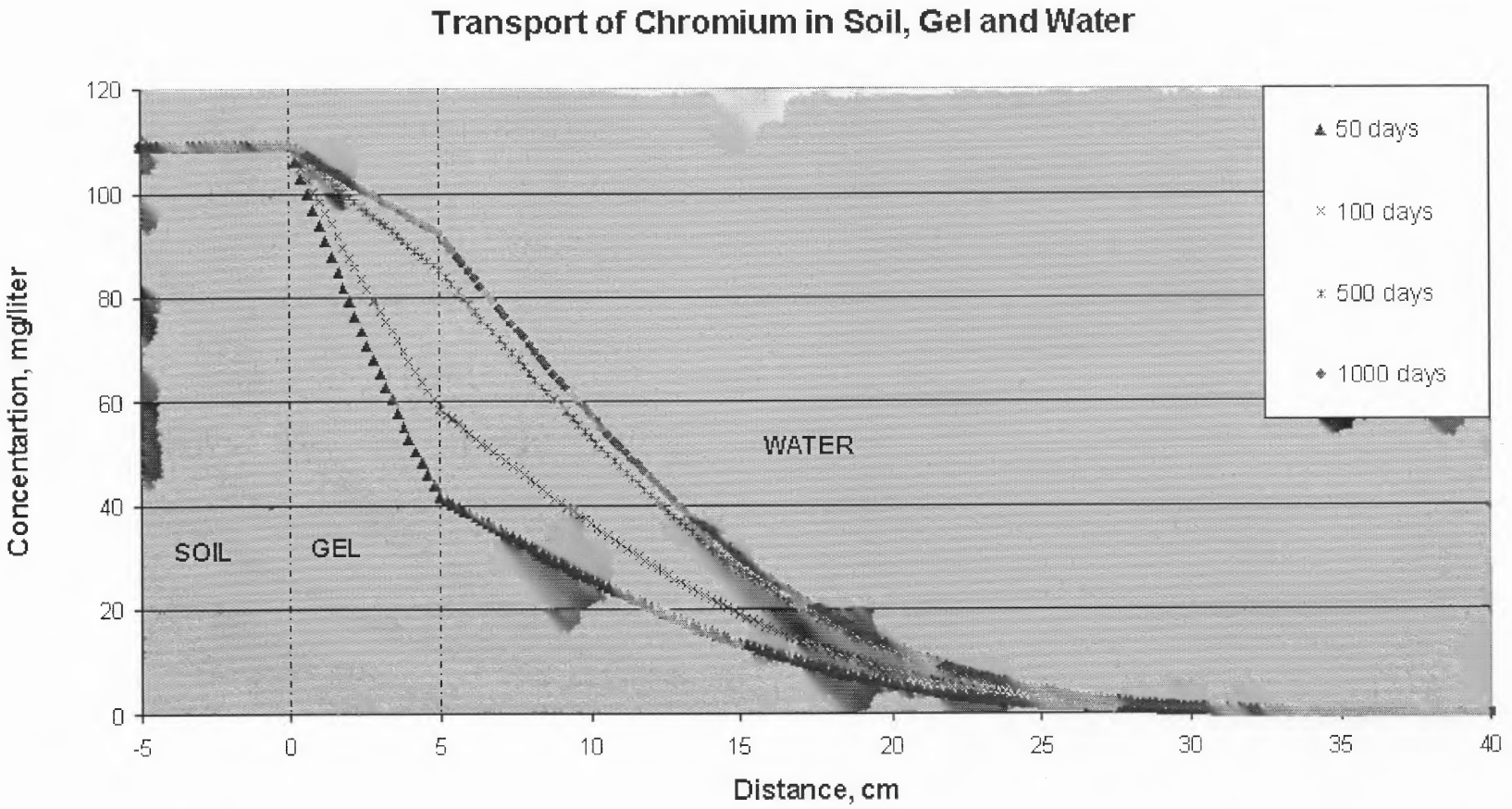

Figure 6.5 The Prediction of Chromium Transport in Colloidal Silica Gel.

Figure 6.5 shows the concentration profiles of soluble chromium in three different media, soil, gel and water. Chromium ions diffuse slightly faster in gel than in water. The simulation shows that diffusion in different media with different diffusion coefficient would yield different concentration profile. With large volume of groundwater, the contaminant concentration would be reduced. Therefore, applying the three-dimensional model would yield different diffusing rate.

6.4 Discussion/Conclusions

The simulation was performed at 240 gm/liter silica content in the gel; the solubility of chromium from the soil was equal to the leaching of chromite ore processing residue, 109.0 mg/l, partition coefficient was 0.549 liter/gm and diffusion coefficient of chromium in gel was 1.36×10^{-10} m^2/sec. Results showed that the concentration of chromium leaching due to diffusion from 5.0 cm thick gel takes approximately eight days to exceed the regulations standard of 0.1 mg/liter. Hence, considering the above calculation of extreme conditions, the colloidal silica technology to treat chromium contaminated soils appear to be ineffective.

However, the study is based on laboratory condition not soil environment, and the model used was one-dimensional model with extreme conditions. The results from this study might be slightly different from those obtained from actual soil with different models and different conditions. Additional research should be performed to better simulate the actual site condition to treat chromium contaminated soils and further investigate the use of other types of colloidal silica that has the ability to oxidize hexavalent chromium to trivalent chromium and retain it inside gel media in treatment of chromium.

Many studies have proven that colloidal silica is applicable to treat contaminated soil. Their conclusions were based on the reduction of groundwater flow due to the pore blocking (Moridis et al., 1996; Zulaski et al., 2000) strength increasing (Persoff et al., 1999) and adsorption of contaminant to silica surface (Borglin et al., 1998; Hakem et al., 1997; Noll et al., 1992). However, Hakem et al. (1997) and Lakatos & Lakatos-Szabó (1998) noted that the possible role of diffusion using gel as a treatment material should be concerned but was overlooked.

In contrary to previous researches, the founding of this research showed that diffusion of chromium in colloidal silica is bulk diffusion in a porous medium which has a large contribution to the effectiveness of the technology. It is strongly suggested that diffusion of contaminant in gel has to be considered and not overlooked if this technology is to be applied in field conditions.

CHAPTER 7

SUMMARY AND CONCLUSIONS

This research seeks theoretical evaluation of one of the potential remediation technology for the treatment of chromium contaminated soils, which is of great concern in New Jersey. In-situ grouting of colloidal silica when injected into soil was shown to create an impermeable wall, preventing the migration of waste (Morisdis et al., 1997; Persoff et al., 1999; Apps et al., 1998). Due to the low cost of colloidal silica, this technology is proven to be economical (Pearlman, 1999; Gellagher & Mitchell, 2001).

Though the in-situ S/S of contaminated soil using colloidal silica is a well-established technology, the theoretical understanding of the technology is deficient. Hence design guides cannot be developed without performing trial test for each situation. This research attempts a theoretical study to understand the stabilization mechanisms of colloidal silica. Specifically it tries to simulate the gelation mechanism and also to evaluate the effectiveness of the treatment technology.

The simulation of the gelation mechanism was performed numerically using Navier-Strokes equation. Then the effectiveness of the treatment technology was evaluated using the study of the diffusion of chromium through the solidified colloidal silica. In order to simulate the transport of chromium in colloidal silica gel, the diffusion coefficient must be known. To estimate the diffusion coefficient of chromium in solidified colloidal silica, a new optical was proposed. This new method expedites the measuring time of the transport of chromium in colloidal silica gel using distinct coloration. Furthermore, it is practical and inexpensive when compared to other commonly used methods.

7.1 Microscopic Behavior of Colloidal Silica Stabilizer in Anisotropic Granular Media

The microstructure of colloidal silica treated contaminated soils was simulated by solving the Navier-Stokes equation with appropriates boundary conditions. It was assumed that porous soil mass consists of spatially periodic spherical particles of a given diameter. Thus, it is possible to analyze a unit representative cell consisting of one particle with its surrounding ambient space. Then it is possible to introduce other variables of soil mass such as, the influence of shape, non-periodic nature, and size by gradual alternation of the unit cell.

The above simulation was performed using a Three-dimensional Finite Element program, RMA7, (King, 1973) and input file generator, MESH, (Meegoda, 1985). These computer programs were originally developed to simulate the flow of water through soil. These programs were modified for the application in this study. The output was processed using graphic operation software.

The gel-time data from Moridis et al. (1999) showing the variation of gel viscosity with time during the solidification of gel was used in the simulation. The simulation began with the injection of colloidal silica solution into contaminated soil, allowing the colloidal silica to move through the spaces in the soil matrix. With the increase in time, viscosity of colloidal silica increased while it moves, causing a reduction of the flow velocity. The above process resulted in increasing the boundary layer thickness, transforming liquid colloidal silica into a gel. The solidified colloidal silica occupied the empty spaces in soil completing the stabilization by trapping the chromium inside the gel mass.

The simulation results showed that during the grouting process, the solidification starts from soil surface and expands out until resides in the empty spaces in soil within

1.2 hours. Different soil particle geometry resulted in the different velocity contours and the different colloidal silica solidified patterns. The greater the ellipsoid axial ratio of soil resulted in the faster solidification.

Further study could be performed at the micro level by having multiple unit cells with different soil particle sizes and shapes to simulate a real soil. The above results are expected to be able to help develop design guides for a large-scale treatment of using colloidal silica including the extent of the treated area and injection time for each injection well.

7.2 Measurement of Diffusion Coefficient

The next part of research includes the modeling of the transport of chromium after the contaminated soil is stabilized. The main mechanism here is molecular diffusion. For the diffusion modeling, the diffusion and the partition coefficient values are needed. Though there are many studies, the diffusion and partition coefficient of chromium in colloidal silica gel is not available in the literatures. Therefore, those two parameters were estimated from laboratory tests.

A new method based on an optical technique that uses computer graphic applications was introduced to measure the diffusion and partition coefficient. The concentration gradient of chromium in gel was recorded digitally and stored as a digital file. It was later converted into concentration using computer software that has the ability to distinguish color level. Then calculation for diffusion coefficient was performed based on Fick's law.

Following are advantages of the proposed digital photography method.

1. The apparatus is easy to setup.
2. The measurement can be performed within a short time.

3. The change of concentration gradient can be monitored in-situ.
4. The diffusion coefficient can be calculated by simple curve fitting of concentration-distance-time data.

Colloidal silica, NYACOL DP5110, was used in this study. The adsorption isotherm and partition coefficient of dichromate in colloidal silica gel were determined by adsorption study. The diffusion coefficient of dichromate in gel at different silica concentration, different initial chromium concentrations and different gelation times were obtained. In small clear plastic vials, colloidal silica was allowed to solidify. After the gel was solidified, 1 ml of chromium solution was added to the top of colloidal silica gel and the diffusion was observed. The optical contrasts were obtained by taking digital pictures of the vials. The pictures were downloaded, analyzed and calibrated to obtain the concentration gradients. The diffusion coefficient was determined by least square estimation.

The adsorption isotherm of dichromate to colloidal silica gel was linear. The partition coefficient calculated from this experiment was 0.549 liter/gm. The diffusion coefficients obtained from the experiments were in the range of 10^{-10} m^2/sec. The average diffusion coefficient with silica concentration 240 gm/liter was $(5.01 \pm 0.15) \times 10^{-10}$ m^2/sec. These values were in the range reported for polymer (10^{-13} to 10^{-9} m^2/sec). The diffusion coefficient depended on silica concentration in gel. Higher silica concentrations yielded the higher diffusion coefficients due to the obstruction to free movement of chromium. Diffusion coefficient increases linearly with initial chromium loading due to the change of gel and chromium compound structure. The tortuosity of colloidal silica gel ranges from 1.25 to 2.00 depends increasing linearly with silica content in gel (ranges 120 to 240 gm/liter). Initial chromium concentration at low concentration (lower than 180 mg/liter) has no attribute to the diffusion coefficient. The

gelation time had no effect to the diffusion coefficient. Thus it was concluded that there is no significant change in gel structure after 3 hours.

Mass balance calculations were performed to confirm the accuracy of the new method. The percent different between the total mass and the calculated from digital method was less than 6.5%. Thus, it was concluded that the measurement of diffusion coefficient by taking digital photograph is accurate. This method is suited for analyzing colored chemical inside clear/white media. The data can be easily analyzed to provide rapid determination of diffusion coefficients.

7.3 Transport of Chromium in Colloidal Silica Gel

The movement of chromium through silica gel was mathematically modeled to evaluate the long-term effectiveness of the in-situ treatment using colloidal silica for chromium contaminated soils. The proposed analysis was based on Fick's law.

Boundary conditions for the simulation assumed that the chromium on soil surface was dissolved into pore water in gel matrix at the soil/gel interface. The solubility of chromium depends on soil properties, species of chromium and chromium concentration in soil, which are site specific. Mostly, the dissolved chromium is in hexavalent states. When chromium ions from the soil/gel interface enters gel matrix, the saturated concentration at the interface is reduced due to the interface resistance. This reduction ratio depends on the properties of the medium, properties of the chemical and the amount of chemical at the interface.

The simulation was performed at 240 gm/liter silica in the gel. The concentration of chromium of the soil-gel interface was assumed equal to 109.0 mg/liter (Rock et al. 1996). The diffusion and partition coefficient of chromium in gel, obtained from the experiments, were 5.01×10^{-10} m^2/sec and 0.549 liter/gm respectively. The simulation

was performed assuming the worst scenario where the chromium in soil was at the highest level and it dissolves continuously into water at the soil-gel interface. The thickness of the gel barrier (based on previous study by Heisher et al. (1997)) was assumed 5 cm for 240 gm/liter silica in the gel. The results showed that in the absent of moving groundwater, the chemical would take slightly over eight days before exceeding the USEPA standard (0.1 mg/l).

Based on the simulation results, colloidal silica, NYACOL DP5110®, technology for in-situ treatment of chromium contaminated soils seems to be ineffective. Further research of more realistic simulation of diffusion and refined gel formulation with capacity to convert the chromium to immobile form is recommended.

7.4 Anticipated Outcome

The work described in this thesis will be able to develop design guidelines for a treatment system by estimating the injection rate, time, and the accumulated leachate over a specific period. The future work should concentrate performing calculation under more realistic site condition to simulate the release of chromium to groundwater and on modifying colloidal silica with the ability to reduce hexavalent chromium to trivalent chromium and retain it inside gel media.

REFERENCES

Aboobaker, N. (2001) "Fractionation and Segregation of Suspended Particle Using Acoustic and Flow Fields." *Doctoral Dissertation,* New Jersey Institute of Technology, New Jersey.

ACR, Analytic & Computational Research, Inc. (2002) "PORFLOW V.5.5." Retrieved June 20th, 2002. From the World Wide Web, http://www.acri-us.com/.

Alan, L. M. & Kukacka, E. L. (1994) "Grout-Treat Soil for Low-Permeability Barrier around Waste Landfill." *ACI material Journal.* Vol.91:355-361.

Allan, M. P. (1997) *Understanding Regression Analysis.* Plenum Press, New York.

Alvarez-Lorenzo, C. et al. (2001) "Reversible adsorption of Calcium ions by Imprinted Temperature Sensitive Gel." *Journal of Chemical Physics.* Vol.114(6):2812-2816.

Apps, A. J., Persoff, P., Moridis, G. J. & Pruess, K. (November 17, 1998) "Method for Formation of Subsurface Barriers Using Viscous Colloidal." *United State Patent 5,836,390.*

Axe, L. & Anderson, P. R. (1995) "Sr Diffusion and Reaction within Fe Oxides:Evaluation of the Rate-Limiting Mechanism for Sorption." *Journal of Colloidal and Interface Science.* Vol.175:157-165.

Axel, T. (1998) "Diffusion of Metal in Polymers." *Material Science and Engineering.* R(22):1-55.

Axelsson, A., Westrin, B. & Loyd, D. (1991) "Application of the Diffusion Cell for the Measurement of Diffusion in Gel." *Chemical Engineering Science.* Vol.46(3):913-915.

Ball, J. W. & Nordstrom, D. K. (1998) "Review:Critical Evaluation and Selection of Standard State Thermodynamic Properties for Chromium Metal and Its Aqueous Ions, Hydrolysis Species, Oxides, and Hydroxides." J. Chem. Eng. Data. Vol.43:895-918.

Bates, D. M. & Watts, D. G. (1988) *Nonlinear Regression Analysis and Its Application.* John Wiley & Sons Inc., New York.

Bear, J. & Bachmat, Y. (1990) *Introduction to Modeling of Transport Phenomena in Porous Media.* Kluwer Academic Publisher, Netherlands.

Berka, M. & Banyái, I. (2001) "Surface Complexation Modeling of K^+, NO_3^-, SO_4^{2-}, Ca^{2+}, F^-, Co^{2+} and Cr^{3+} Ion adsorption on Silica Gel." *Journal of Colloidal and Interface Science.* Vol.233:131-135.

Bird, R. B., Stewart, W. E. & Lightfoot, E. N. (1960) *Transport Phenomena.* John Wiley & Sons Inc, USA.

Borglin, S. E., Lamble, G. M. & Moridis, G. J. (1998) "Studies of Adsorption of Contaminants onto Viscous Liquid Barriers" Earth Sciences Division, Lawrence Berkeley National Laboratory, Berkeley.
Retrieved August 1st, 2001. From the World Wide Web
http://alspubs.lbl.gov/AbstractManager/uploads/lamble4.pdf.

Buerge I. J. and S. J. Hug. (1999) "Influent of Mineral Surface on Chromium(VI) Reduction by Iron(II)." *Environ. Sci. Tech.* Vol.33:4285-4291.

Burke, M. D., Park, J. O., Srinivasarao, M. & Khan, S. A. (2000) "Diffusion of Macromolecules in Polymer Solution and Gel: A Laser Scanning Confucian Microscopy Study." *Macromolecule.* Vol.33:7500-7507.

Camera-Roda, G. & Sarti G. C. (1990) "Mass Transport with Relaxation in Polymers" *AIChE Journal.* Vol.36(6): 851-860.

Cifra, P. & Bleha, T. (2001) "Partition Coefficients and the Free energy of Confinement from Simulation of Nonideal Polymer Systems." *Macromolecules.* Vol.34(4):605-613.

Chen, Y & Yang, R. T. (1998) "Surface and Mesoporous Diffusion with Multilayer Adsorption." *Carbon* Vol.36(10):1525-1537.

Clark, M. M. (1996) *Transport Modeling for Environmental Engineers and Scientists.* Wiley-Interscience Publication, New York.

Crank, J. (1979) *The Mathematics of Diffusion.* Oxford University Press, New York.

Csobán, K., Parkanyi-Berka, M., Joó, P. &. Behra, Ph. (1998) "Sorption Experiment of Cr(III) onto Silica." *Colloidals and Surfaces A: Physical and Engineering Aspects.* Vol.141:347-364.

Csobán, K. & Joó, P. (1999) "Sorption of Cr(III) on Silica and Aluminum Oxide: experiments and Modeling." *Colloidals and Surfaces A: Physical and Engineering Aspects.* Vol.151:97-112.

Cussler, E. L. (1997) *Diffusion Mass Transport in Fluid System.* Cambridge University Press, New York.

Dean, A. J. (1992) *Lange's Handbook of Chemistry.* McGraw-Hill Inc., New York.

Doung, D. D. (1998) *Adsorption Analysis: Equilibrium and Kinetics.* Imperial College Press, Singapore.

Dragun, J., Kostecki, P. & Knowles, B. (1997) "Chromium in Soil: Perspective in Chemistry, Health, and Environmental Regulation." *Journal of Soil Contamination: volume 6*, New York.

Dunmire, E. N., Plenys, A. M., & Katz, D. F. (1999) "Spectrophotometric Analysis of Molecular Transport in Gel." *Journal of Control Release.* Vol. 57:127-140.

Durmusoglu, E. & Corapcioglu, M. Y. (2000) "Experimental Study of Horizontal Barrier Formation by Colloidal Silica." *Journal of Environmental Engineering.* Vol.126(9):833-841.

Eary, L. E. & Rai, D. (1989) "Kinetics of Chromium Reduction by Ferrous Ions Derived from Hematite and Biotite at 25°C." *America Journal of Science.* Vol.289:180-213.

Eidsath, A., Cablnell, R. G., Whitaker, S. & Herrman, L. R. (1983) "Dispersion in Pulsed System-III." *Chemical Engineering Science.* Vol.35(11):1803-1816.

Ellis & Perry (2001)-Host by Hoslink. (2002) "ABC of Safe Practices." Retrieved August 1st, 2002. From the World Wide Web http://www.hoslink.com/Ellis/SOLCHART.htm.

ESTL TechTra Inc. (2001) "Colloidal Silica Properties." Retrieved February 20th, 2001. From the World Wide Web http://www.labrorea.com/products/chemical/silica/colloidalsilica.htm.

Faupel, F., Willecke, R. & Thran, A. (1998) "Diffusion of Metal in Polymer" *Material Science and Engineering.* R(22:1-55).

Fendorf, E. S. (1992) "Oxidation and Sorption Mechanisms of Hydrolyzable Metal Ions on Oxide Surface." *Doctoral Dissertation,* University of Delaware, Delaware.

Fendrof, E. S. (1995) "Surface Reactions of Chromium in Soils and Water." *Geoderma.* Vol.67:55-71.

Fendorf, E. S., Lamble, G. M., Stapleton, M. G., Kelly, M. J. & Sparks, L. D. (1994) "Mechanisms of Chromium(III) Sorption on Silica. 1. Cr(III) Surface Structure Derived by Extended X-ray Absorption Fine Structure Spectroscopy." *Environ. Sci. Technol.* Vol.28(2):284-289.

Fendorf, E. S. & Sparks, L. D. (1994) "Mechanisms of Chromium(III) Sorption on Silica. 2. Effect of Reaction Condition." *Environ. Sci. Technol.* Vol.28(2):290-297.

Fendorf, E. S. & Li, G. (1996) "Kinetics of Chromate Reduction by Ferrous Iron." *Environ. Sci. Technology.* Vol.30:1614-1617.

Fendorf, E. S., Li, G & Gunter M. E. (1996) "Micromorphologies and Stability of Chromium(III) Surface Precipitates Elucidated by Scanning Force Microscopy." *Soil. Sci. Soc. Am. J.* Vol.60:99-106.

Finsterle, S., Moridis, G. J., Pruess, K. & Persoff, P. (January 1994) "Physical Barriers Formed from Gelling Liquids: 1 Numerical Design of Laboratory and Field Experiment." *LBNL-35113: UC-2000.* Earth Science Division, Ernest Orlando Lawrence Berkeley National Laboratory.

Finsterle, S. (October 1995) "Direct and Inverse Modeling Multiphase Flow Systems." *LBNL-38151 UC-400.* Earth Science Division, Ernest Orlando Lawrence Berkeley National Laboratory.

Finsterle, S., Oldenburg, C. M., James, A. L., Pruess, K. & Moridis, G. J. (September 1996) "Mathematical Modeling of Permeation Grouting and Subsurface Barrier Performance." *LBNL-39419: UC-2000.* Earth Science Division, Ernest Orlando Lawrence Berkeley National Laboratory.

Finsterle, S. (March 1998) "Multiphase Inverse Modeling: An Overview." *LBNL-41638.* Earth Science Division, Ernest Orlando Lawrence Berkeley National Laboratory.

Freeze, R. A. & Cherry J. A. (1979) *Groundwater.* Prentice-Hall Inc., New Jersey.

Friedman, A. & Rossi, G. (1997) "Note:Phenomenological Continuum Equations To Describe Case II Diffusion in Polymeric Material." *Macromolecules.* Vol.30:153-154.

Fugita, H. (1992) *Encyclopedia of Polymer Science and Technology:Plastics, Resins, Rubbers, Fibers (Volume 5).* Interscience Publishers, John Wiley & Son Inc., New York.

Gallagher, M. P. (October 27, 2000) *Passive Site Remediation for Mitigation of Liquefaction Risk.* Doctoral Dissertation, Virginia Polytechnic Institute and State University, Virginia.

Gallagher, M. P. & Mitchell, J. K. (2001) Multidisciplinary Center for Earthquake Engineering Research. "Passive Site Remediation for Mitigation of Liquefaction Risk."
Retrieved October 22nd, 2001. From the World Wide Web
http://mceer.buffalo.edu/publications/resaccom/0001/rpa_pdfs/13mitchell.pdf.

Gerhartz, W. & Elvers, B. (1993) *Ullmann's Encyclopedia of Industrial Chemistry.* New York.

Gudmundsson, K. (2001) "An Approach to Water Vapor Transport Mechanisms in Building Materials."
Retrieved July 23rd, 2001. From the World Wide Web,
http://bim.ce.kth.se/PersWeb/byte/kjartan/gas2000.html.

Hakem, N., Al Mahamid, I., Apps, J. & Moridis, G. J (January, 1997) "Sorption of Cesium and Strontium on Savanah River Soils Impregnated with Colloidal Silica." *LBNL-39498 UC-600.* Earth Science Division, Ernest Orlando Lawrence Berkeley National Laboratory.

Heiney, P. A., Butera, R. J., Londono, J. D., Davidson, R. B. & Mazur, S. (2000) "Network Growth in the Flocculation of Concentrated Colloidal Silica Dispersions." *J. Phys,. Chem. B.* Vol.104:8807-8821.

Heisher, H. J., Milian, L., Clinton, J. & Colombo, P. (1994) "Durability of Polymers for Containment Barriers." *In-situ Remediation:Scientific Basis for Current and Future Technologies: 33rd Hanford Symposium on Health and the Environment: November 7-11 1994. Pasco, Washington, D.C.* 61-101.

Heisher, H. J. (1997) "Summary Report on Close-Coupled Subsurface Barrier Technology Initial Field Trials to Full-scale Demonstration." *NBL-52531.* Brookhaven National Laboratory.

Heisher, H. J., Sullivan, T. & North-Abbott, M. (1998) "Viscous Liquid Barrier Demonstration at the Brookhaven National Laboratory LINAC Isotope Producer." *BNL-67336.* Brookhaven National Laboratory.

Hemond, F. H. & Fechner-Levy, E. J. (1996) *Chemical Fate and Transport in the Environment: 2nd edition.* Academic Press, New York.

Hood, P. (1976) "Fontal Solution Program for Unsymmetric Matrices" *Int. J. Numer. Methods Eng.* Vol.10:379-399.

Iler, K. R. (1989) *The Chemistry of Silica; Solubility, Polymerization, Colloid and Surface Properties, and Biochemistry.* John Wiley & Sons Inc., New York.

Irons, B. M. (1970) "A Frontal Solution Program for Finite Element Analysis" *Int. J. Number. Methods Eng.* Vol.2:5-32.

Jardine, P. M. & Fendorf, E. S. (1999) "Fate and Transport of Hexavalent Chromium in Undisturbed Heterogeneous Soil." *Environ Sci. Tech.* Vol.33(17): 2939-2944.

Jokinen, M., Györvary E. & Rosenholm, G. B. (1998) "Viscoelastic Characterization of Three Different Sol-gel Derived Silica gels." *Colloids and Surfaces A: Physicochemical and Engineering Aspects.* Vol.141(2):161-278.

Kärger, J., & Ruthven, G. M. (1992) *Diffusion in Zeolites and Other Macroporous Solids.* John Wiley & Sons Inc., New York.

Karim, N. & Gerald J. G. (2002) Howstuffworks, Inc. "How Digital Cameras Work." Retrieved July 25th, 2002. From the Words Wide Web http://www.howstuffworks.com/digital-camera12.htm.

Katz, A. S. & Salew, H. (1994) *The Biological and Environmental Chemistry of Chromium.* John Wiley & Sons Inc., New York.

Kim, M. (December 1999) *Modeling of a Subsurface Barrier Formation by a Gelling Liquid-Colloidal Silica.* Doctoral Dissertation. Texas A&M University, Texas.

King, I. P. (1982) *A Finite Element Model for Three Dimensional Flow.* Report Prepared for U.S. Army Crops of Engineering Waterways Experiment Station, Vicksburg, Mississippi.

King, I. P., Norton, W. R. & Orlob, G. T. (1973) *A finite Element Solution for Two-Dimensional Density Stratified Flow.* Final Report, prepared by Water Resource Engineer, Inc. for Office of Water Resource Research, the U.S. Department of Interior.

Kodak Co. Ltd., (2002) Kodak digital learning center. "Introduction to Digital Image." Retrieved February 8th, 2002. From the World Wide Web http://www.kodak.com/US/en/digital/dlc/index.jhtml.

Kožuh, N., J. Štupar & B. Gorenc. (2000) "Reduction and Oxidation Processes of Chromium in Soil." *Environ. Sci. Technol.* Vol.34(1):112-119.

Lakatos, I., Bauer, k., Lakatos-Szabó, J. & Kretzschmar, H. J. (1997) "Mass Transport of Heavy Metal Ions and Radon in Gels Used as Sealing Agents in Containment Technologies." *International Containment Technology Conference: February 9-12, 1997. St. Petersburg, FL.*

Lakatos, I., Lakatos-Szabó, J. & Kosztin, B. (1998) " Role of Diffusion Mass Transport in Design of Profile Correction Method Based on Sequential Injection of Gel-Forming Materials." *1998 SPE/DOE Improved Oil Recovery Symposium:18-22 April 1998.* Tulsa, Oklahoma.

Lakatos, I. & Lakatos-Szabó, J. (1998) "Diffusion of Chromium ions in polymer/silicate gels" *Colloidal and Surfaces A: Physicochemical and Engineering Aspects* Vol.141:425-434.

Lay, A. P. & A. Levina. (1996) "Kinetics and Mechanism of Chromium(VI) Reduction to Chromium(III) by L-Cysteine in Neutral Aqueous Solution." *Inorg. Chem.* Vol.35:7709-7717.

Lekkerkerker, H. N. W., Dhont, J. K. G., Verduin, H., Smits, C. & Duijneveldt J. S. (1995) "Interactions, Phase Transition and Metastable States in Concentrated Colloidal Dispersions." *Physica A.* Vol. 213:18-29.

Lide, D. R. (2001) *CRC Handbook of Chemistry and Physics, 82nd Edition.* CRC Press.

Mahmoud, M. E. & Gohar, G. A. (2000) "Silica Gel-immobilized-dithioacetal Derivatives as Potential Solid Phase Extractors for Mercury(II)." *Talanta.* Vol.51: 77–87.

Manchester, K., Zaluski, M., North-Abbott, M., Trudnowski, J., Bickford, J. & Wraith, J. (2001) "Grout Selection and Characterization in Support of the Colloidal Silica Barrier Deployment at Brookhaven National Laboratory." *In: Proc. 2001 International Contain. and Remed. Technol. Conf. and Exhib., 10-13 June, 2001. Orlando, FL.*

Masaro, L. & Zhu, X. X. (1999) "Physical Model of Diffusion in Polymer Solutions, Gels and Solids". Prog. Polym. Sci. Vol. 24:731-775.

McDonald, P. J., Godward, J., Sackin, K. & Sear, R. P. (2001) "Surface Flux Limited Diffusion of Solvent into Polymer." *Macromolecule.* Vol. 34:1048-1057.

Meegoda, J. N., King, I. P. & Arulanandan, K. (1989) "An Expression for the Permeability of Anisotropic Granular Media." *International Journal for Numerical and Analytical Methods in Geomechanics.* Vol.13:575-598.

Meegoda, J. N. (1997) "Micro-Mechanics and Microscopic Modeling in Geotechnical Engineering Current Status and Future." *Computer Methods and Advance in Geomechanics.* Balkema, Rotterdam. 197-206.

Mikolaichuk, V. & Stoch, E. (1993) "Chromium Oxide Layer Structure on the surface of Dispersed Silica." *Kinetics and Catalysis.* Vol.34(3):467-469.

Moridis, G. J. (1994) "Containment of Contaminants through Physical Barriers Formed from Viscous Liquids Emplaced under Controlled Viscosity Conditions." *FY 1993 Annual Report LBNL-29400.* Ernest Orlando Lawrence Berkeley National Laboratory.

Moridis, G. J., Yen, P., Persoff, P., Finsterle, S., Williams, P., Myer, L. & Pruess, K. (September 1996). "A Design Study for a Medium-Scale Field Demonstration of the Viscous Barrier Technology." *LBNL-38916 UC-2000.* Earth Science Division, Ernest Orlando Lawrence Berkeley National Laboratory.

Moridis, G. J., Persoff, P., Myer, L., Muller, S., Yen, P. & Pruess, K. (August 1996) "A Field Test of a Waste Containment Technology Using a New Generation of Injectable Barrier Liquids" *LBNL-38817 UC-2000.* Earth Science Division, Ernest Orlando Lawrence Berkeley National Laboratory.

Moridis, G. J., James, A. & Oldenburg, C. (October 1996.) "Development of a Design Package for a Viscous Barrier at the Savannah River Site." *LBNL-39487 UC-2000.* Earth Science Division, Ernest Orlando Lawrence Berkeley National Laboratory.

Moridis, G. J., Persoff, P., Apps, A., James, A., Oldenburg, C., McGrath, A., Myer, L., Pellerin, L., & Pruess, K. (November 1996) "A Design Study for the Isolation of the 281-3H Retention Basin at the Savannah River Site Using the Viscous Liquid Barrier Technology." *LBNL-38920 UC-2000.* Earth Science Division, Ernest Orlando Lawrence Berkeley National Laboratory.

Moridis, G. J. & Persoff, P. (1997) "A Field Test of Permeation Grouting in Heterogeneous Soils Using a New Generation of Barrier Liquids" *Barrier Technologies for Environmental Management: Summary of a Workshop (1997).* Retrieved June 18th, 2001. From the Words Wide Web http://books.nap.edu/books/0309056853/html/150.html#pagetop.

Moridis, G. J., James, A. & Oldenburg, C. (1997) "Development of a Design Package for a Viscous Barrier at the Savannah River Site." *LBNL-39487 UC-2000.* Earth Science Division, Ernest Orlando Lawrence Berkeley National Laboratory.

Moridis, G. J. (1998) "A set of Semianalytical Solutions for Parameter Estimation in Diffusion Cell Experiments." *LBNL-41857.* Earth Science Division Lawrence Berkeley National Laboratory.

Moridis, G. J., Finsterle, S. & Heiser, J. (1999) "Evaluation of Alternative Designs for an Injectable Subsurface Barrier at the Brookhaven National Laboratory Site, Long Island, New York." *Water Resource Research.* Vol.35(10):8937-2953.

Moridis, G. J. (June 1999) "Semianalytical Solutions for Parameter Estimation in Diffusion Cell Experiments" *Water resource Research.* Vol. 35(6):1729-1740.

Morrissey, P. & Vessely, D. (2000) "Accurate Measurement of Diffusion Rate of Small Molecules Through Polymers." *Polymer.* Vol.41(5):1865-1872.

Morohashi, S., Akakabe, S., Isobe, T. & Sasakura, T. 1990. "Adsorption properties of Metal Ions onto Hydrolyzed Polycrylamide Gel." *Journal of Chemical Engineering of Japan.* Vol.23(3):275-279.

Motulsky, H. (1996) "The GraphPad Guide to Nonlinear Regression." Retrieved March 20th, 2002. From the World Wide Web http://www.graphpad.com/www/nonling1.htm.

Nakano, Y., Takeshita, K. & Tsutsumi, T. (2001) "Adsorption Mechanism of Hexavalent Chromium by Redox within Condensed-Tannin Gel." *Water Research.* Vol.35(2):496-500.

Netz, A. P. & Dorfüller, T. (1997) "Computer Simulation Studies of Diffusion in Gels: Model Structures." *J. Chem. Physic.* Vol.107: 9221-9233.

New Jersey Department of Environmental Protection Agency, NJDEP, Site Remediation Program. (2000) *Chrome Update 28 (June 1999).* Retrieved June 18th, 2000. From the World Wide Web http/www.state.nj.us/dep/srp/chrome/bkgrnd.html.

New Jersey Department of Environmental Protection Agency, NJDEP, Site Remediation Program. (2000) *Hudson County Chromate Chemical Production Waste Site.* Retrieved June 1st, 2002. From the World Wide Web http://www.state.nj.us/dep/srp/chrome/update28.htm.

Noll, R. M., Bratlett, C. & Dochat, T. M. (1992) "In Situ Permeability Reduction and Chemical Fixation Using Colloidal Silica." *Proceeding of the Sixth National Outdoor Action Conference on Aquifer Restoration, Ground Water Monitoring, and Geophysical Method, National Ground Water Association.* 443-457.

North-Abbott, M. A., Heisher, J. H., Manchester, K. R., Trudnowski, J. M., Martin, J. M., Bickford, J. L. & Zaluski, M. H. (2001) "Colloidal Silica Barrier Deployment at Brookhaven National Laboratory." *HLW, LLW, Mixed Wastes and Environmental Restoration-Working towards A Cleaner Environment., February 25- March1, 2001.,* Tucson, Arizona.

Olazabal, M. A., Nikolaidis, N. P., Suib, S. A. & Madariaga, J. M. (1997) "Precipitation Equilibria of the Chromium(VI)/Iron(III) System and Spectroscopic Characterization of the Precipitates." *Environmental Science and Technology.* Vol.31:2898-2902.

Oya, T. & Enoki, T. (1999) "Reversible Molecular Adsorption Based on Multiple-Point Interaction by Shrinkable Gels." *Science.* Vol.286:1543-1545.

Pagilla, R. K. & Canter, W. L. (March 1999) "Laboratory Studied in Remediation of Chromium Contaminated Soils." *Journal of Environmental Engineering.* 243-248.

Palmer, D. C. & Wittbrodt, P. R. (1991) "Processes Affecting the Remediation of Chromium-Contaminated Sites." *Environmental Health Perspectives.* Vol.92:25-40.

Papirer, E. (Editor) (2000) *Adsorption on Silica Surface: Surfactant Science Series. Volume 90.* Marcel Dekker, Inc., USA.

Park, Y. J., Jung, K. g-Hoon & Park, K. K. (1994) "Effect of Complexing Ligands on the Adsorption of Cu(II) onto the Silica Gel Surface: I Adsorption of Ligands Complex" *Journal of Colloidal and Interface Science.* Vol.171: 205-210.

Park, Y. J., Jung, K. g-Hoon & Park, K. K. (1994) "Effect of Complexing Ligands on the Adsorption of Cu(II) onto the Silica Gel Surface: II Adsorption of Cu(II)-Ligands Complex" *Journal of Colloidal and Interface Science.* Vol.171:447-458.

Patterson, E. R. (1992) *Kirk-Othmer Encyclopedia of Chemical Technology Vol.21:4th edition.* John Wiley & Sons Inc., New York. 977-1029.

Pearlman, L. (1999) "Subsurface Containment and Monitoring Systems: Barriers and Beyond: Overview Report." National Network of Environmental Management Studies Fellow for U.S. Environmental Protection Agency Office of Solid Waste and Emergency Response Technology Innovation Office. Washington, DC. Retrieved March 24th, 2002. From the World Wide Web http://www.clu-in.org/products/intern/pearlman/#_Toc445174071.

Persoff, P., Finsterle, S., Moridis, G. J., Apps, J. A., Pruess, K. & Muller, S. J. (March 1995) "Injectable Barriers for Waste Isolation" *LBNL-36739 UC-600.* Earth Science Division, Ernest Orlando Lawrence Berkeley National Laboratory.

Persoff, P., Apps, J. A., Moridis, G. J. & Whang, J. M. (October 1996) "Effect of Dilution and Contaminates on Strength and Hydraulic Conductivity of Sand Grouted with Colloidal Silica Gel" *LBNL-39347 UC-000.* Earth Science Division, Ernest Orlando Lawrence Berkeley National Laboratory.

Persoff, P., Moridis, G. J., Apps, J. A. & Pruess, K. (1998) "Technical Note: Evaluation Tests for Colloidal Silica for Use in Grouting Applications." *The America Society for Testing and Materials.* Vol.21(3) 264-269.

Persoff, P., Apps, J. A. & Moridis, G. J. (May 1998) "Effect of Dilution and Contaminants on Ludox® Colloidal Silica Grout." *LBNL-42385.* Earth Science Division, Ernest Orlando Lawrence Berkeley National Laboratory.

Persoff, P., Apps, J. A., Moridis, G. J. & Whang, J. M. (June 1999) "Effect of Dilution and Contaminants on Sand Grout with Colloidal Silica." *Journal of Geotechnical and Geoenvironmental Engineering.* Vol.125(6):461-469.

Plus, R. W., Clark, D. A., Paul, C. J. & Vardy, J. (1994) "Transport and Transformation of Hexavalent Chromium through Soils and into Ground Water." *Journal of Soil Contamination.* Vol.3(2):203-224.

Poon, W. C. & Haw, M. D. (1997) "Mesoscopic Structure Formation in Colloidal Aggregation and Gelation." *Advance in Colloidal and Interface Science.* Vol.73:71-126.

Pozrikidis, C. (1998) *Numerical Computation in Science and Engineering.* Oxford University Press, New York. 375-382.

Pradhan, J., Das, S. N. & Thakur, R. S. (1999) "Adsorption of Hexavalent Chromium from Aqueous Solution by Using Activated Red Mud." *Journal of Colloid and Interface Science.* Vol.217:137–141.

Rai, D., Sass, B. M. and Moore, D. A. (1987) "Chromium(III) Hydrolysis Constant and Solubility of Chromium(III) Hydroxide." *Inorg. Chem.* Vol.26:345-349.

Rock, M. L., James, B. J. & Helz, G. R. (2001) "Hydrogen Peroxide Effects on Chromium Oxidation State and Solubility in Four Diverse Chromium-Enrich Soils." *Environmental Science and Technology.* Vol.35:4054-4059.

Rutherford, S. W. (2001) "Mechanism Sorption and Diffusion in a High Free-Volume Polymer." *Ind. Eng. Chem. Res.* Vol.40:1370-1376.

Ruthven, D. M. (1991) *Encyclopedia of chemical technology:volumn1, 4th edition.* John Wiley & Sons Inc., USA.

SAS Institute Inc. (2002) *SAS/STAT Software Manual: Changes and Enhancements, Release 8.2: The GAM Procedure.*
Retrieved March 15th, 2002. From the World Wide Web
http://www.sas.com/rnd/app/da/new/802ce/stat/chap5/sect16.htm.

Sattar, S. & Francis, L. F. (1995) "Formation of Chromium Hydroxide Particles in Silica Xerogel." *Journal of Material Science Letters.* Vol.14:1354-1356.

Seaman, C. J., Bertsch, P. M. & Schwallie, L. (1999) "In Situ Cr(VI) Reduction within Coarse-Textures, Oxide-Coated Soil and Aquifer Systems Using Fe(II) Solutions." *Environmental Science and Technology.* Vol.33:938-944.

Simonoff, J. S. (1996) *Smoothing Methods in Statistics.* Springer, New York.

Shackelford, C. D. (1991) "Review Paper:Laboratory Diffusion Testing for Waste Disposal-A Review." *Journal of Contaminant Hydrology.* Vol.7:177-217.

StatSoft Inc. (2002) Electronic Statistics Textbook (EST). *Nonlinear Estimation.*
Retrieved March 15th, 2002. From the World Wide Web

http://www.statsoftinc.com/textbook/stnonlin.html.

Stumm, W. (1992) *Chemistry of the Solid Water-Interface.* A Willey-Interscience Publication, John Wiley & Sons, Inc., Singapore.

Sunderrajan, S., Hall, C. K. & Freeman, B. D. (1996) "Estimation of Mutual Diffusion Coefficients in Polymer/penetrant Systems Using Nonequilibrium Molecular Dynamics Simulations" *J. Chem. Phys.* Vol.105(4):1621-1632.

Takahashi, R., Sato, S., Sodesawa, T. & Kamomae, Y. (2000.) "Measurement of the Diffusion Coefficient of Nickel Nitrate in Wet Silica gel Using UV/VIS Spectroscope Equipped with a Flow Cell." *Phys. Chem. Chem. Phys.* Vol.(2):1199-1204.

Teasdale, P. R., Hayward, S. & Davison, W. (June 1, 1999) "In situ, High-Resolution Measurement of Dissolved Sulfide Using Diffusion Gradients in Thin Films with Computer Imaging Densitometry." *Anal. Chem.* Vol. 71(11):2186-2191.

Teraoka, I. (1996) "*Polymer Solutions in Confining Geometries.*" Prog. Polym. Sci. Vol.21:89-149.

The School of Chemical Engineering and Industrial Chemistry, The University of New South Wales, Australia. *CEIC0010 Mass Transfer Fundamentals.* Retrieved May 1st, 2002. From the World Wide Web http://www.ceic.unsw.edu.au/classnotes/CEIC0010/MTLec4.pdf.

Tran, H. H., Roddick, F. A. & O'Donnell, J. A. (1999) "Comparison of Chromatography and Desiccant Silica Gels for the Adsorption if Metal Ions-I. Adsorption and Kinetics." *Water Resource.* Vol.33(13):2992-3000.

Tran, H. H., Roddick, F. A. & O'Donnell, J. A. (1999) "Comparison of Chromatography Silica Gels for the Adsorption of Metal Ions: II. Fixed-Bed Study." *Water Resource.* Vol.33(13):3001-3011.

Thibodeaux, L. J. (1995) *Environmental Chemodynamics: Movement of Chemicals in Air Water and Soil.* John Wiley &Sons Inc., New York.

United State Environmental Protection Agency, USEPA, Office of Research and Development. Washington, D.C. (May 1989) "Stabilization/solidification of CERCLA and RCRA Waste." *EPA-625-6-89-022.*

United State Environmental Protection Agency, USEPA, Office of Research and Development. Washington, D.C. (August 1991) "Handbook: Stabilization Technology for RCRA Corrective Actions." *EPA-625-6-91-026.*

United State Environmental Protection Agency, USEPA, Office of Research and Development. Washington, D.C. (July 1995) "Contaminated and Remediation Options at Selected Metal-Contaminated Sites." *EPA-540-R-95-512.*

United State Environmental Protection Agency, USEPA, Office of Research and Development. Washington, D.C. (October 2000) "In Situ Treatment of Soil and Groundwater Contaminated with Chromium." *EPA-625-R-00-005.*

United State Environmental Protection Agency, USEPA, Office of Solid Waste and Emergency Response. Washington, D.C. (March 1997) "Recent Developments for In Situ Treatment of Metal Contaminated Soils." *EPA-542-R-97-004.*

United State Environmental Protection Agency, USEPA. (August 2000) *Sodium Dichromate Listing Background Document for the Inorganic Chemical Listing Determination.* Washington, D.C.
Retrieved May 1st, 2002. From the World Wide Web
http://www.epa.gov/OSWRCRA/hazwaste/id/inorchem/docs/sod-dich.pdf.

United State Environmental Protection Agency, USEPA, Integrated Risk Information System (IRIS). (1998) *Toxicology Review of Hexavalent Chromium (CAS No. 18540-29-9).*
Retrieved May 1st, 2002. From the World Wide Web
www.chromiumcentral.com/toxicology.html.

United State Environmental Protection Agency, USEPA, Integrated Risk Information System (IRIS). (1998) *Toxicology Review of Trivalent Chromium (CAS No. 16065-83-1).*
Retrieved May 1st, 2002. From the World Wide Web
www.chromiumcentral.com/toxicology.html.

University of Pittsburgh. (2002) *An Introductory, Lecture to Environmental Epidemiology: Part 2. Time Series Studies.*
Retrieved April 1st, 2002. From the World Wide Web
http://www.pitt.edu/~super1/lecture/lec1641/010.htm.

Vipulananda, C. & Wang, S. (2000) "Solidification/stabilization of Cr(VI) with Cement Leachability and XRD analyses." *Cement and Concrete Research.* Vol.30:385-389.

Valsaraj, K. T. (2000) *Elements of Environmental Engineering: Thermodynamic and Kinetics (Second Edition).* Lewis Publication, London.

Wang, K. Suda, H. & Haraya, K. (2001) "Permeation Time Lag and the Concentration Dependence of the Diffusion Coefficient of CO_2 in a Carbon Molecular Sieve Membrane." *Ind. Eng. Chem. Res.* Vol.40:2942-2946.

Watanabe, Y., Okumura, E., Ando, M. & all of Funabashi, Japan. (February 27, 1990) "Chemical Grout for Ground Injection and Method for Accretion." *US patent 4,904,304.*

Weckhuysen, B. M., Wachs, I. E. & Schoonheydt, R. A. (1996) "Surface Chemistry and Spectroscopy of Chromium in Inorganic Oxide." *Chem. Rev.* Vol.96(8):3327-3349.

Westrin, B. A., Axelsson, A. & Zacchi, G. (1994) "Review:Diffusion Measurement in Gels." *Journal of Controlled Release.* Vol.(30):189-199.

Willecke, R. & Faupel, F. (1997) "Diffusion of Gold and Silver in Bisphenol A Polycarbonate" *Macromolecules.* Vol. (30): 567-573.

White, J. A. & Deen, W. M. (2001) "Effects of Solute Concentration on Equilibrium Partitioning of Flexible Macromolecules in Fibrous Membranes and Gels" *Macromolecules.* Vol. 34:8278-8285.

Worldwide Performance and Innovative. (1996) "Physical plums barrier stop plume in their track." *Initiative online Vol.3 August 1996.* Retrieved March 23rd, 2002. From the World Wide Web http://www.wpi.org/Initiatives/init/aug96/barriers.html.

Xrefer Inc. (2002) Electronic Reference. *Definition of Partition Coefficient from A Dictionary of Science.* Oxford University Press, © Market House Books Ltd 1999. Retrieved May 15th, 2002. From the World Wide Web http://w2.xrefer.com/entry.jsp?xrefid=491018.

Yonekura, R. & Miwa, M. (May 1993) "Fundamental Properties of Sodium Silicate Based Grout." *Eleventh Southeast Asia Geotechnical Conference: May 1993.* Singapore. 439-444.

Zorrilla, E. S. & Rubiolo, A. C. (1994) " A Model For Using The Diffusion Cell in the Determination of Multicomponent Diffusion Coefficients in Gels or Foods." *Chemical Engineering Science.* Vol. 49(13):2123-2128.

Zulaski, M. H., Manchester K. R. & North-Abbott, M. A. (2000) "Modeling of Unsaturated Flow in Soil Solidified with Colloidal Silica." *Proceeding of the Business and Industry Simulation Symposium 2000 Advance Simulation Technologies Conference. April 16-20, 2000.* Washington, D.C.

Zulaski, M. H., Manchester, K. R., North-Abbott, M. A. & Wraith, J. M. (2000) "Impact of Colloidal-Silica Solidification on Unsaturated Flow Regime, the Modeling Study." *Proceeding of the Fifth International Symposium and Exhibition on Environmental Contamination in Central and Eastern Europe, September 12-14, 2000.* Prague, Czech Republic.

Zulaski, M. H., Manchester, K. R., North-Abbott, M. A. & Wraith, J. M. (2001) "Performance of the Colloidal Silica Barrier Installed at Brookhaven National Laboratory, A Computer Modeling Study." *Proceeding of 2001 International Containment and Remediation Technology Conference and Exhibit, 10-13 June, 2001.* Orlando, FL.